Study the Mechanical Properties of SiC Material by Using Molecular Dynamic Simulation (lammps)

A Thesis Submitted to

the Council of the College of Education – Al-Qadisiyah University

In Partial Fulfillment of the Requirements for the Degree of

Master of Science in Physics

Submitted by

Shurooq Hayder Abd alnebee Al-mehanyah

Supervised by
Assistant Professor
Dr. Hisham Mohammed ali Hasan AL-Barmany

2017 A.D   **1438 A.H**

بِسْمِ اللهِ الرَّحْمَنِ الرَّحِيمِ

﴿يَرْفَعِ اللَّهُ الَّذِينَ آمَنُوا مِنْكُمْ وَالَّذِينَ أُوتُوا الْعِلْمَ دَرَجَاتٍ وَاللَّهُ بِمَا تَعْمَلُونَ خَبِيرٌ﴾

صدق الله العلي العظيم

سورة المجادلة
الآية (11)

CERTIFICATION OF THE SUPERVISOR

I certify that this thesis entitled " **Study the mechanical properties of SiC material by using molecular dynamic simulation (lammps)**" was prepared by "**Shurooq Hayder Abd alnebee**" under my supervision at Department of Physics, Faculty of education, University of AL-Qadisiyah, as a partial fulfillment of the requirements for the Degree of Master in Physics science.

Signature:

Name: Dr.Hisham Mohammed ali Al-Barmany(Supervisor)

Title: Assistant Professor

Address: /University of AL-Qadisiyah

Date:23/ /d 2016

Based on the recommendation of (Assist. Prof. Dr. Hisham Mohammed ali Hasan) I refer this thesis to the masters defense committee for their opinin.

Signature:

Name: Dr.: Abd AL-Hussain Abbas Khudhaier

Title: Assistant Professor

Address: Physics Department/Faculty of

Education /University of AL-Qadisiyah

Date:2}/ (∘/ 2016

CERTIFICATION OF LINGUISTIC EVALUATOR

I certify that this thesis entitled " **Study the mechanical properties of SiC material by using molecular dynamic simulation (lammps)**" was prepared by **"Shurooq Hayder Abd alnebee"** was evaluated linguistically, and I forward it for debate by the examination committee.

Signature:

Name: Jenan Atiya

Title: Lecturer

Address: Department of English /College of Education /University of AL-Qadisiyah
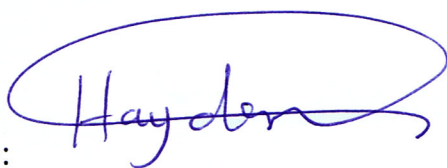
Date:

CERTIFICATION OF SCIENTIST EVALUATOR

I certify that this thesis entitled **"Study the mechanical properties of (SiC) material by using molecular dynamic simulation (lammps)"** was prepared by **"Shurooq Hayder Abd alnebee"** was evaluated scientifically, and I forward it for debate by the examination committee.

Signature:

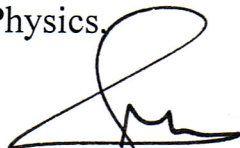Name: Hayder M. Abduljalil

Title: Assis. Prof

Date: 26 - 1 - 2017

Examining Committee Certification

We, the members of examining committee, certify that we have read this thesis entitled **"Study the mechanical properties of SiC material by using molecular dynamic simulation (lammps)"** and examined the student **"Shurooq Hayder Abd alnebee"** in its contents and that, in our opinion it is adequate for the partial fulfillment of the Requirements for the degree of Master of Science in Physics.

Signature

Name : Assist. Prof. Dr. Majeed Ali Habeeb

Address : University of Babylon, College of Education for Pure Sciences

Date : 19/4/2017

(Chairman)

Signature   Signature

Name : Assist. Prof. Dr. Burhan R. Nori   Name : Assist. Prof. Dr. Saleem A. Hussain

Address : University of Kerbala,   Address : University of Al- Qadisiayh,
College of Education for Pure Sciences   College of Education
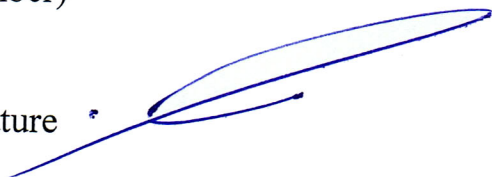
Date :   Date : 18-4- 2017

(Member)   (Member)

Signature

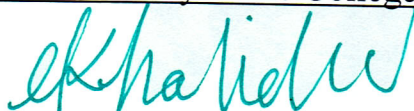Name : Assist. Prof. Dr. Hisham Mohammed ali Al-Barmany

Address : University of Al-Qadisiyah, College of Computer Science and information Technology

Date : 20-4-2017

(Member and Supervisor)

Approved by the Deanery of the College of Education

Signature

Name : Prof. Dr. Khalid Jawad Kadhim Al-Adilee

Rank: Professor

Position: Dean of College of Education   Date: 30/ 4 / 2017

Dedication

To my great teacher: Prophet Mohammed and his progeny (PBUT).

To these whom I owe my life: Mother and father And to those who seek knowledge everywhere.

Shurooq
2017

Acknowledgments

Abstract

In this thesis, the crack and modified embedded atom method (MEAM) by using molecular dynamics simulation was studied, simulator (lammps) of crack propagation in hexagonal lattice and in modified embedded atom method (MEAM) for material silicon carbide (SiC). The mechanisms of crack including emission of dislocations and creation of stacking faults.

In crack code the time steps used was (0.044,0.04,0.03, 0.02, 0.01, 0.009, 0.008, 0.007, 0.006, 0.005, 0.004, 0.003, 0.002, 0.001and 0.00001 tau) and in modified embedded atom method code time steps used was (0.003, 0.002, 0.001, 0.0009, 0.0008, 0.0007, 0.0006, 0.0005 and 0.0001 Ps), the time step must be chosen small enough to ensure energy conservation and to avoid large discretization errors, so the best choice time step in crack was (0.00001 reduced) and in Modified Embedded Atom Method (MEAM) is (0.0001 Ps). In crack code increase (decreases in negative) potential energy because the crack was not initiated, while the crack initiate at step (run) =10600, while potential energy was (-3.2511ϵ) at step (run) =10600 resulting by breaking the bonds between atoms while the increase in temperature indicates that the crack propagated. The increase (decreases in negative) pressure of the system because there is no crack initiation, then decreases (increasing in negative) pressure resulting from breaking the bonds between atoms at crack propagation. In this code the volume or area of crack is constant.

In Modified Embedded Atom Method (MEAM) the increases in negative potential energy because the embedded atom within the group of atoms (stable system) need sufficient energy in order to break the bonds between the atoms. And the increases of the kinetic energy of the

system can be attributed to the rapid breaking. Although the energy of the system is conserved, the temperature will increase when potential energy is transferred into thermal kinetic energy , resulting in breaking the bonds between atoms. And an increases in negative pressure result of breaking the bonds between atoms.

LIST OF CONTENTS

LIST SYMBOL OF ABBREVIATION

The symbol	The meaning of the symbol	Unit reduced	Unit metal
MD	Molecular Dynamics		
EAM	Embedded Atom Method		
MEAM	Modified Embedded Atom Method		
FCC	Face Centered Cubic		
BCC	Body Centered Cubic		
HCP	Hexagonal Close Packing		
MC	Monte Carlo		
LAMMPS	Large-scale Atomic/Molecular Massively Parallel Simulator		
CNA	Common Neighbor Analysis		
CTMD	Constant Temperature Molecular Dynamics		

DFT	Density Functional Theory		
H-K	Hohenberg and Kohn		
K-S	Kohn-Sham		
LDA	Local Density Approximation		
GGA	Generalized Gradient Approximation		
PAW	projector-augmented wave		
OPWs	Orthogonalized plane waves		
NC-PP	Norm-Conserving Pseudopotentials		
US-PP	Ultrasoft Pseudopotentials		
LJ	Lennard-Jones		
NVE	(constant number of particles, constant volume, constant energy) microcanonical ensemble		
NVT	(constant number of particles, constant volume, constant temperature) canonical ensemble		
NPT	constant number of particles, constant pressure, constant temperature) isothermal–isobaric ensemble		
F_i	Force of atom (i)	$\dfrac{\in}{\sigma}$	$\dfrac{eV}{Angstrom}$
m_i	Mass of atom (i)	m	$\dfrac{grams}{mole}$
a_i	Acceleration of atom (i)		
v_i	Velocity of atom (i)	$\dfrac{\sigma}{tau}$	$\dfrac{Angstrom}{picosecond}$
r_i	Position of atom (i)		
R, r	Distance between the two atoms, Bond	σ	Angstroms

	length		
ϵ	Well depth		
Q_1, Q_2	The charges		
ϵ_0	Permittivity of free space		
K_b, K_{ij}^r	Bond length		
r_0	Equilibrium bond length		
K_{ijk}^θ, K_θ	Angle spring		
θ, θ_{ijk}	Bond angles		
θ_0	Equilibrium angle		
$K_{ijkl}^{\emptyset,m}, K_\emptyset$	Torsion angle		
p	Momentum		
H	Energy or hamiltouian		
k	Kinetic energy	ϵ	eV
U	Potential energy	ϵ	eV
t	Time	tau	picosecond
$\delta t, \Delta t$	Time step	tau	picosecond
E, E*	Total energy	ϵ	eV
V	Volume	σ	Cm^3
N	Number of atoms		
T	Temperature	$\dfrac{K_b}{\epsilon}$	Kelvin
$\widehat{H}$	Hamiltonian		
$\widehat{H}_{NN}$	Represents the kinetic energy and the interaction of the nuclei		
$\widehat{H}_{Ne}$	Represents the interaction between the electron and nuclei		
$\widehat{H}_{ee}$	Represents the interaction between the		

	electrons		
h	Plank constant		
M_α	Mass of nuclei		
Z_α, Z_β	Charges of the nucleus		
e	Charge of the electron		
R_α, R_β	Radius of nucleus		
r_i, r_j	Radius of electron		
$\psi, \emptyset$	Wave function		
φ	Wave function of the nuclei		
$\hat{T}$	The operator for the kinetic energy		
$\hat{V}_{ext}$	The potential acting on the electrons due to the nuclei		
$\hat{V}_{int}$	The electron-electron interaction		
E_{II}	The interaction of the nuclei		
$\hat{O}$	The expectation value of an operator		
n(r)	The particle density		
$E_{Hartree}$	Hartree energy		
V_{XC}	The exchange-correlation potential		
ϵ_{XC}	Exchange-correlation energy density		
$\emptyset\rangle$	The pseudo wave function		
$X_n\rangle$	The core wave functions		
F_i, G_i	Embedding functional		
ρ_j^a	The contribution of the atom(j) of type (a) to the electron charge density		
R_{ij}	The distance between atoms (i) and(j)		
ϕ_{ij}	The short-range pair potential		
Z	The atomic number of the atoms		

$\bar{\rho}_i^0(R)$	The background electron density for the reference structure of atom i		
$E_i^u(R)$	The energy per atom of the reference structure as a function of nearest neighbor distance		
E_c	Cohesive energy		
r_e	Nearest-neighbor distance		
Ω	atomic volume		
B	bulk modulus		
$F(\rho)$	Embedding function		
A	An adjustable parameter		
ρ_0	Density scaling parameter		
$\rho^{a(h)}$	radial functions		
2D	Two dimension		
k	Spring constant		
a	Lattice constant		
k_B	Boltzmann constant		
Ps	picoseconds		

LIST OF TABLES

LIST OF FIGARES

CHAPTER ONE
INTRODUCTION

1-1 Introduction

Molecular dynamics (MD) is a computer program simulation method (installation of program and the input data in appendix I) , for examining the physical movements of N-atoms and molecules [1], the atoms and molecules are allowed to interact for a fixed period of time [2], the equations of motion for a system of interacting particles are determined by numerically solved Newton's equations, where forces between the particles and their potential energies are calculated using interatomic potentials or molecular mechanics force fields [3]. Molecular dynamics (MD) simulation have been widely used in various academic fields, such as physics, biophysics, chemistry, and materials science [1].

Molecular dynamics (MD) is one of the first simulation methods has been applied to study the dynamics of liquids by Alder, Wainwright [4] and by Rahman [5] in the late 1950 and early 1960. Molecular dynamics (MD) has become an important tool in many areas of physics. Since the 1970 molecular dynamics (MD) has been used widely to study the structure and dynamics of macromolecules, such as crack or fracture and Modified Embedded Atom Method (MEAM) [6].

Molecular dynamics (MD) simulations use to understanding the properties of assemblies of molecules in terms of their structure and the microscopic interactions between them. Computer simulations act as a bridge between microscopic length and time scales and the macroscopic world of the laboratory, Molecular dynamics (MD) provide a guess at the interactions between molecules, and obtain `exact' predictions of bulk properties [7] .

The molecular dynamics (MD) simulation is being used for investigating physical in the field of solid-state physics (metal structure

conversion, cracks initiated by pressure and shear stresses, and fracture) and fluid dynamics [8]. Molecular dynamics (MD) runs in crack propagation or fracture, Modified Embedded Atom Method (MEAM), flow, body, balance, colloid, deposit, dipole, friction, melt and shear, in this thesis used crack and Modified Embedded Atom Method (MEAM).

Fracture is the separation of a body into two or more pieces in response to an stress .The applied stress which may be tensile, compressive, shear, or torsional. There are two fracture modes; ductile and brittle. Ductile materials typically exhibit substantial plastic deformation with high energy absorption before fracture while brittle fracture is normally little or no plastic deformation with low energy absorption [9].

Fracture normally occurs through the enlargement of existing defects, in solid voids, grain boundaries, or micro-cracks, all such defects concentrate stress,the fact that failure stresses lie far below ideal crystal strengths shows that the stress concentration is large [10]. Apply the embedded atom method to basic parts of the fracture process sach as dislocation dynamics, and crack tip plasticity [11].

The embedded atom method (EAM), developed by Daw and Baskes [12,13] in the early 1980, is a semi-empirical N-body potential useful for the atomistic simulations of metal systems. It has successfully been utilized to calculate the energetics and structures of complex metallic systems involving free surfaces, defects and grain boundaries [14,15].

The embedded atom method (EAM) construction is based on the use of density functional theory, in which the energy of a collection of atoms can be expressed exactly by function of its electronic density. In the embedded atom method (EAM), each atom is embedded in a host electron gas created by its neighboring atoms. The atom host interaction

is described using the embedding function incorporating some important many-atom interactions. It is possible to describe and understand interatomic interactions at defects in terms of either the embedding function or the effective many-atom interactions that arise from it. Embedded atom method (EAM) potentials have been applied to study many aspects of materials behavior in face centered cubic (fcc), body centered cubic (bcc) and hexagonal close packing (hcp) metals . Although the embedded atom method (EAM) gives a more detals of crystal properties than can be obtained by pair potentials, there are two assumptions, first, spherically averaged free atom densities represent the atomic electron densities, second, the host electron density is approximated by a linear superposition of the atomic densities of the constituents [16].

Recent modifications have been made to generalize the Embedded Atom Method (EAM) to describe bonding in diverse materials. By including angular dependence of the electron density in an empirical way, the Modified Embedded Atom Method (MEAM) has been able to reproduce the basic energetic and structural properties of forty-five elements. This method is ideally suited for examining the interfacial behavior of dissimilar materials.

A basic limitation of the Embedded Atom Method (EAM) is that it spherically averages the electron density which precludes directional bonding. Baskes modified the EAM to include directional bonding and applied it to silicon metal. The silicon EAM model was extended by Baskes, et al. to the silicon/germanium system where the Modified Embedded Atom Method (MEAM) was developed [17] . The modified embedded atom method (MEAM) assumes that the energy per atom is a known function of the nearest neighbor distance in the reference structure

for the element under consideration. An analytic form for the electron density at a given atom site arising from the other atoms and an analytic form for the embedding energy as a function of the electron density are also assumed [16].

More programe simulations used in molecular dynamics such as Monte Carlo(MC) [18], Finit Element [19] and Large-scale Atomic/Molecular Massively Parallel Simulator (lammps) (lammps.org) which we used in this thesis, a freely-available open-source code. According to the website of the project \LAMMPS is a classical molecular dynamics code that models an ensemble of particles in a liquid, solid, or gaseous state. It can be an model atomic, polymeric, biological, metallic, granular, and coarsegrained systems using a variety of force fields and boundary conditions[20, 21]. It runs on computer installed memory (RAM): 4.00 GB (3.56 usabe) , processor : intal(R) i5-3320M CPU @ 2060 GHZ 2060 GHZ and system type: 64-bit. The operating system runs on the Windows and the linax, and the output could be graphs, picture or movies. The program of input file are c++, MATLAB and python programs.

1-2 Literatures review

Wang et al. (2012) [22] studied the fracture of graphene sheets with Stone–Wales type defects and vacancies were investigated using molecular dynamics simulations at different temperatures. The initiation of defects via bond rotation was also investigated. The results indicate that the defects and vacancies can cause significant strength loss in graphene.

Bohumir et al. (2012) [23] studied a set of Modified Embedded-Atom Method (MEAM) potentials for the interactions between Al, Si, Mg, Cu, and Fe was developed from a combination of each element's MEAM potential in order to study metal alloying. The new MEAM potentials were validated by comparing the formation energies of defects, equilibrium volumes, elastic moduli, and heat of formation for several binary compounds with ab initio simulations and experiments.

Minh-Quy and Romesh (2013) [24] used the molecular dynamics simulations to study crack initiation and propagation in pre-cracked single layer arm chair graphene sheets. Results computed for axial strain rates of 2.6×10^6, 2.6×10^7 and 2.6×10^8 s−1 reveal that values of the J-integral are essentially the same for the first two strain rates but different for the third strain rate even though the response of the pristine sheet is essentially the same for the three strain rates.

G. D. et al. (2013) [25] have been used a molecular dynamics technique to study the impact of single vacancies and small vacancy clusters/micvoids on thermal conductivity of β-SiC. It is found that single vacancies reduce thermal conductivity more significantly than do micro

5

voids with the same total number of vacancies in the crystal. The vacancy concentration dependence of the relative change of thermal resistivity of both Si and SiC changes from linear at low concentrations to square-root at higher values.

Mazdak et al. (2014) [26] have been simulated dynamic fracture of a polycrystalline microstructure (alumina ceramic). The influence of the grain boundary and grain interior fracture energies on the interacting and competing fracture modes of polycrystalline materials, i.e. intergranular and transgranular fracture, has been studied.

Laalitha et al. (2014) [27] studied structural, elastic, and thermal properties of cementite (Fe3C) using a modified embedded atom method (MEAM) potential for iron-carbon (Fe-C) alloys. The stability of cementite was investigated by molecular dynamics simulations at high temperatures. The formation energies of (001), (010), and (100) surfaces of cementite were also calculated.

Alireza and Xiaonan (2015) [28] used molecular dynamics (MD) modeling to study the fracture properties of monolayer hexagonal boron nitride (h-BN) under mixed mode I and II loading. The molecular dynamics (MD) used results predict that under all the loading phase angles cracks prefer to propagate along a zigzag direction and the critical stress intensity factors of zigzag cracks are higher than those of armchair cracks.

Ebrahim et al. (2015) [29] studied the two-phase solid–liquid coexisting structures of Ni, Cu, and Al by molecular dynamics (MD) simulations using the Second Nearest-Neighbor (2NN) Modified-
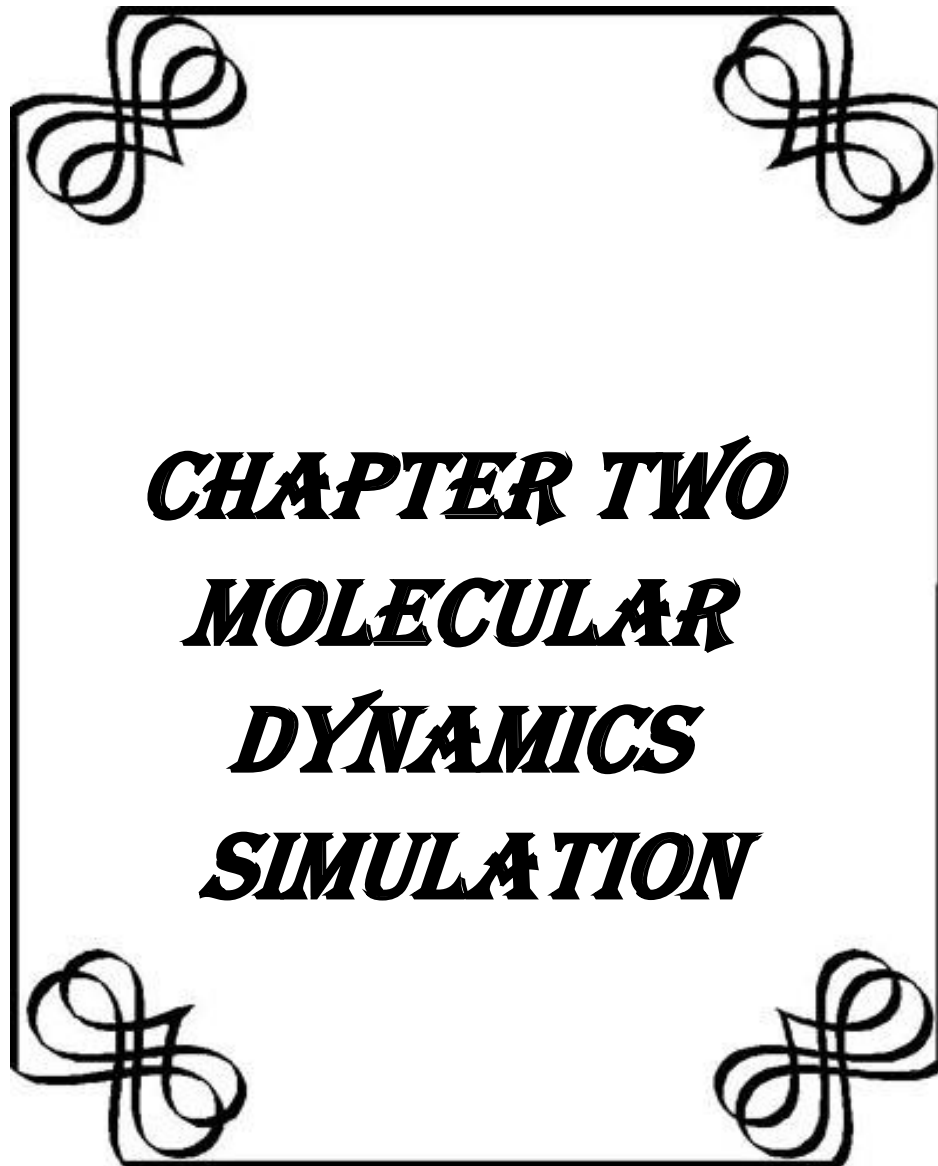
Embedded Atom Method (MEAM) potential. Using these potentials, to compare calculated low-temperature properties of Ni, Cu, and Al, such as elastic constants, structural energy differences, vacancy formation energy, stacking fault energies, surface energies, specific heat and thermal expansion coefficient with experimental data.

Qi-lin et al. (2016) [30] studied the fracture strength and crack propagation of monolayer molybdenum disulfide (MoS2) sheets with various pre-existing cracks are investigated using Molecular Dynamics Simulation (MDS). The results show that the configuration of crack tip can influence significantly the fracture behaviors of monolayer MoS2 sheets while the location of crack does not influence the fracture strength.

Naigen et al. (2016) [31] studied molecular dynamics simulations of crystal growth of SiC in the reduced temperature range of 0.51−1.02 have been carried out. The results show that the growth rate increases first with the temperature and then decreases dramatically after passing through a maximum.

1-3 The goal

In this research , we will study The crack propagation in brittle materials and the Modified Embedded Atom Method (MEAM) models by using molecular dynamics simulation . Calculating the temperature, total energy, kinetic energy, potential energy, pressure and volume in order to study and analyzing the effects of these parameters on the crack propagation and Modified Embedded Atom Method (MEAM) specially in the electronic devices.

CHAPTER TWO
MOLECULAR DYNAMICS SIMULATION

2-1 Molecular Interactions

Molecular dynamics simulation is a numerical, step-by-step, solution of the classical equations of motion (Newton) , which for a simple atomic system may be written as:

$$F_i = m_i\, a_i = m_i\, \frac{dv_i}{dt} = m_i\, \frac{dr_i{}^2}{dt^2}, \quad F_i = -\frac{dU}{dr_i} \qquad (2\text{-}1)$$

Where m_i , r_i, v_i, a_i are the mass, position, velocity and acceleration of atom i in a defined coordinate system, respectively. For this purpose need to be able to calculate the forces F_i acting on the atoms, and these are usually derived from a potential energy $U(r^N)$, where $r^N = (r_1, r_2, \cdots r_N)$ represents the complete set of 3N atomic coordinates[32,33]. So the non-bound potential energy (intra-molecular) and bound potential energy (inter-molecular) discussed.

2-1-1 Non-bonded Potential Energy

The part of the potential energy $U_{non-bonded}$ representing non-bonded interactions between atoms is traditionally split into 1-body, 2-body, 3-body and higher order terms:

$$U_{\text{non-bonded}}(r^N) = \sum_i u(r_i) + \sum_i \sum_{j>i} v(r_i, r_j) + \sum_{i,j,k} v(r_i, r_j, r_k) + \cdots \qquad (2\text{-}2)$$

The first term is the one-body potential $u(r_i)$ represents the effect of an external field on the system. Such as external, magnetic or electric fields or fields which model container walls, it is usually dropped for fully periodic simulations of bulk systems. The second term is the two-body potential describes dependence of the potential energy on the distances between pairs of atoms in the system, it is usual to concentrate on the pair potential $v(r_i, r_j) = v(r_{ij})$. The third term is the three-body potential are sufficient to give the relative positions of three atoms i,j,k in three-dimensional space. Higher order terms are expected to be small compared

9

to the two-body and three-body terms and are consequently neglected [7,33-37,38].

For an isolated system there are no external influences, so the first term of equation (2-2) is zero. The effective pair potential is a function of the pair separation $r_{ij} = \| r_i - r_j \|$ and is constructed in such a way as to include the true pair potential and average effects of higher order terms; it often includes also electrostatic and dipolar effects. The total potential energy of the system is then a sum over all distinct pairs of particles.

$$v_{eff} = \frac{1}{2} \sum_{i,j} v_{eff}(r_{ij})$$ (2-3)

Interactions can be described using different attributes, but from a computational point of view the most important dividing line is between long-range and short-range forces. The prototypical short-range interaction is the ubiquitous Lennard-Jones potential [35,36].

The Lennard-Jones potential is one of the simplest mathematical model that attempts to describe the interaction between a pair of neutral atoms or molecules. It is used for calculating the Van der Waals forces. The most common expression of the Lennard-Jones potential is the one following:

$$U(R) = 4\epsilon \left[\left(\frac{\sigma}{R} \right)^{12} - \left(\frac{\sigma}{R} \right)^{6} \right],$$ (2-4)

In this equation (ϵ) shows the bonding/dislocation energy (minimum of the function to occur for an atomic pair in equilibrium) is well depth, (σ) is the finite distance at which the potential between two particles is zero, and (R) is the distance between the particles. As shown in the Figure (2-1) , this potential is strongly repulsive at shorter distance and after reaching the minimum around (1.122 σ), it has an attractive tail for larger

(r). The parameters (ϵ) and (σ) are chosen to fit the physical properties of the material.

The repulsion between atoms when they are very close to each other is modeled by the term $\sim 1/R^{12}$, this is because of the Pauli principle, thus when electronic clouds surrounding the atoms overlap, the energy of the system increases. The second term represents the attractive part, which is more dominating at a large distance. It is originated by the Van der Waals forces, who are weaker but dominate the character of closed shell systems [39,40].
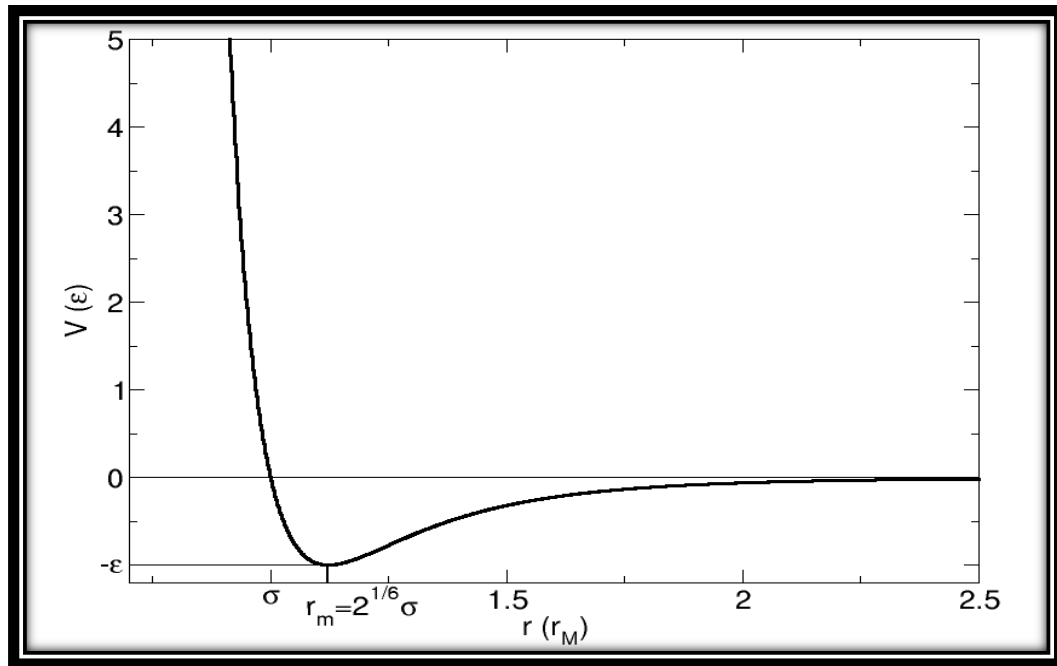
Figure (2-1) Lennard-Jones potential [39]

The Coulomb interaction is an example of a long-range interaction [8,32]. If electrostatic charges are present, we add the appropriate Coulomb potentials

$$V^{coulomb}(r) = \frac{Q_1 Q_2}{4\pi\epsilon_0 r},$$
(2-5)

where Q_1, Q_2 are the charges and ϵ_0 is the permittivity of free space [33,7,37].

2-1-2 Bonding Potentials

For molecular systems, simply build the molecules of site-site potentials of the form of equation (2-4) or similar. Typically, a single-molecule quantum-mechanics calculation may be used to estimate the electron density throughout the molecule, which may then be modelled by a distribution of partial charges by equation (2-5), or more accurately by a distribution of electrostatic multipoles . In Figure (2-2) For molecules must also consider the intramolecular bonding interactions. The simplest molecular model will include terms in the following equation [33,7,27,41]:
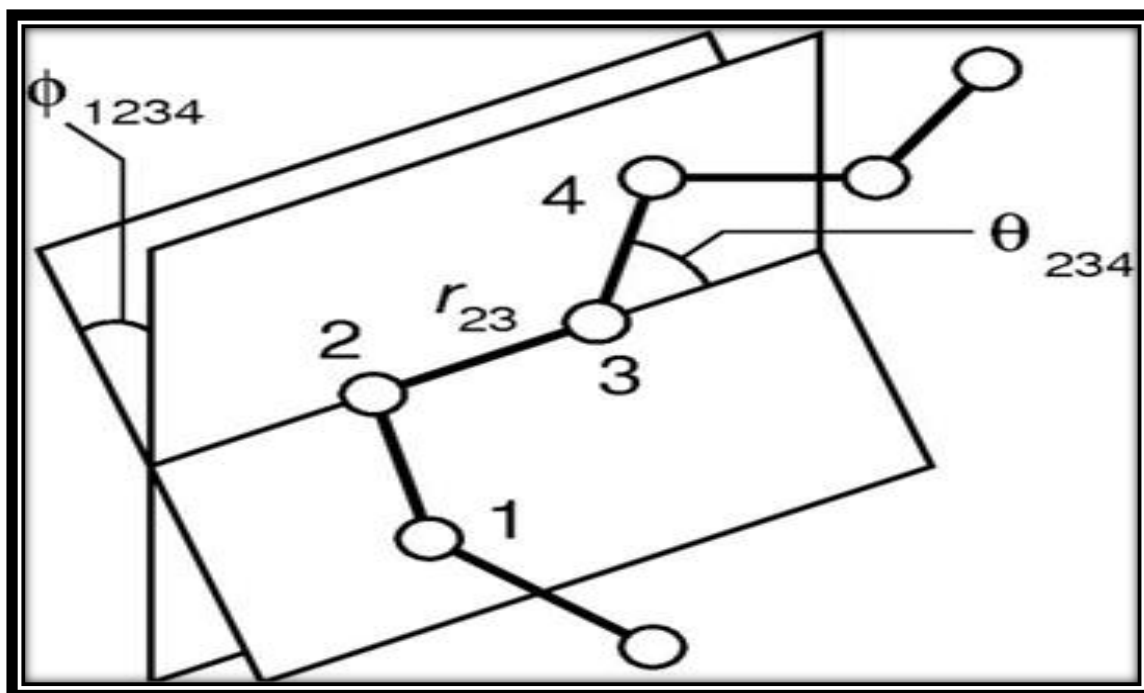
Figure (2-2). Geometry of a simple chain molecule, illustrating the definition of interatomic distance r_{23}, bend angle θ_{234}, and torsion angle $\emptyset_{1234}$**[7].**

$$U_{intramolecular} = \frac{1}{2} \sum_{bonds} K_{ij}^{r} \left(r_{ij} - r_0\right)^2$$

$$+\frac{1}{2} \sum_{\substack{torsion \\ angles}} \sum_{m} K_{ijkl}^{\emptyset,m} \left(1+\cos\left(m\emptyset_{ijkl}-\gamma_m\right)\right)$$

$$+\frac{1}{2} \sum_{\substack{bond \\ angles}} K_{ijk}^{\theta}(\theta_{ijk} - \theta_0)^2 \qquad\qquad (2-6)$$

There are three types of interaction between bonded atoms according to above equation (2-6).

2-1-2-1 The Bond Length

The bond length will typically involve the separation $r_{ij} = |r_i - r_j|$ between adjacent pairs of atoms in a molecular framework [7, 33,37] . Potential energy as a function of bond length, r, rises sharply at very short bond distances, reaches a minimum at an optimal or reference bond length (r_0) and then rises gradually as the bond length increases away from the reference bond length.

In the region around (r_0) the bond length potential behaves as a harmonic potential and can thus be described by Hooke's Law in which the potential energy varies as the square of the deviation of bond length from its reference value Figure (2-3). The harmonic potential has the functional form.

$$U = \frac{1}{2} K_b (r - r_0)^2 \tag{2-7}$$

where (r) is the bond length and (r_0)is the reference bond length. The parameter (r_0) is often referred to as the equilibrium bond length, and (k_b) parameter controls the stiffness of the bond spring [30]. Unique (k_b) and (r_0) parameters are assigned to each pair of bonded atoms based on their types (e.g. C-C, C-H, O-C, etc.). Where (r) is the distance between two atoms, equation (2-7) estimates the energy associated with vibration about the equilibrium bond length. This is the equation of a parabola Figure (2-3), as shown in the right side of Figure (2-3) [25,43].
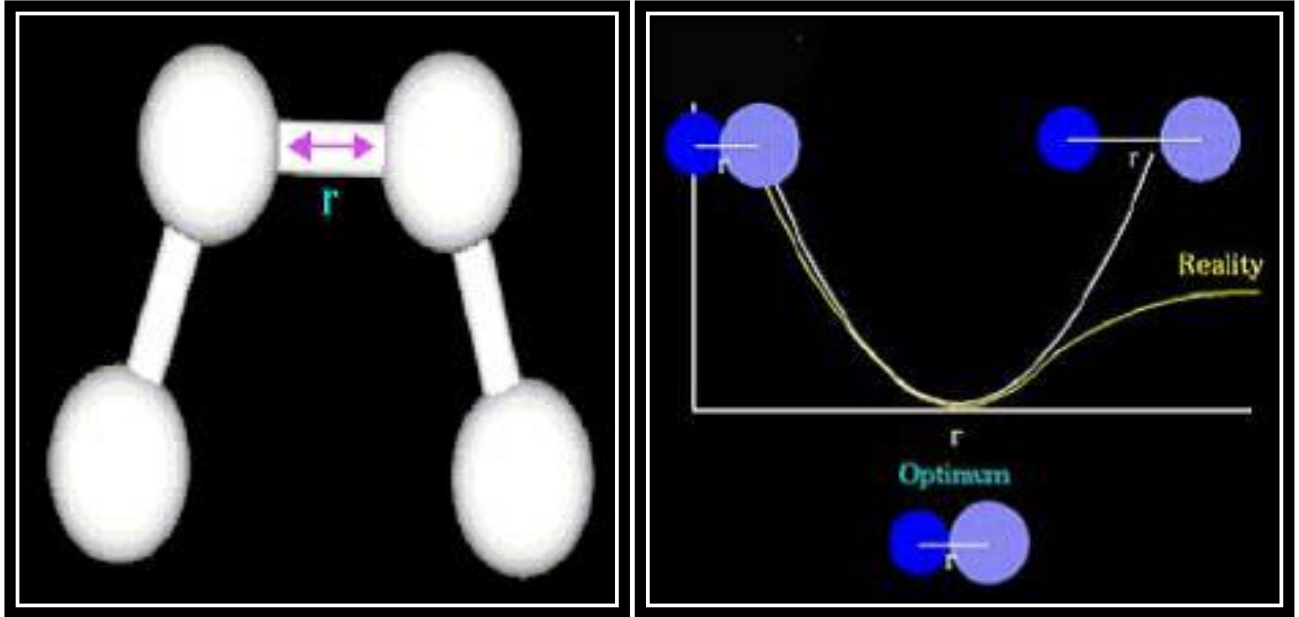
Figure (2-3) The bond length [43].

2-1-2-2 The Bond Angles

The bond angles θ_{ijk} are between successive bond vectors such as :

$r_i - r_j$ and $r_j - r_k$, and therefore involve three atom coordinates:

$$\cos \theta_{ijk} = \hat{r}_{ij} \cdot \hat{r}_{jk} = \left(r_{ij} \cdot r_{ij}\right)^{-1/2} \left(r_{jk} \cdot r_{jk}\right)^{-1/2} \left(r_{ij} \cdot r_{jk}\right) \qquad (2\text{-}8)$$

where $\hat{r} = \frac{\vec{r}}{r}$. Usually this bending term is taken to be quadratic in the angular displacement from the equilibrium value [33,7,37].

The potential energy associated with variation in bond angles(θ), from their reference values (θ_0) , is also frequently described by a harmonic potential. The functional form of angle bending harmonic potential is

$$U = \frac{1}{2} K_\theta (\theta - \theta_0)^2 \qquad (2\text{-}9)$$

The description of the energetic contribution of bond angle deformation requires two parameters: a force constant (k_θ) and a reference angle (θ_0) [42].

15

The bending energy equation is also based on Hook's law. The (k_θ) parameter controls the stiffness of the angle spring, while the (θ) defines it equilibrium angle. This equation estimates the energy associated with vibration about the equilibrium bond angle .Unique parameters for angle bending are assigned to each bonded triplet of atoms based on their types. (e.g. C-C-C, C-O-C, etc.), as shown in the Figure (2-4) [25,43].
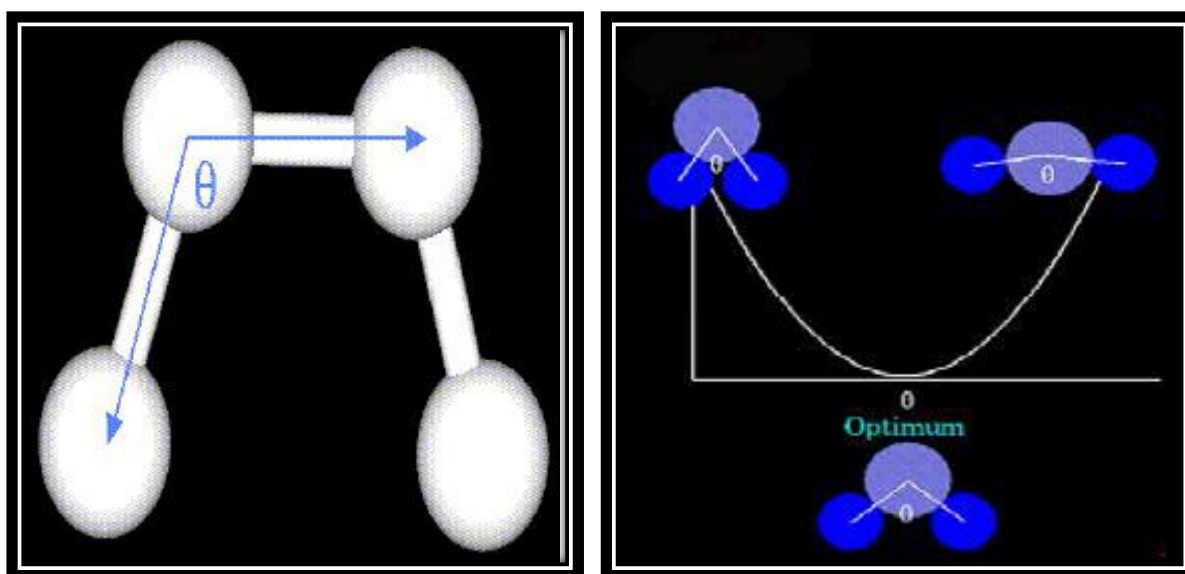
Figure (2-4) The bond angles [43].

2-1-2-3 The Torsion Angles

The torsion angles $\emptyset_{ijkl}$ are defined in terms of three connected bonds as shown in Figure (2- 5), hence four atomic coordinates:

$$\cos\emptyset_{ijkl} = -\hat{n}_{ijk}.\hat{n}_{jkl} \text{ , where } n_{ijk} = r_{ij} \times r_{jk} \text{ , } n_{jkl} = r_{jk} \times r_{kl} \quad (2\text{-}10)$$

and $\hat{n} = \frac{n}{n}$, the unit normal to the plane defined by each pair of bonds [33,7,37].

Intramolecular rotations (rotations about torsion or dihedral angles) require energy (equation (2-11) and Figure (2-5)). Torsional energies are usually important only for single bonds because double and triple bonds are too rigid to permit rotation.

$$U = \frac{1}{2} K_\emptyset \left(1 + \cos(m\emptyset_{ijkl} - \gamma_m)\right) \quad (2\text{-}11)$$

The $(k_\emptyset)$ parameter controls the amplitude of the Figure (2-5-2), the (n) parameter controls its periodicity, and (γ_m) is the offset or phase shift , $(\emptyset)$ is torsion angle value. The parameters are determined from Figure (2-5-2) fitting. Unique parameters for torsional rotation are assigned to each bonded quartet of atoms based on their types (e.g. C-C-C-C, C-O-C-N, H-C-C-H, etc.) [25, 43].

| -1- | -2- |
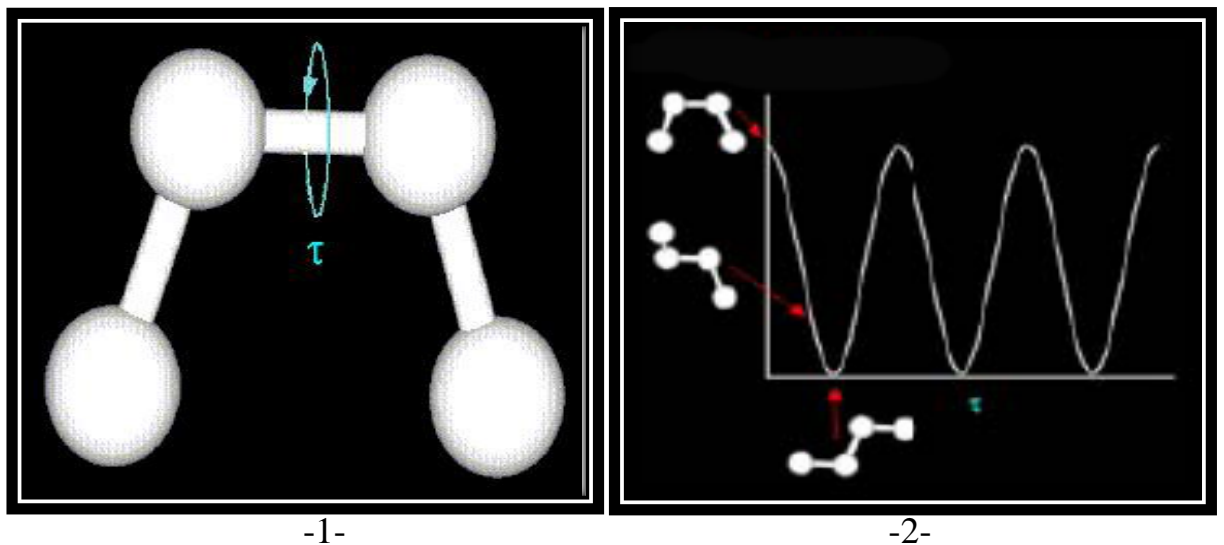
Figure (2-5) The torsion angles [43].

2-2 The Molecular Dynamics (MD) Algorithm

The molecular dynamics algorithm have been known to Newton equations [7,31], a system composed of atoms with coordinates $r^N = (r_1, r_2, \dots r_N)$ and potential energy $U(r^N)$, introduce the atomic momenta $p^N = (p_1, p_2, \dots p_N)$,in terms of which the kinetic energy may be written $K(p^N) = \sum_{i=1}^{N} |p_i|^2 / 2m_i$, then the energy (or the Hamiltonian) written as a sum of kinetic and potential terms H = K + U. Write the classical equations of motion as

$$\dot{r}_i = p_i/m_i \quad \text{and} \quad \dot{p}_i = f_i \tag{2-12}$$

This is a system of coupled ordinary differential equations. Many methods exist to perform step-by-step numerical integration of them. Characteristics of these equations are: (a) they may be short and long timescales, and the algorithm must cope with both; (b) calculating the forces is expensive, typically involving a sum over pairs of atoms [7, 33,41].

The potential energy is a function of the atomic positions (3N) of all the atoms in the system. Due to the complicated nature of this function, there is no analytical solution to the equations of motion; they must be solved numerically. Numerous numerical algorithms have been developed for integrating the equations of motion.

All the integration algorithms assume the positions, velocities and accelerations can be approximated by a Taylor series expansion:

$$y(t_{i+1}) = y(t_i) + h\,\dot{y}(t_i) + \frac{h^2}{2}\ddot{y}(t_i) + \cdots + \frac{h^n}{n}y^{(n)}$$

$$+ \frac{h^{n+1}}{(n+1)}y^{(n+1)}(t_i) \tag{2-13}$$

$$r(t + \delta t) = r(t) + v(t)\,\delta t + \frac{1}{2}a(t)\delta t^2 + \cdots \tag{2-14}$$

$$v(t + \delta t) = v(t) + a(t)\delta t + \frac{1}{2}b(t)\delta t^2 + \cdots \tag{2-15}$$

$$a(t + \delta t) = a(t) + b(t)\delta t + \cdots \tag{2-16}$$

Where (r) is the position,(v) is the velocity (the first derivative with respect to time), (a) is the acceleration (the second derivative with respect to time).

2-2-1 The Verlet Algorithm

Verlet algorithm is derived as follows:

$$r_j(t_0 + \Delta t) = r_j(t_0) + v_j(t_0)\,\Delta t + \tfrac{1}{2}a_j(t_0)(\Delta t)^2 + \cdots \qquad (2-17)$$

$$r_j(t_0 - \Delta t) = r_j(t_0) - v_j(t_0)\,\Delta t + \tfrac{1}{2}a_j(t_0)(\Delta t)^2 + \cdots \qquad (2-18)$$

Summing these two equations, we obtain

$$r_j(t_0 + \Delta t) + r_j(t_0 - \Delta t) = 2r_j(t_0) + a_j(t_0)(\Delta t)^2 \qquad (2-19)$$

$$r_j(t_0 + \Delta t) = 2r_j(t_0) - r_j(t_0 - \Delta t) + a_j(t_0)(\Delta t)^2 \qquad (2-20)$$

The Verlet algorithm uses positions and accelerations at time t and the positions from time (t-dt) to calculate new positions at time (t+dt) [39,42,43, 45]. Important features of the Verlet algorithm are:

1- It is exactly time reversible.

2- It is symplectic.

3- It is low order in time thus permitting long timesteps.

4- It requires just one force evaluation per timestep.

5- It is easy to implement [33,7].

2-2-2 Common Neighbor Analysis Approach

Common neighbor analysis (CNA), first proposed by Honeycutt and Anderson [49], is based on the analysis of common neighbors of a pair of atoms. They introduce three properties to describe an atom pair:

1- whether they are near-neighbors.

2- the number of near neighbors they have in common.

3- the structure of these common neighbors.

According to the dislocation about common neighbor analysis (CNA) in one parametrization using four indexes to describe the local structure of an atom pair. In Fig. (2-6), for the pair formed by atom i and j with blue atoms k being the common neighbors, the following indicators

i- indicates if i,j are nearest neighbors (1 = yes, 2 = no).

ii- indicates the number of common neighbors (number of k atoms).

iii- indicates the number of bonds among common neighbor atoms.

iv- indicates the bonding configuration if first three indexes are the same.

For example as (Figure 2-6), every face centered cubic (fcc) atom has 12 pairs with index 1421 as picture (a), hexagonal close packing(hcp) atom has 6 pairs with index 1421 and 6 pairs with index 1422 as picture b as in Figure (2-6).

For above approach, atoms can be classified into have a local face centered cubic (fcc), or body centered cubic (bcc), or hexagonal close packing (hcp), or icosahedron configuration. If one atom does not belong to any type above, the common neighbor analysis will return the value disordered, which in most cases represents dislocation core or crack surface. In LAMMPS, common neighbor analysis(CNA) has been implemented by using command "compute cna/atom", the output returns a per atom value array [46].
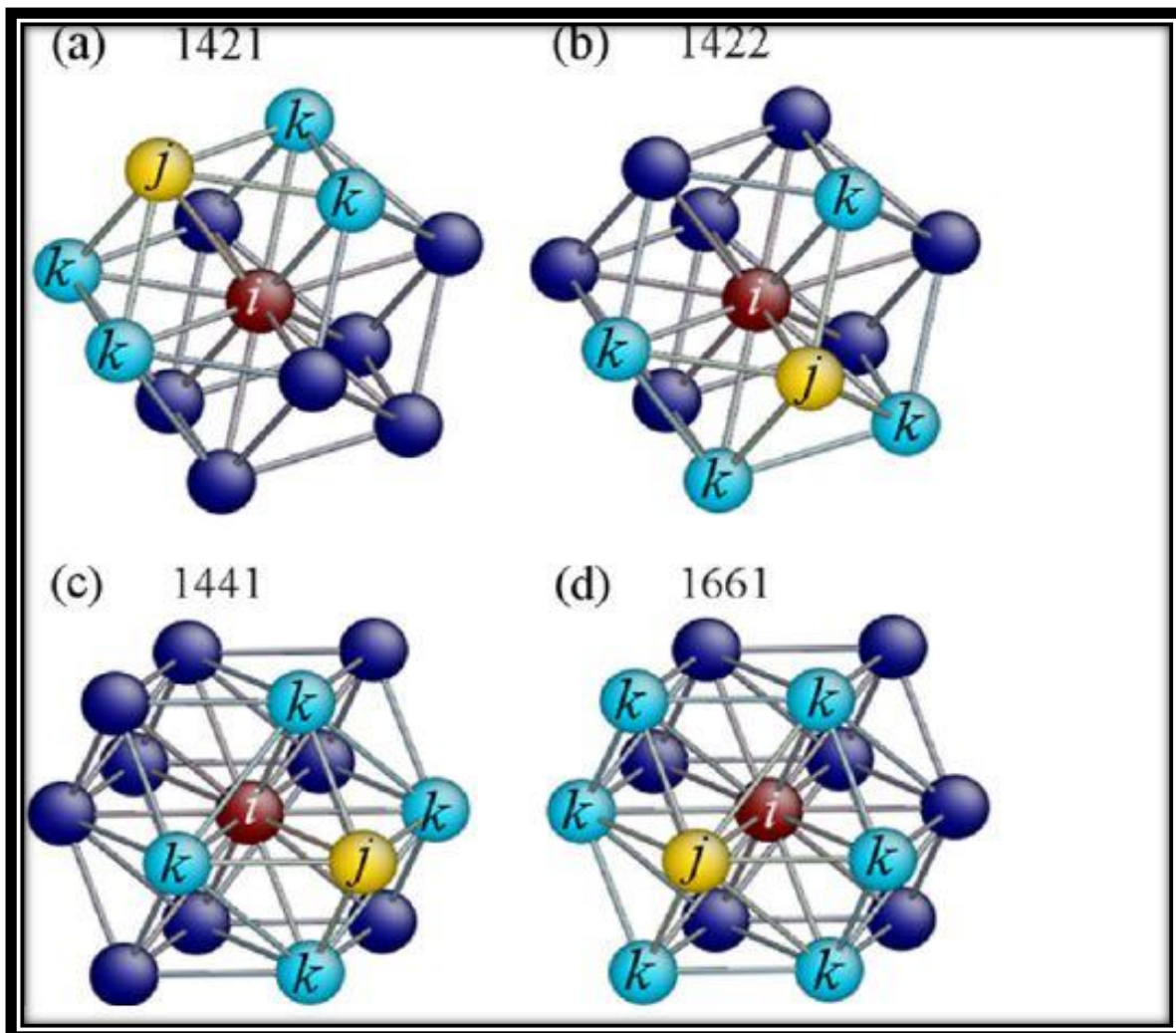
Figure (2-6): Illustration of several common neighbor atoms structure in different lattice type [46].

2-2-3 Schematic of the Molecular Dynamics (MD) Algorithm

START

Initialize Positions $\vec{r}_i(t_0)$ and Velocities with Gaussian distribution $\vec{v}_i(t_0)$

Calculate forces for all molecules using Potential

$$\vec{F}_i = -\vec{\nabla}_n U\left(\vec{r}_1, \vec{r}_2, \vec{r}_3, \cdots, \vec{r}_N\right)$$

Apply Thermostat and Volume Changes

Solve equation of the motion for all particles in the system at a short enough timestep Δt. With $\vec{r}_i(t_n) \rightarrow \vec{r}_i(t_{n-1})$, $\vec{v}_i(t_n) \rightarrow \vec{v}_i(t_{n-1})$ and $t_{n-1} = t_n + \Delta t$ then Update Position and Velocities

Calculate desired physical quantities and write data to trajectory file

No

Is $t_n > t_{max}$?

Yes

Finish

Figure (2-7) Schematic diagram of the basic MD simulation code [32]

2-3 Molecular Dynamics in Different Ensembles

Molecular dynamics allows use to explore the constant-energy surface of a system. under conditions the total energy of the system is conserved and hence different forms (i.e. ensembles) of molecular dynamics are required. An ensemble is a collection of all possible systems which have different microscopic states but have an identical macroscopic or thermodynamic state. Depending on which state variables (for example, the energy (E), volume (V), temperature (T), pressure (P), and number of particles (N)) are kept fixed, different statistical ensembles can be generated. A variety of structural, energetic, and dynamic properties can then be calculated from the averages or the fluctuations of these quantities over the ensemble generated. There exist different ensembles with different characteristics [47].

2-3-1 Micro-Canonical or NVE Ensemble

This ensemble is characterized by a fixed number of atoms (N), a fixed volume (V), and a fixed energy (E), is obtained by solving Newton's standard equation of motion without any temperature and pressure control. Energy is conserved when this ensemble is generated. However, because of rounding and truncation errors during the integration process, there is always a slight drift in energy. It is interested in exploring the constant-energy surface of the conformational space. The results can be used to calculate the thermodynamic response function

2-3-2 Canonical or NVT Ensemble

This ensemble is characterized by a fixed number of atoms (N), a fixed volume (V), and a fixed temperature (T). It is also sometimes called constant temperature molecular dynamics (CTMD). In NVT, the energy of endothermic and exothermic processes is exchanged with a thermostat. A variety of thermostat methods is available to add and remove energy from the boundaries of an MD system in a more or less realistic way, approximating the canonical ensemble.

2-3-3 Isothermal–Isobaric or NPT Ensemble

This ensemble is characterized by a fixed number of atoms (N), a fixed pressure (P), and a fixed temperature (T). In addition to a thermostat, a barostat is needed to control the pressure to approximate real situation[42,47].
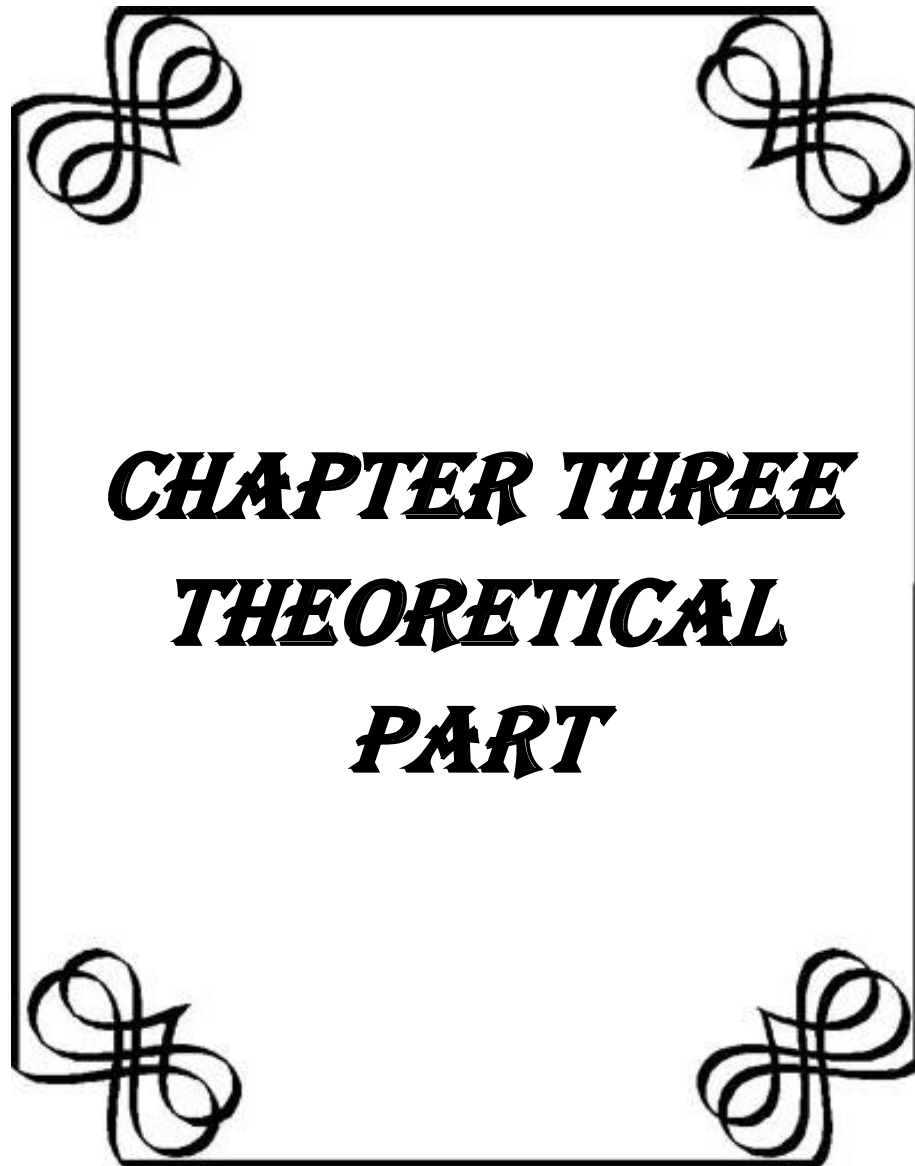
CHAPTER THREE
THEORETICAL PART

3-1 Quantum Many-Body Problem

In quantum mechanics the operator for the total energy is the Hamiltonian. For a system of electrons and nuclei it can be written as

$$\widehat{H} = \widehat{H}_{NN} + \widehat{H}_{ee} + \widehat{H}_{Ne} \qquad (3\text{-}1)$$

There are three contributions with the indices (N) for nuclei and e for electrons. The first term in (2-1) represents the kinetic energy and the interaction of the nucleus:

$$\widehat{H}_{NN} = -\sum_{\alpha} \frac{\hbar^2}{2M_\alpha} \nabla_\alpha^2 + \frac{1}{2} \sum_{\substack{\alpha,\beta \\ \alpha \neq \beta}} \frac{Z_\alpha Z_\beta e^2}{|R_\alpha - R_\beta|} \qquad (3-2)$$

Where $(\hbar = \frac{h}{2\pi})$, (h) is Plank constant , (M_α) is a mass of nuclei , (Z_α, Z_β) is the charges of the nucleus, (e) is the charge of the electron, (R_α, R_β) is radius of nucleus.

Upper case and greet subscript letters are used to indicate nuclei, lower case and latin subscripts for electrons. The second term, $(\widehat{H}_{ee})$, is equivalent to the first one, except it describes electrons.

$$\widehat{H}_{ee} = -\sum_{i} \frac{\hbar^2}{2m} \nabla_i^2 + \frac{1}{2} \sum_{\substack{i,j \\ i \neq j}} \frac{e^2}{|r_i - r_j|} \qquad (3-3)$$

Where (m) is mass of electron, (r_i, r_j) is radius of electrons.

The third term represents the interaction between the electrons and the nuclei:

$$\widehat{H}_{Ne} = -\sum_{\alpha} \sum_{i} \frac{Z_\alpha e^2}{|r_i - R_\alpha|} \qquad (3-4)$$

The ground state of a non-relativistic quantum system can be calculated with the time-independent Schrödinger equation [48],

$$\widehat{H}\psi(r_i, R_\alpha) = E\psi(r_i, R_\alpha) \qquad (3-5)$$

where the many-body wavefunction

$$\psi(r_i, R_\alpha) \equiv \psi(r_1, \dots, r_n, R_1, \dots, R_N) \tag{3-6}$$

depends on the coordinates of the (n) electrons and the (N) nuclei [48-53]. The time evolution of the eigenstates of Eq. (3-5) is then given by $(\psi e^{-i(E/\hbar)t})$.

Solving the Schrödinger equation for the Hamiltonian given in Eq. (2-1) is not possible, even for small systems containing only a few atoms the complexity of this problem is far beyond the capabilities of any currently available computer. For a single oxygen atom with eight electrons the amount of data is already incredibly large. Assuming (10) bytes are required to store a single value of the many-body wavefunction at a discrete point in space, the storage capacity needed for the entire function can be calculated. For a 10×10×10 grid about 10^{24} bytes are needed, which could be stored on a trillion (1 TB) hard drives.

The quantum many-body problem is thus only solvable within some approximations [48].

3-1-1 The Born-Oppenheimer Approximation

The Born-Oppenheimer is a very fundamental part of most theoretical approaches to the quantum many-body problem. It makes use of the fact, that the mass of the electrons is much smaller than the mass of the nuclei. Therefore the term for the kinetic energy of the nucleus is "small" when compared to the electron. The Born-Oppenheimer approximation can be thought of in different ways:

1- The nuclei are decoupled from the electrons.

2- The electrons follow the motion of the nuclei a diabatically.

3- There is no exchange of energy between nuclei and electrons [48].

As a consequence the first term in Eq. (3-2) can be neglected and the nuclei are considered as frozen at the positions $\{R_\alpha\}$. The Schrödinger equation (3-5) can then be written as

$$\left[\widehat{H}_{ee} + \widehat{H}_{Ne} + \frac{1}{2}\sum_{\alpha,\beta}\frac{Z_\alpha Z_\beta e^2}{|R_\alpha - R_\beta|}\right]\emptyset = \epsilon\emptyset \qquad (3-7)$$

The wave function ($\emptyset$) and the energy (ϵ) depend on the positions of the nuclei only as parameters

$$\emptyset = \emptyset(r_i, \{R_\alpha\}) \qquad and \qquad \epsilon = \epsilon(\{R_\alpha\}) \qquad (3-8)$$

The $\epsilon(\{R_\alpha\})$ can be identified as a potential energy of the nuclei [48]. Rephrasing Eq. (3-5) yields

$$\left[-\sum_\alpha\frac{\hbar^2}{2M_\alpha}\nabla_\alpha^2 + \epsilon(\{R_\alpha\})\right]\varphi = E^*\varphi \qquad (3-9)$$

Where $\varphi = \varphi(R_\alpha)$ is the wave function of the nuclei. The energy (E^*) is the total energy (E) from Eq. (3-5). Using this approach, the wavefunction (ψ) can be separated into a part for the nuclei and a part for the electrons:

$$\psi(r_i, R_\alpha) = \emptyset(r_i, \{R_\alpha\}) \cdot \varphi(R_\alpha) \qquad (3-10)$$

Ignoring the nuclear kinetic energy, the Hamiltonian for the electrons can then be written as

$$\widehat{H} = \widehat{T} + \widehat{V}_{ext} + \widehat{V}_{int} + E_{II} \qquad (3-11)$$

The operator for the kinetic energy of the electrons is

$$\widehat{T} = -\sum_i\frac{\hbar^2}{2m}\nabla_i^2 \qquad (3-12)$$

$\widehat{V}_{ext}$ is the potential acting on the electrons due to the nuclei,

$$\widehat{V}_{ext} = \sum_{i,\alpha}V_\alpha(|r_i - R_\alpha|) \qquad (3-13)$$

and $\hat{V}_{int}$ is the electron-electron interaction,

$$\hat{V}_{int} = \frac{1}{2} \sum_{i \neq j} \frac{e^2}{|r_i - r_j|} \tag{3 – 14}$$

The final term E_{II} in Eq. (3-11) is the interaction of the nuclei with each other and also includes terms that contribute to the total energy of the system. The effect of the nuclei upon the electrons is put into an effective external potential for the electrons, $(\hat{V}_{ext})$ [48,49,50,52].

3-1-2 The Variational Principle

The expectation value of an operator $(\hat{O})$ for an eigenstate is given by the time independent expression

$$\langle \hat{O} \rangle = \frac{\langle \Psi | \hat{O} | \Psi \rangle}{\langle \Psi | \Psi \rangle} \tag{3 – 15}$$

which involves an integral over all coordinates. For the total energy, which is represented by the Hamiltonian from equation (3-11), this yields

$$E = \frac{\langle \Psi | \hat{H} | \Psi \rangle}{\langle \Psi | \Psi \rangle} \equiv \langle \hat{H} \rangle = \langle \hat{T} \rangle + \langle \hat{V}_{int} \rangle + \int dr \, V_{ext}(r) n(r) + E_{II} \tag{3 – 16}$$

The expectation value of the external potential has been explicitly written as an integral over the particle density n(r), defined as

$$n(r) = \frac{\langle \Psi | \hat{n}(r) | \Psi \rangle}{\langle \Psi | \Psi \rangle}, \qquad where \qquad \hat{n}(r) = \sum_i \delta(r - r_i) \tag{3 – 17}$$

The nucleus-nucleus term E_{II} is important for total energy calculations, for the electronic structure, i.e. the wavefunctions, it is only a classical additive term [48].

The basic task of ab initio simulation programs is finding the eigenstates of the many-body Hamiltonian. These eigenstates are stationary points of the energy expression Eq. (3-16). Using the variational principle this can be expressed as:

$$\delta\left[\langle\Psi|\hat{H}|\Psi\rangle - E(\langle\Psi|\Psi\rangle - 1)\right] = 0 \qquad\qquad (3-18)$$

where the orthonormality of the wavefunction ($\langle\Psi|\Psi\rangle = 1$) is ensured with a Lagrange multiplier. This is equivalent to the Rayleigh-Ritz variation method.

The ground state wave function (Ψ_0) can thus be obtained by minimizing the total energy with respect to all parameters in $\Psi\{r_i\}$ [48,52,54].

3-2 Density Functional Theory [55]

Density functional theory (DFT) is the most methods for calculations (structure of atoms, molecules, crystals, surfaces and their interactions). And also it is a ground-state theory in which the emphasis is on the charge density as the relevant physical quantity. Density functional theory (DFT) has been highly describing structural of most of materials and electronic properties in a vast class of materials ranging from atoms and molecules to simple crystals to complex extended systems (including glasses and liquids). Furthermore density functional theory (DFT) is computationally very simple. For these reasons density functional theory (DFT) has become a common tool in first-principle calculations aimed at describing or even predicting properties of molecular and condensed matter systems.

3-2-1 Hohenberg and Kohn (H-K) Theorems

Formulation of density functional theory as an exact theory of a many-body system. This formalism can be applied to any system of interacting particles in an external potential $V_{ext}(r)$, especially to electrons and fixed nuclei, where the Hamiltonian can be written as

$$\hat{H} = -\frac{\hbar^2}{2m_e}\sum_i \nabla_i^2 + \sum_i V_{ext}(r_i) + \frac{1}{2}\sum_{i\neq j}\frac{e^2}{|r_i - r_j|} \qquad (3-19)$$

The basis are the following two theorems , which can be proven very easily [48] :

Theorem I: For any system of interacting particles in an external potential $V_{ext}(r)$, the potential $V_{ext}(r)$ is determined uniquely, except for a constant, by the ground state particle density $n_0(r)$.

As a conclusion of this theorem, the Hamiltonian is fully determined, except for a constant shift of the energy. Thus the many-body wavefunction is also fully determined for all ground and excited states. This means that all properties of the system are completely determined simply be the ground state density $n_0(r)$.

Theorem II: A universal functional for the energy E[n] in terms of the density n(r) can be defined, valid for any external potential $V_{ext}(r)$. For any particular $V_{ext}(r)$, the exact ground state energy is the global minimum value of this functional, and the density n(r) that minimizes the functional is the exact ground state density $n_0(r)$.

This implies, that the functional E[n] is sufficient to determine the exact ground state energy and density. This only holds for ground states, for excited states requires additional information, such as the free-energy functional [54-59] .

The total energy functional for a system of interacting particles is given by

$$E_{HK}[n] = T[n] + E_{int}[n] + \int dr\, V_{ext}(r)n(r) + E_{II} \qquad (3-20)$$

$$\equiv F_{HK}[n] + \int dr\, V_{ext}(r)n(r) + E_{II} \qquad (3-21)$$

which can be derived from Eq. (3-11). The functional $F_{HK}[n]$ includes all internal energies, potential and kinetic, of the interacting electron system,

$$F_{HK}[n] = T[n] + E_{int}[n] \qquad (3-22)$$

The Hohenberg-Kohn theorems however are not enough to perform electron structure calculations. An instruction on how to determine the energy functional E[n] is required, which was given only one year later[48,56,61,62].

3-2-2 Kohn-Sham (K-S) Equation

The Ansatz assumes that the density of the ground state of the original interacting system is equal to that of some chosen non-interacting system [28,29]. This leads to independent-particle equations for the non-interacting system. They can be solved exactly with numerical methods, the complicated many-body terms are incorporated into an exchange-correlation functional of the density. It can be shown that the accuracy of the results for this auxiliary system depends only on the approximation for the exchange-correlation functional [48].

The Kohn-Sham equations are based on the total energy functional of the Hohenberg-Kohn theorem. The ground state energy functional is rewritten in the form

$$E_{KS} = T_S[n] + \int dr\, V_{ext}(r)n(r) + E_{Hartree}[n] + E_{II} + E_{XC}[n] \qquad (3-23)$$

with the independent-particle kinetic energy (T_S) and the classical Coulomb interaction energy of the electron density n(r) with itself,

$$E_{Hartree}[n] = \frac{1}{2}\int dr\, d\acute{r}\, \frac{n(r)n(\acute{r})}{|r - \acute{r}|} \qquad (3-24)$$

known as the Hartree energy.

All many-body effects of exchange and correlation in Eq. (3-23) are grouped into the exchange-correlation energy E_{XC}, it can be written in the form

$$E_{XC}[n] = \langle \hat{T} \rangle - T_S[n] + \langle \hat{V}_{int} \rangle - E_{Hartree}[n] \qquad (3-25)$$

Applying the variational principle leads to the Kohn-Sham Schrödinger-like equations:

$$(H_{KS} - \epsilon_i)\psi_i(r) = 0 \qquad\qquad (3-26)$$

where the (ϵ_i) are the eigenvalues and (H_{KS}) is the effective Hamiltonian

$$H_{KS}(r) = -\frac{\hbar^2}{2m}\nabla^2 + V_{KS}(r) \qquad\qquad (3-27)$$

With

$$V_{KS}(r) = V_{ext}(r) + \frac{\delta E_{Hartree}}{\delta n(r)} + \frac{\delta E_{XC}}{\delta n(r)}$$

$$= V_{ext}(r) + V_{Hartree}(r) + V_{XC}(r) \qquad\qquad (3-28)$$

If the exchange-correlation potential (V_{XC}) were known, these equations would lead to the exact ground state density and energy for the interacting system. The advantage of this approach is that the remaining functional $E_{XC}[n]$ can be expressed as a local or nearly local functional of the density [48]. The long range Hartree terms and the independent particle kinetic energies are separated out. This means that the energy E_{XC} can be expressed in the form

$$E_{XC}[n] = \int dr\, n(r)\epsilon_{XC}([n], r) \qquad\qquad (3-29)$$

where $\epsilon_{XC}([n], r)$ is an energy per electron at point (r) that depends only upon the density n(r) in some neighborhood of point (r) [48,62-64].

3-2-3 Functionals for Exchange and Correlation

The crucial quantity in the Kohn-Sham approach is the exchange-correlation energy, expressed as a functional of the density $E_{XC}[n]$. There are different approaches on how to choose an appropriate functional, the two most popular being the local density approximation (LDA) and the generalized-gradient approximation (GGA) [62].

3-2-3-1 The Local Density Approximation (LDA)

The idea for the local density approximation (LDA) is very simple. It was already presented by Kohn and Sham in their original publication.

Solids are often well described as a homogeneous electron gas. The exchange-correlation energy is then simply an integral over all space where the exchange-correlation energy density at each point is the same as in a homogeneous electron gas with that density [48,65]

$$E_{XC}^{LDA}[n] = \int dr\, n(r)\epsilon_{XC}^{hom}(n(r)) \qquad (3-30)$$

Despite of this approximation the local density approximation (LDA) yields reasonable results for a wide range of solids. It is implemented in most modern computer codes and has lead to improved functionals, like generalized-gradient approximation (GGA) [48].

3-2-3-2 The Generalized Gradient Approximation (GGA)

A natural approach to improve the results of the local density approximation (LDA) for inhomogeneous densities is the incorporation of the gradient. The "gradient expansion approximation" (GEA) was already proposed by Kohn and Sham in the original paper and realized by Herman et al. in 1969. The form

$$E_{XC}[n] = \int dr\, n(r)f_{XC}(n(r), \nabla n(r), \nabla^2 n(r)) \qquad (3-31)$$

however has some drawbacks. The first order derivatives often worsen the result, while second order terms may have divergences. The basic problem is that gradients in real materials are so large that the expansion breaks down [48].

To deal with these problems the generalized-gradient approximation (GGA) was developed. It splits the exchange-correlation energy density

(ϵ_{XC}) into the local exchange energy of the homogeneous gas and a dimensionless gradient-dependent part (F_{XC}),

$$E_{XC}^{GGA}[n] = \int dr\, n(r)\epsilon_{XC}(n(r), \nabla n(r), \dots)$$

$$= \int dr\, n(r)\epsilon_{XC}^{hom}(n)F_{XC}(n(r), \nabla n(r), \dots) \qquad (3-32)$$

The functional form of the F_{XC} term is rather complicated. It is usually written as an expansion, for which the coefficients have to be determined from training data or from mathematical constraints [48,66].

3-2-4 Pseudopotentials

One of the most expensive parts of electronic structure calculations is the treatment of the core electrons. These tightly bound electrons have a strongly localized wavefunction, which can vary on short distances. For numerical calculations that is very unfavorable. To reduce the efforts needed for the core electrons the concept of pseudopotentials was established. The idea is to replace the strong Coulomb potential of the nucleus and the effects of the tightly bound core electrons by an effective ionic potential that acts on the valence electrons[48,67].

3-2-4-1 Frozen Core Approximation

The motivation for the introduction of pseudopotentials is the frozen core approximation. It assumes that the core electrons do not participate in chemical bonding or other electronic properties. Only the valence electrons have an overlap with electrons from other atoms. The inner shells can thus be treated as frozen and their wavefunctions be calculated independently from the many-body system. This can be done either by replacing the inner shells with an effective potential, like for most pseudopotential methods, or by using pseudopotential operators but

retaining the full core wavefunctions, like in the projector augmented wave (PAW) approach [48].

3-2-4-2 Formal Justification for Pseudopotentials

A short proof for the justification of pseudopotentials, which also gives some insight into their construction, shall be given here. It uses the ansatz

$$\Psi\rangle = \emptyset\rangle + \sum_n c_n X_n\rangle \qquad (3-33)$$

where $\Psi\rangle$ is the true wavefunction, $\emptyset\rangle$ the pseudo wavefunction and $X_n\rangle$ are the core wavefunctions. The core and the true wavefunctions need to be orthogonal, from which one can deduce

$$0 = \langle X_n|\Psi\rangle = \langle X_n|\emptyset\rangle + c_n \quad \rightarrow \quad c_n = -\langle X_n|\emptyset\rangle \qquad (3-34)$$

$$and \ \Psi\rangle = \psi\rangle - \sum_n \langle X_n|\emptyset\rangle|X_n\rangle \qquad (3-35)$$

The Schrödinger equation then yields

$$\hat{H}\ \Psi\rangle = \hat{H}\ \emptyset\rangle - \sum_n \hat{H}X_n\rangle \langle X_n|\emptyset\rangle = E\ \Psi\rangle$$

$$= E\ \emptyset\rangle - \sum_n X_n\rangle \langle X_n|\emptyset\rangle \qquad (3-36)$$

$$where \ \ \hat{H}\ X_n\rangle = E_n\ X_n\rangle$$

Rearranging these terms leads to

$$\left\{\hat{H} + \sum_n (E - E_n)\ X_n\rangle\langle X_n\right\}\emptyset\rangle = E\emptyset\rangle \qquad (3-37)$$

where (E) is the exact eigenvalue of the true wave function (Ψ).Solving this equation in a self-consistent way, the pseudo wave function as well as the correct energy values can be obtained [48].

The basic idea of pseudopotentials is illustrated in Figure (3-1). For distances smaller than a certain cutoff radius (r_c) the real potential is

replaced by the pseudopotential Vpseudo. The real wave function, which has several knots in the core region, is then replaced by a pseudo wave function without any knots. For distances greater than (r_c), the all electron wave function and the pseudo wave function are identical.

The important property, which must be conserved by the pseudopotential, is the phase shift $\delta_l(\epsilon)$. The index (l) stands for the angular momentum of the scattered wave function and for its energy. The scattering properties of a localized spherical potential can be formulated in terms of this phase shift. The scattering cross-section and all properties of the wave function outside the localized region are determined by it.

By choosing a potential with more desirable properties, which can reproduce the phase shift up to a modulo of(2πn), the numerical effort can be reduced greatly. This does not change the properties of the wave functions outside of the scattering region, they are invariant for such phase shifts [48].

3-2-4-3 Different Approaches for Pseudopotentials

The first ideas on how to effectively describe electron scattering from electrons were published in the 1930 by Fermi and coworkers. A first application of pseudopotentials to solids was presented by Hellmann in 1935. The orthogonalized plane waves (OPWs) method of Herring was the basis for the pseudopotential research [48].
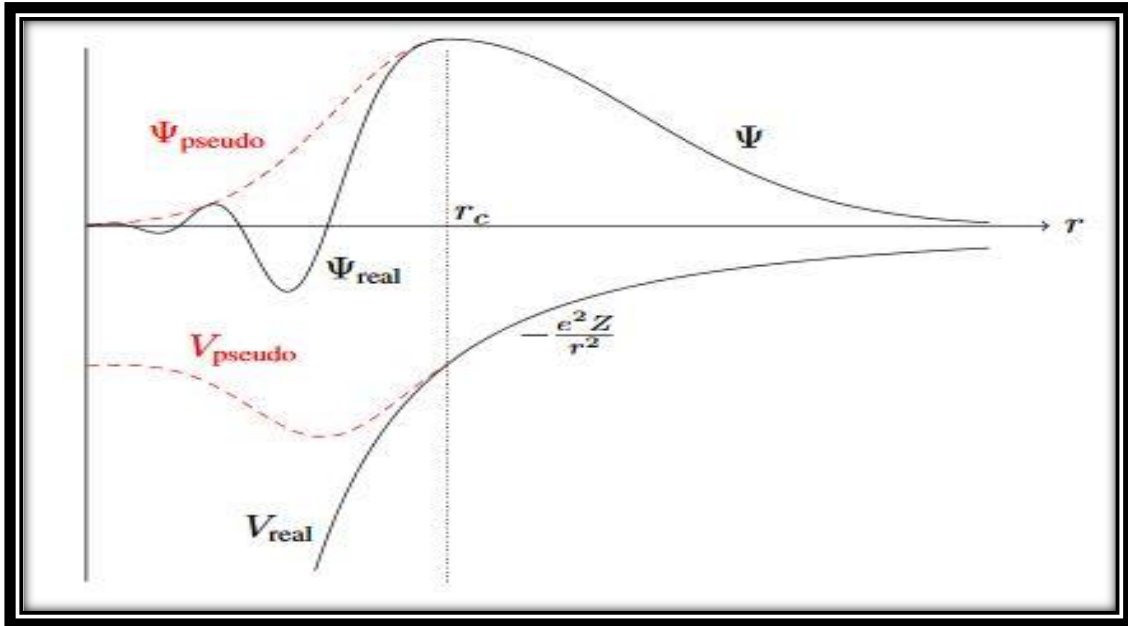
Figure (3-1): Schematic representation of pseudopotentials and the corresponding wavefunctions [48].

in the 1950s. It yielded accurate descriptions which led to the basic understanding of many properties of sp-bonded metals and semiconductors. In modern computer codes usually there are several different approaches to pseudopotentials available. They are briefly discussed in the next paragraphs [48].

3-2-4-3-1 Norm-Conserving Pseudopotentials (NC-PP)

There are the basis for most modern pseudopotential calculations. In 1979 Hamann et al. published a list of requirements for a "good" pseudopotential. It comprises the following points:

1- All-electron and pseudo valence eigenvalues agree for the chosen atomic reference configuration.

2- All-electron and pseudo valence wave functions agree beyond a chosen core radius (r_c).

3- The logarithmic derivatives of the all-electron and pseudo wave functions agree at (r_c).

4- The integrated charge inside (r_c) for each wave function agrees (norm conservation).

The points (1) and (2) are already clear from the definition of pseudopotentials. Point (3) follows from the requirement of a smooth potential, the dimensionless logarithmic derivative (D) is defined as

$$D_l(\epsilon, r) \equiv r\dot{\psi}(\epsilon, r)/\psi_l(\epsilon, r) = r\frac{d}{dr}\ln\psi_l(\epsilon, r) \qquad (3-38)$$

where (l) is either the all-electron or pseudo wave function.

Inside of the core radius (r_c)the integrated charge (Q_l) has to be the same for the all-electron (AE) and pseudo (PS) wave function [48],

$$Q_l = \int_0^{r_c} dr\ r^2 |\psi_l^{AE}|^2 = \int_0^{r_c} dr\ r^2 |\psi_l^{PS}|^2 \qquad (3-39)$$

This conservation ensures that the total charge in the core region is correct and that the normalized pseudo-orbital is equal to the true orbital outside of (r_c). For solids this means, that the pseudo-orbitals are correct between the atoms, in the region where the bonding occurs.

3-2-4-3-2 Ultrasoft Pseudopotentials (US-PP)

There are another approach to reducing the computational efforts. Usually the goal of pseudopotentials is to have a function that is as "smooth" as possible and yet accurate, one reason for this is that smooth functions can be expressed with less Fourier components, which in turn require less computational time. Increasing the "smoothness" of a pseudopotential is equivalent to reducing the size of the Fourier space needed to describe the valence properties with a given accuracy. For

norm-conserving pseudopotentials this accuracy is usually reached by sacrificing some of the "smoothness".

The ultrasoft pseudopotentials maintain the smoothness with a different approach. The wave function is split up into two parts, a smooth function and an auxiliary function that represents the rapidly varying part close to the core. In cases where most of the orbitals are tightly bound in the core region, US-PP can yield a huge speed up compared to norm-conserving pseudopotentials, while keeping the accuracy the same [48].

3-2-4-3-3 Projector Augmented Waves (PAW)

There are a general approach to the solution of the electronic structure problem with the help of modern computational methods. As the ultrasoft pseudopotentials it includes auxiliary localized functions. The full wave function in all space can be written as

$$\Psi\rangle = \widetilde{\Psi}\rangle + \sum_m \langle \tilde{P}_m | \widetilde{\Psi} \rangle \{ \Psi_m \rangle - \widetilde{\Psi}_m \rangle \} \qquad (3-40)$$

where $\Psi\rangle$ and $\widetilde{\Psi}\rangle$ are the all-electron and the smooth wave functions, respectively. Both can be expanded into partial waves m in a sphere, $\Psi\rangle = \sum_m c_m \Psi_m\rangle = \sum_m \langle \tilde{P}_m | \widetilde{\Psi} \rangle \Psi_m\rangle$, which are the solution of the Schrödinger equation for an isolated atom. The projection operators $(\tilde{P})$ are defined by $\langle \tilde{P}_m | \widetilde{\Psi}_{\acute{m}} \rangle = \delta_{m\acute{m}}$.

With the PAW Ansatz the full all-electron wave function is kept for the valence part while the smoothness is also incorporated in the core region. Especially for systems with both localized and delocalized valence states it can be beneficial. The PAW method combines the accuracy of all-electron methods with the efficiency of pseudopotentials. It is available in many simulation packages[48,67].

3-3 Embedded Atom Method (EAM)

A realistic simulation of different Semi-empirical properties of low-symmetric metallic surfaces such as those with defects requires methods that can simulate large numbers of atoms. Semi-empirical potentials are good alternatives to ab-initio methods owing to their lower computational cost. One of the early simple potentials is the two-body Lennard-Jones (LJ) potential, which was successfully used in studying the properties of rare gases. The first Embedded-Atom Method (EAM) potential was proposed by Baskes and Daw [24] in 1984 on the basis of the concept of local density, which is considered as the key variable in inter-atomic potentials. The idea behind the EAM potential model is based on the Quasi-atom . In the Embedded Atom Method (EAM), it is assumed that each atom in the system is embedded in a host consisting of all the other atoms as shown in Figure (3-2). The energy to embed an atom within the host (embedding energy) is described as being dependent on the electron density.

$$E_{tot} = \sum_i F_i\left(\rho_{h,i}\right) + \frac{1}{2}\sum_{\substack{i,j \\ (i \neq j)}} \phi_{ij}(R_{ij}) \qquad \rho_{h,i} = \sum_{j(\neq i)} \rho_j^a(R_{ij})$$

Embedding energy   Two-body term

ρ_i

Electron gas
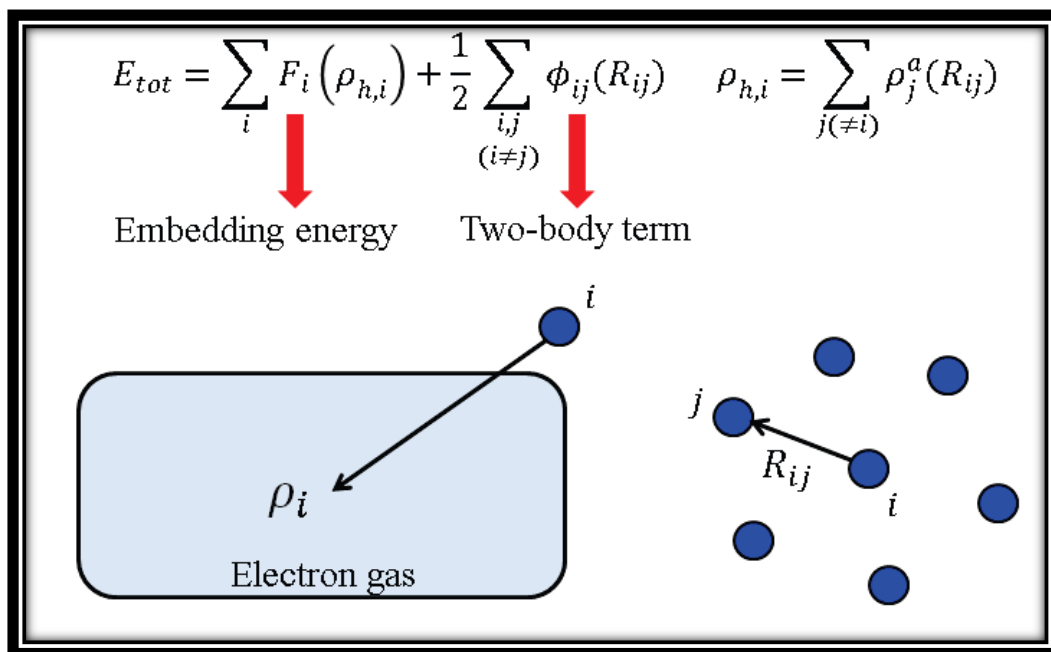
Figure 3-2. Schematic representation of the Embedded Atom Method [66].

In the embedded atom method (EAM), the total energy of the system is written as the addition of the embedding energy and that of the two-body terms, as in Equation (3-41),

$$E_{tot} = \sum_i F_i\left(\rho_{h,i}\right) + \frac{1}{2}\sum_{\substack{i,j \\ i \neq j}} \emptyset_{ij}\left(R_{ij}\right) \qquad (3-41)$$

In the former term of Equation (3-41), $(\rho_{h,i})$ is the sum of the individual atomic densities (ρ_j^a) as given by Equation (3-42),

$$\rho_{h,i} = \sum_{j(\neq i)} \rho_j^a\left(R_{ij}\right) \qquad (3-42)$$

where ρ_j^a is the contribution of the atom(j) of type (a) to the electron charge density at the location of the atom (I), and (F_i) is an embedding functional that represents the energy required to place atom(i) into the electron cloud when (R_{ij}) is the distance between atoms (i) and(j). Therefore, the total energy of the system is a function of the atomic positions.

In the latter term of Equation (3-41),(ϕ_{ij}) is the short-range pair potential, where (Z) is the atomic number of the atoms.

$$\emptyset_{ij}(r) = \frac{Z_i(r)Z_j(r)}{r} \qquad (3-43)$$

The total energy of the system given in Equation (3-41) has an attractive and a repulsive part. The attractive part (first term) describes the embedding of a positively charged core in to the electron density formed by the surrounding atoms, while the repulsive part (second term) describes the interactions between the ion cores [66].

To derive an approximate expression for the cohesive energy of a metallic system that is an explicit function of the positions of the atoms and which is simple to evaluate (i.e. equation (3-41)). This derivation has been discussed in detail by Daw , and only summarize it here [24].

Start with the density-functional expression for the cohesive energy of a solid is [25].

$$E_{tot} = G[\rho] + \frac{1}{2} \sum_{i,j} \frac{Z_i Z_j}{R_{ij}} - \sum \frac{Z_i \, \rho(r)}{|r - R_i|} dr + \frac{1}{2} \int \int \frac{\rho(r_1) \, \rho(r_2)}{r_{12}} dr_1 dr_2$$

$$- E_{atoms} \qquad\qquad (3 - 44)$$

where the sums over (i) and (j) are over the nuclei of the solid, the primed sum indicates omission of the (i =j) term, (Z_i) and (R_i) are the charge and position of the ith nucleus, the integrals are over [r (or r_1 and r_2)], and $r_{12} = |r_1 - r_2|$. where the first term in the right side of Equation (3-44) $(G[\rho])$ is the kinetic, exchange, and correlation energy functional, $G[\rho] = E_{XC}[\rho] + T_e[\rho]$, where $E_{XC}[\rho]$ is the exchange and correlation energy, and $T_e[\rho]$ is the electronic kinetic energy. The second term is the core-core repulsion potential, the third term is the electron-core coulomb interaction, the fourth term is the electron-electron coulomb interaction, the fifth term (E_{atoms}) is the collective energy of the isolated atoms[24,68].

Can go from equation(2-44) to equation (2-41) if make the following two assumptions:

a): $G[\rho]$can be described by $G[\rho] = \int g(\rho(r), \nabla\rho(r), \nabla^2(\rho(r) \cdots)dr$ where (g) is the density and is assumed to be a function of the local electron density and its lower derivatives.

b): the electron density of the solid can be described as a linear superposition of the densities of the individual atoms $(\rho_s(r) = \sum_i \rho_i^a (r - R_i))$. The first approximation is motivated by studies of the response function of the nearly uniform electron gas. The second approximation is justified by the observation that, in many metals, the electron distribution in the solid is closely represented by a superposition of atomic densities. In addition, due to the variational nature of the energy

functional, errors in the assumed density should only affect the energy to second order. It is also useful for to define the embedding energy for an atom in an electron gas of some constant density $(\overline{\rho})$ (neutralized by a positive background): $G_i(\overline{\rho}_i) = G[\rho_i^a + \overline{\rho}_i] - G[\rho_i^a - G[\overline{\rho}_i]$. Using these two assumptions and the definition for the embedding energy, can obtain from eq. (2-44):

$$E_{coh} = \sum_i G_i \left(\sum_{j \neq i} \rho_i^a (R_{ij}) \right) + \frac{1}{2} \sum_{i,j(j \neq i)} U_{ij}(R_{ij}) + E_{err} \qquad (3-45)$$

The error (E_{err}) is a function of the background density $\overline{\rho}_i$. Setting the error to zero gives an equation for the optimal background density. The solution to $E_{err} = 0$ is discussed in detail by Daw [24].

3-4 Modified Embedded Atom Method (MEAM) [27, 25,69,70,71]

The total energy (E) of a system of atoms in the Embedded Atom Method (EAM) has been shown to be given by an approximation of the form:

$$E = \sum_i \left(F_i(\overline{\rho}_i) + \frac{1}{2} \sum_{j \neq i} \emptyset_{ij}(R_{ij}) \right) \qquad (3-46)$$

where the sums are over the atoms i and j. In this approximation, the embedding function (F_i) is the energy to embed an atom of type (i) into the background electron density at site i, $\overline{\rho}_i$; and $\emptyset_{ij}$ is a pair interaction between atoms (i) and (j) whose separation is given by R_{ij}. In the EAM, $\overline{\rho}_i$ is given by a linear supposition of spherically averaged atomic electron densities, while in the Modified Embedded Atom Method (MEAM), $\overline{\rho}_i$ is augmented by angularly dependent terms. Let denote the term in brackets in Eq. (3-46), i.e., the direct contribution to the energy from the ith atom:

as E_i. Atom i also indirectly contributes to the energy through its interactions with its neighbors. Then E_i may be written as follows:

$$E_i = F_i(\bar{\rho}_l) + \frac{1}{2}\sum_{j \neq i} \emptyset_{ij}(R_{ij}) \qquad (3-47)$$

As in Baskes et al. consider the case of a homogeneous monatomic solid with interactions limited to first neighbors only. In a specific reference structure (usually the equilibrium structure) for an atom of type i have:

$$E_i^u(R) = F_i\left(\bar{\rho}_i^0(R)\right) + \frac{1}{2}Z_i\emptyset_{ii}(R) \qquad (3-48)$$

where $\bar{\rho}_i^0(R)$ is the background electron density for the reference structure of atom i, Z_i is the coordination, and (R) is the nearest neighbor distance. Here $E_i^u(R)$ is the energy per atom of the reference structure as a function of nearest neighbor distance, obtained, e.g., from first principles calculations or the universal equation of state of Rose et al. Here choose the latter:

$$E_i^u(R) = -E_c\left(1 + \alpha\left(\frac{R}{r_e} - 1\right)\right)e^{-\alpha(R/r_e - 1)} \qquad (3-49)$$

with

$$\alpha^2 = \frac{9\Omega B}{E_c} \qquad (3-50)$$

where E_c, r_e, Ω, and B are the cohesive energy, nearest-neighbor distance, atomic volume, and bulk modulus, respectively, all evaluated at equilibrium in the reference state. The pair potential for like atoms is then given by:

$$\emptyset_{ii}(R) = \frac{2}{Z_i}\left\{E_i^u(R) - F_i\left(\bar{\rho}_i^0(R)\right)\right\} \qquad (3-51)$$

At equilibrium (denoted by $|_{re}$), with the use of this form, $E|_{re} = -E_c$, $dE/dr|_{re} = 0$, and $d^2E/dr^2|_{re} = 9\Omega B/r_e^2$ so that agreement is assured

between the model and the input cohesive energy, atomic volume, and bulk modulus. The pair potential for unlike atom pairs will be discussed below.

In the MEAM the embedding function $F(\rho)$ is taken as

$$F(\rho) = AE_c \frac{\rho}{\rho_0} \ln \frac{\rho}{\rho_0} \qquad (3-52)$$

Where (A) is an adjustable parameter and (ρ_0) is a density scaling parameter. The density scaling parameter was initially taken to be the coordination times the atomic density scaling factor (see Eq. 2-56 below) and more recently as the density in the equilibrium reference structure. The SiC calculations presented below use the latter definition. face centered cubic (fcc), body centered cubic (bcc) reference lattices the definitions are identical. For and hexagonal close packing (hcp) and diamond cubic. there is a small difference.

The background electron density, $\bar{\rho}_i$, is assumed to be a function of what call partial electron densities. These partial electron densities contain the angular reformation in the model. The reader should be cautioned that even though the electron density may be thought of as qualitatively similar to a real electron density, there is no expectation that the electron densities calculated here would be in agreement with those obtained from first principles calculations.

For example, the square of the electron density at a given site has previously been defined as the sum of terms with s, p, d, and f symmetry from the neighboring atoms. By including these angular terms in the background electron density, introduce angular forces into the model. Thus at a particular atom:

$$\bar{\rho}^2 = \sum_{h=0}^{3} t^{(h)} \rho^{(h)2} \qquad (3-53)$$

with h=0 to 3 corresponding to s, p, d, and f symmetry, respectively, and for convenience take $t^{(0)} = 1$. Note that in a crystal the s, p, d, and f terms may be considered as measures of volume, polarization, shear, and lack of inversion symmetry, respectively . For example, as vary the volume of a perfect face centered cubic (fcc) lattice, only $\rho^{(0)}$ is not equal to zero and, thus it can simply be related to the volume. Similarly as shear the face centered cubic (fcc) lattice, contributions from $\rho^{(2)}$ arise. An alternative exponential form with the same asymptotic behavior near the perfect lattice has also been used :

$$\bar{\rho} = \rho^{(0)} e^{\left[\frac{1}{2}\Sigma_{h=0}^{3} t^{(h)}\left(\rho^{(h)}/\rho^{(0)}\right)^{2}\right]} \qquad (3-54)$$

The contributions to the density are given by:

$$\rho^{(0)} = \sum_{i} \rho^{a(0)}(r^{i}) \qquad (3-55a)$$

$$(\rho^{(1)})^{2} = \sum_{\alpha} \left[\sum_{i} \rho^{a(1)}(r^{i}) \frac{r_{\alpha}^{i}}{r^{i}}\right]^{2} \qquad (3-55b)$$

$$(\rho^{(2)})^{2} = \sum_{\alpha,\beta} \left[\sum_{i} \rho^{a(2)}(r^{i}) \frac{r_{\alpha}^{i}r_{\beta}^{i}}{r^{i2}}\right]^{2} - \frac{1}{3}\left[\sum_{i} \rho^{a(2)}(r^{i})\right]^{2} \qquad (3-55c)$$

$$(\rho^{(3)})^{2} = \sum_{\alpha,\beta,\gamma} \left[\sum_{i} \rho^{a(3)}(r^{i}) \frac{r_{\alpha}^{i}r_{\beta}^{i}r_{\gamma}^{i}}{r^{i3}}\right]^{2} \qquad (3-55d)$$

Here, the $\rho^{a(h)}$ are radial functions which represent the decrease in the contribution with distance (r^{1}) from the site in question, the superscript (i) indicates neighboring atoms to the site in question, and the $\alpha, \beta,$ and γ summations are each over the three coordinate directions with r_{α}^{1} .being the distance from the site in question in that direction. The functional forms for the partial electron densities (h=1,3) were chosen to be translationally and rotationally invariant and equal to zero for crystals

with cubic symmetry. Finally, the individual contributions are assumed to decrease exponentially, i.e.,

$$\rho^{a(0)}(R) = \rho_0^a e^{-\beta^{(h)}(R/r_e - 1)} \tag{3-56}$$

where ρ_0^a and $\beta^{(h)}$ are constants. For alloys the coefficients $t^{(h)}$ were initially assumed to depend on the properties of the atom at which the average electron density was calculated. agreement with defect properties in SiC could be obtained if the properties of the atoms surrounding this atom were included. The latter averaging procedure is used below for the SiC calculations:

$$t^{(h)} = \sum_i t_i^{(h)} \rho^{a(0)}/\rho^{(0)} \tag{3-57}$$

3-5 Molecular Dynamics (MD) Modeling of Fracture

3-5-1 Model Potentials for Brittle Materials

The most critical input parameter in Molecular Dynamics (MD) is the choice of interatomic potentials, it is difficult to identify generic relationships between potential parameters and macroscopic observables such as the crack limiting or instability speeds when using such complicated potentials. Deliberately avoid these complexities by adopting a simple pair potential based on a harmonic interatomic potential with spring constant (k) [72]. In this case, the interatomic potential between pairs of atoms is expressed as

$$\emptyset(r) = a_0 + \frac{1}{2}k_0(r - r_0)^2 \tag{3-58}$$

where (r_0) denotes the equilibrium distance between atoms, for a two dimensions (2D) triangular lattice, as schematically shown in the inlay of Fig. (3-3). This harmonic potential is a first-order approximation of the Lennard-Jones potential , one of the simplest and most widely used pair potentials defined as

$$\emptyset(r) = 4\varepsilon \left(\left[\frac{\sigma}{r} \right]^{12} - \left[\frac{\sigma}{r} \right]^{6} \right) \tag{3-59}$$

Express all quantities in reduced units, so that lengths are scaled by the LJ-parameter (σ) which is assumed to be unity, and energies are scaled by the parameter (ε) , the depth of the minimum of the LJ potential. Corresponding to choosing $\varepsilon = 1$ in Eq. (3-59), choose ($a_0 = -1$) in the harmonic approximation shown in Eq. (3-58). Further, more ($r_0 = \sqrt[6]{2} \approx 1.12246$) (see Fig. (3-3)). The parameter (σ) is coupled to the lattice constant (a) as ($\sigma = a / \sqrt[2]{2} / \sqrt[6]{2}$). The reduced temperature is ($k_B T / \varepsilon$) with (k_B) being the Boltzmann constant. The mass of each atoms in the models is assumed to be unity, relative to the reference mass (m^*) . The reference time unit is then given by ($t^* = \sqrt{m^* \sigma^2 / \varepsilon}$) . For example, when choosing electron volt as reference energy ($\varepsilon = 1eV$), Angstrom as reference length ($\sigma = 1$ Å), and the atomic mass unit as reference mass ($m^* = 1$ amu), the reference time unit corresponds to ($t^* \approx$ 1.01805E-14 seconds) [72].

Although the choice of a simple harmonic interatomic potential can not lead to quantitative calculations of fracture properties in a particular material, it allows to draw certain generic conclusions about fundamental, material-independent mechanisms that can help elucidating the physical foundations of brittle fracture. The harmonic potential leads to linear elastic material properties, and thus serves as the starting point when comparing simulation results to predictions by the classical linear theories of fracture.

In Fig (3-3), (a) the geometry is characterized by the slab width l_x and slab length l_y , and the initial crack length a. Consider different loading cases, including mode I, mode II (indicated in the figure) and mode III (not shown). Subplots (b) and (c) illustrate two different

possible crack orientations. The orientation shown in subplot (c) has lower fracture surface energy than the orientation shown in subplot (b) [72].
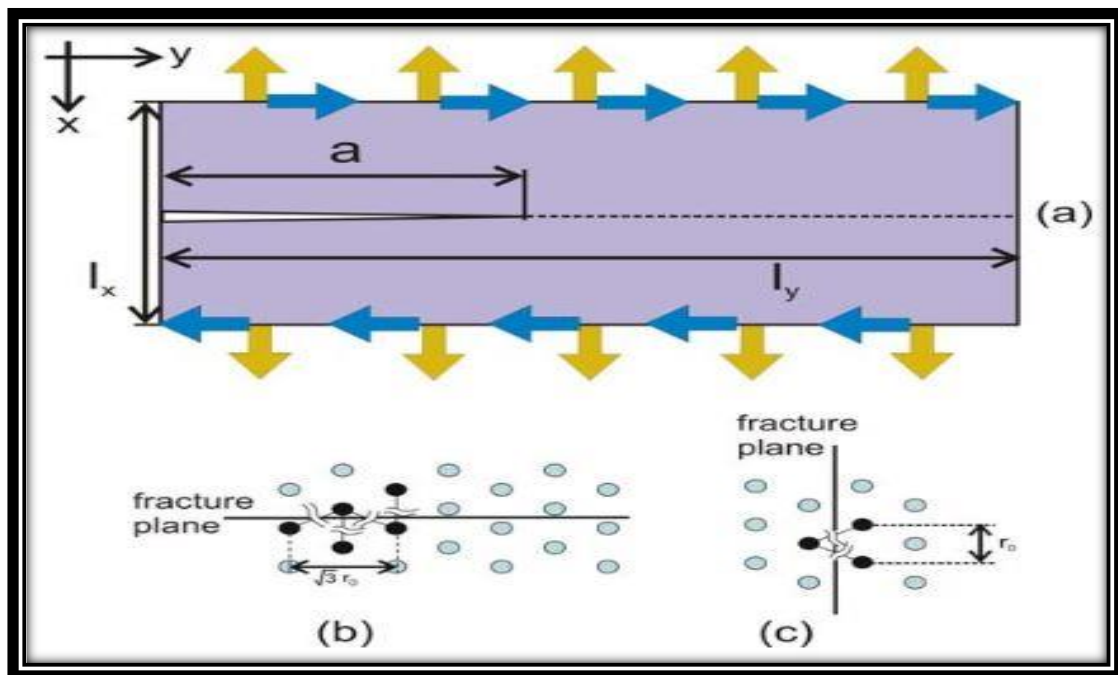
Figure 3-3. A schematic illustration of the simulation geometry used in our large-scale atomistic studies of fracture [72].

3-5-2 Model Geometry and Simulation Procedure

A crack in a two-dimensional geometry with slab size ($l_x \times l_y$) and initial crack length (a), as schematically shown in Fig. (3-3). The slab size is chosen large enough such that waves reflected from the boundary do not interfere with the propagating crack at early stages of the simulation. The slab size in the crack direction is chosen between 2 and 4 times larger than the size orthogonal to the initial crack. The slab is initialized at zero temperature prior to simulation. Most of studies are carried out in a two-dimensional, hexagonal lattice. The three-dimensional studies are performed in a face centered cubic (FCC) lattice, with periodic boundary conditions in the out-of-plane in Z-direction [72].

CHAPTER FOUR

RESULTS
AND
DISCUSSION

4-1 Crack code

Dynamic fracture is investigated for two-dimensional notched solids under tension using million atom systems [74]. The material which test in this code is brittle material with hexagonal style in two dimension (2d) lattice, the unit cell is rectangular, with miller indices $a_1 = [1\ 0\ 0]$ and $a_2 = [0\ \text{sqrt}(3)\ 0]$. In crack used time step (0.044.0.04,0.03, 0.02, 0.01, 0.009, 0.008, 0.007, 0.006, 0.005, 0.004, 0.003, 0.002, 0.001and 0.00001 tau ($t^* = \sqrt{m^*\sigma^2/\varepsilon}$) as shown in Table (4-1). The output obtained from Large-scale Atomic/Molecular Massively Parallel Simulator (LAMMPS) is used to calculate various values such as temperature, total energy, kinetic energy, potential energy, pressure and volume. Statistica used to plot graphs. After implementation of the simulation program the results of crack code shown in the table (4-1) and table (4-2).

The total energy in each time step (E = K(t)+U(t)) is conserved by Newtonian dynamics. Moving each atom in a time in separate steps known as time-steps, run command continues dynamics for a specified number of time steps [74]. Time step command sets time step size (δt) for molecular dynamics simulations [76] , time step exist in the Euler equation and other equations according to the equation (2-14). We choose time step small to minimize the error and these idea is consistent with [77] where they chose time step small enough to ensure energy conservation and avoid large discretization errors. The step (run) evolution of the total energy as shown in Figure (4-1) and Table (4-1), where the (0.044, 0.04, 0.03, 0.03, 0.01 tau ($t^* = \sqrt{m^*\sigma^2/\varepsilon}$) time step (the input data in appendix I) gives increased then rise to small oscillations in total energy, furthermore, the (0.001,0.002, 0.003, 0.004, 0.005, 0.006, 0.007, 0.008, 0.009 tau ($t^* = \sqrt{m^*\sigma^2/\varepsilon}$) time step where increasing the

51

total energy and this is violates energy conservation, a time step of (0.00001 tau ($t^* = \sqrt{m^*\sigma^2/\varepsilon}$) has therefore been to be the optimum choice, balancing energy conservation.

Table 4-1: Total energy vs. step (run) at run= 5000 in crack

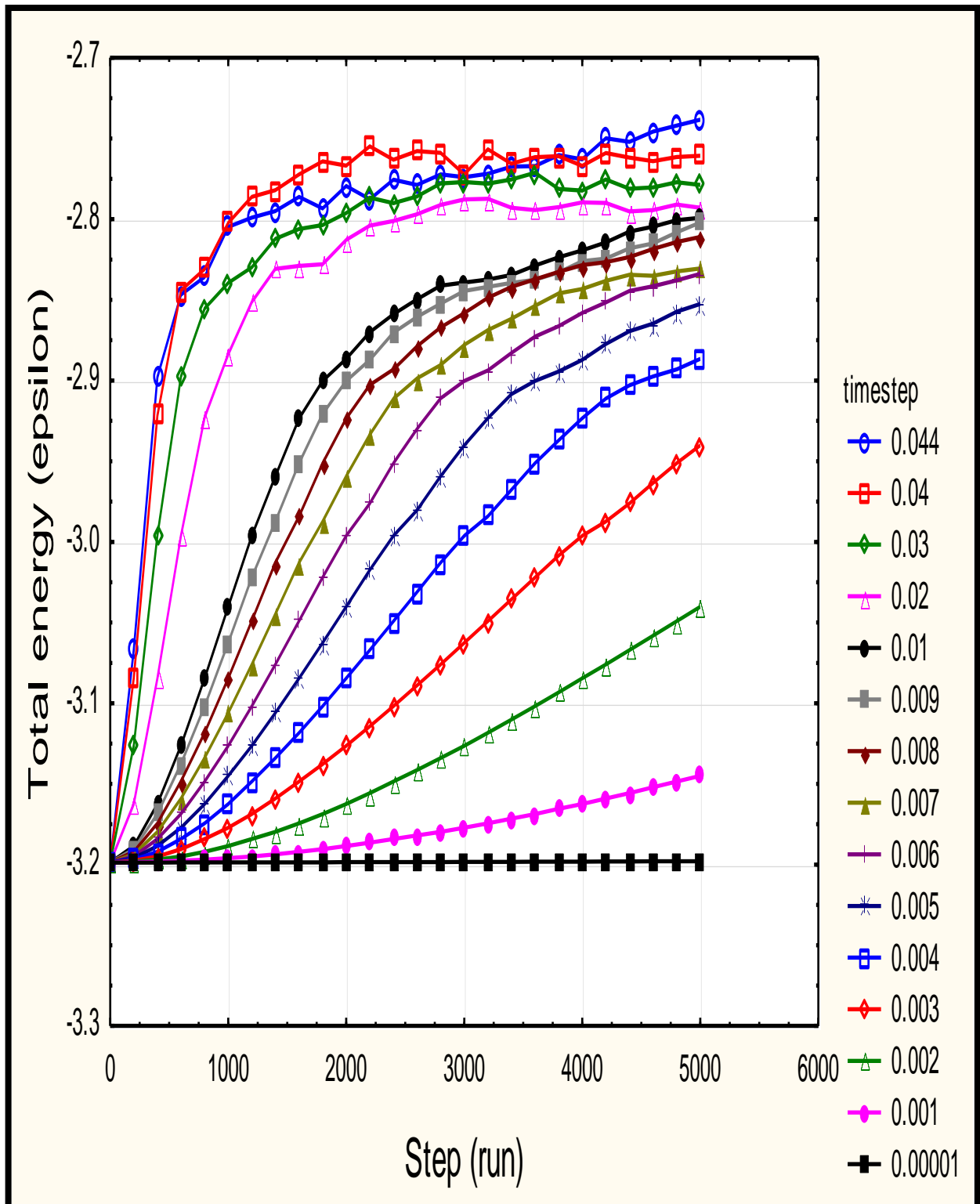| Step (run)	0.00001	0.001	0.002	0.003	0.004	0.005	0.006	0.007	0.008	0.009	0.01	0.02	0.03	0.04	0.044
0	-3.19251	-3.19251	-3.19251	-3.19132	-3.19251	-3.19251	-3.19251	-3.19251	-3.19251	-3.19251	-3.19251	-3.19251	-3.19251	-3.19251	-3.19251
200	-3.19251	-3.19231	-3.19193	-3.19132	-3.19062	-3.18975	-3.18867	-3.18733	-3.18576	-3.18407	-3.18219	-3.15599	-3.11974	-3.07758	-3.05998
400	-3.19251	-3.19193	-3.19062	-3.18868	-3.18577	-3.18221	-3.17791	-3.1734	-3.16808	-3.16228	-3.15604	-3.07783	-2.98922	-2.91419	-2.89018
600	-3.19251	-3.19132	-3.18868	-3.18409	-3.17792	-3.17085	-3.16229	-3.15275	-3.14208	-3.13126	-3.11989	2.98943	-2.8895	-2.83514	-2.83733
800	-3.19251	-3.19062	-3.18577	-3.17792	-3.16809	-3.15605	-3.14209	-3.12748	-3.11185	-3.09521	-3.07789	-2.91538	-2.84675	-2.82615	-2.82615
1000	-3.1925	-3.18975	-3.18221	-3.17085	-3.15605	-3.1386	-3.1199	-3.09946	-3.0779	-3.05584	-3.03333	-2.87583	-2.83026	-2.79208	-2.7952
1200	-3.1925	-3.18868	-3.17792	-3.1623	-3.14209	-3.1199	-3.09521	-3.06922	-3.04228	-3.01527	-2.98954	-2.84227	-2.82021	-2.77596	-2.78909
1400	-3.1925	-3.18734	-3.17341	-3.15275	-3.12749	-3.09946	-3.06922	-3.03785	-3.00609	-2.98061	-2.95249	-2.82171	-2.82171	-2.7721	-2.78504
1600	-3.1925	-3.18577	-3.16809	-3.1421	-3.11186	-3.07791	-3.04228	-3.00609	-2.97729	-2.94409	-2.916	-2.81929	2.79567	-2.76209	-2.77568
1800	-3.1925	-3.18409	-3.1623	-3.13127	-3.09522	-3.05583	-3.01528	-2.98062	-2.9441	-2.91308	-2.89256	-2.81817	-2.79324	-2.75368	-2.78208
2000	-3.1925	-3.18221	-3.15606	-3.1199	-3.07791	-3.03334	-2.98955	-2.95248	-2.91599	-2.89257	-2.87868	-2.80291	2.78532	-2.75639	-2.76829
2200	-3.19249	-3.18011	-3.14925	-3.10779	-3.06033	-3.01067	-2.9695	-2.92598	-2.89512	-2.87944	-2.86164	-2.79383	-2.77592	-2.74362	-2.77631
2400	-3.19249	-3.17792	-3.1421	-3.09522	-3.04229	-2.98956	-2.94413	-2.90351	-2.88536	-2.86229	-2.85034	-2.79071	-2.77924	-2.75176	-2.76439
2600	-3.19249	-3.17568	-3.13504	-3.08231	-3.02427	-2.97356	-2.92268	-2.89096	-2.8522	-2.8522	-2.84061	-2.7868	-2.77492	-2.74661	-2.76801
2800	-3.19249	-3.17341	-3.12749	-3.06922	-3.0061	-2.95251	-2.90336	-2.88252	-2.8588	-2.84322	-2.83181	-2.78082	-2.76664	-2.74751	-2.76163
3000	-3.19249	-3.17085	-3.1199	-3.05583	-2.98956	-2.9323	-2.89256	-2.86956	-2.84957	-2.83239	-2.82954	-2.77756	-2.7653	-2.76075	-2.76313
3200	-3.19248	-3.16809	-3.11186	-3.04229	-2.97728	-2.91593	-2.88585	-2.86052	-2.83935	-2.83239	-2.82774	-2.77703	-2.76625	-2.74542	-2.76072
3400	-3.19248	-3.16525	-3.10366	-3.02875	-2.96112	-2.90063	-2.87464	-2.85296	-2.83233	-2.82898	-2.82479	-2.78221	-2.76409	-2.75443	-2.75567
3600	-3.19248	-3.1623	-3.09522	-3.01529	-2.94412	-2.89255	-2.86434	-2.84498	-2.82782	-2.82665	-2.81848	-2.78364	-2.76041	-2.75241	-2.7553
3800	-3.19248	-3.15917	-3.08665	-3.00167	-2.92921	-2.88664	-2.85763	-2.83669	-2.82302	-2.82297	-2.81416	-2.78146	-2.76988	-2.74921	-2.7486
4000	-3.19249	-3.15606	-3.07791	-2.98957	-2.91586	-2.87926	-2.84962	-2.83347	-2.81894	-2.81601	-2.80921	-2.77849	-2.77052	-2.7556	-2.75179
4200	-3.19248	-3.15276	-3.06922	-2.98061	-2.90345	-2.86908	-2.84269	-2.82899	-2.81721	-2.81383	-2.80486	-2.77879	-2.7636	-2.74697	-2.73843
4400	-3.19247	-3.14925	-3.06034	-2.96948	-2.89532	-2.8611	-2.83534	-2.82464	-2.81351	-2.8079	-2.79803	-2.78376	-2.76895	-2.75014	-2.74014
4600	-3.19247	-3.14573	-3.05137	-2.95676	-2.88974	-2.85629	-2.83216	-2.82545	-2.80858	-2.80489	-2.79428	-2.78257	2.76896	-2.75241	-2.73368
4800	-3.19247	-3.1421	-3.04229	-2.94413	-2.88544	-2.84894	-2.8285	-2.82312	-2.80399	-2.79822	-2.79044	-2.77987	-2.76517	-2.7503	-2.72977
5000	-3.19247	-3.13861	-3.03334	-2.94011	-2.87874	-2.84367	-2.8244	-2.82063	-2.80145	-2.79192	-2.7888	-2.78104	-2.76683	-2.74916	-2.72638

Total energies (epsilon)

53

Figure (4-1) : The total energy vs. step (run) in crack

In molecular mechanics atoms movement based on their potential energy instead of the calculated force. Energy minimization is a way to relax the system before any runs by finding a stable equilibrium for that system, energy minimization can also be used to find the most stable state of molecules, If the simulation box contains 3200 atoms, then potential would be calculated 3199 times for each atom per time step, an atom-atom distance calculated, and computing the Lennard-Jones potential gives a total of more than 20 million calculations. If any atom is closer to target atom than this distance, then can proceed with calculating the potential. If the atom-atom distance is larger than the cutoff, then the potential calculation is ignored. This cuts the number of calculations roughly in half. LAMMPS does not support these functions and simply set the potentials to zero for distances above cutoff [73].

The potential energy in crack is its Lennard-Jones potential (non-bonded), the potential energy is negative because of negative cohesive energy, in energy versus distance between two atoms plot in LJ (Lennard-Jones) type of potential , see a drop in energy at the equilibrium position of two atoms.

At the atomic level, when an external load is applied to a material the atoms are displaced from their original equilibrium position straining their bonds. In order for a bond to be severed and an atom to be permanently displaced from its equilibrium position, the external load on the material must translate to an acting atomic level force that is greater than the cohesive force binding the atoms. Additionally, this force must perform a minimum amount of work equal to the bond energy. The equilibrium atomic separation or bond length occurs at the minimum of the potential energy where the force is zero. The magnitude of the force (slope of the potential) on the atoms is shown for distances beyond

equilibrium. Here the binding/bond energy is shown to be the minimum of the potential energy graph. If the straining force is larger than the maximum restoring force, the atoms will continue to separate and the bond between them will be severed [78].

From Table (4-2) and Fig. (4-2) the increase (decreases in negative) potential energy indicate that there is no crack initiation, at step (10600) the crack will be propagate at negative energy (-3.25211epsilon) i.e the bound will be break.

Table 4-2: Values of the crack at time step 0.00001tau and run = 18000

Step (run)	Potential energy (epsilon)	Kinetic energy (epsilon)	Temperature (reduced)	Pressure (reduced)	Volume
0	-3.2595	0.066987	0.066996	-0.03624	8605.592
200	-3.25949	0.06698	0.066988	-0.037	8605.592
400	-3.25947	0.066958	0.066967	-0.03765	8605.592
600	-3.25943	0.066922	0.066931	-0.0382	8605.592
800	-3.25938	0.066872	0.06688	-0.03865	8605.592
1000	-3.25931	0.066808	0.066816	-0.03899	8605.592
1200	-3.25923	0.06673	0.066738	-0.03923	8605.592
1400	-3.25914	0.066639	0.066647	-0.03938	8605.592
1600	-3.25904	0.066535	0.066543	-0.03943	8605.592
1800	-3.25892	0.066418	0.066427	-0.03939	8605.592
2000	-3.25879	0.06629	0.066298	-0.03926	8605.592
2200	-3.25865	0.06615	0.066158	-0.03905	8605.592
2400	-3.25849	0.065999	0.066007	-0.03875	8605.592
2600	-3.25833	0.065837	0.065845	-0.03839	8605.592
2800	-3.25816	0.065666	0.065674	-0.03795	8605.592
3000	-3.25798	0.065486	0.065494	-0.03745	8605.592
3200	-3.25779	0.065298	0.065306	-0.03689	8605.592
3400	-3.25759	0.065102	0.06511	-0.03628	8605.592
3600	-3.25739	0.0649	0.064908	-0.03562	8605.592
3800	-3.25718	0.064692	0.0647	-0.03492	8605.592

4000	-3.25696	0.064479	0.064487	-0.03419	8605.592
4200	-3.25674	0.064262	0.06427	-0.03342	8605.592
4400	-3.25652	0.064042	0.064049	-0.03264	8605.592
4600	-3.2563	0.063819	0.063827	-0.03184	8605.592
4800	-3.25607	0.063595	0.063602	-0.03103	8605.592
5000	-3.25585	0.06337	0.063378	-0.03022	8605.592
5200	-3.25562	0.063145	0.063153	-0.02941	8605.592
5400	-3.2554	0.062922	0.062929	-0.02862	8605.592
5600	-3.25517	0.0627	0.062708	-0.02784	8605.592
5800	-3.25495	0.062481	0.062489	-0.02708	8605.592
6000	-3.25474	0.062266	0.062274	-0.02636	8605.592
6200	-3.25452	0.062056	0.062064	-0.02567	8605.592
6400	-3.25432	0.061851	0.061858	-0.02502	8605.592
6600	-3.25412	0.061651	0.061659	-0.02442	8605.592
6800	-3.25392	0.061458	0.061466	-0.02386	8605.592
7000	-3.25374	0.061273	0.061281	-0.02337	8605.592
7200	-3.25356	0.061096	0.061103	-0.02294	8605.592
7400	-3.25339	0.060927	0.060934	-0.02257	8605.592
7600	-3.25323	0.060767	0.060774	-0.02228	8605.592
7800	-3.25308	0.060617	0.060624	-0.02205	8605.592
8000	-3.25293	0.060476	0.060484	-0.0219	8605.592
8200	-3.2528	0.060347	0.060354	-0.02184	8605.592
8400	-3.25268	0.060228	0.060235	-0.02185	8605.592
8600	-3.25257	0.06012	0.060127	-0.02195	8605.592
8800	-3.25248	0.060023	0.06003	-0.02213	8605.592
9000	-3.25239	0.059937	0.059945	-0.0224	8605.592
9200	-3.25232	0.059863	0.059871	-0.02275	8605.592
9400	-3.25225	0.059801	0.059809	-0.0232	8605.592
9600	-3.2522	0.05975	0.059758	-0.02373	8605.592
9800	-3.25216	0.059711	0.059719	-0.02434	8605.592
10000	-3.25213	0.059684	0.059691	-0.02505	8605.592
10200	-3.25211	0.059667	0.059675	-0.02584	8605.592
10400	-3.25211	0.059662	0.059669	-0.02671	8605.592
10600	-3.25211	0.059667	0.059675	-0.02766	8605.592
10800	-3.25213	0.059683	0.059691	-0.02869	8605.592
11000	-3.25215	0.05971	0.059717	-0.0298	8605.592
11200	-3.25219	0.059746	0.059753	-0.03098	8605.592
11400	-3.25223	0.059791	0.059798	-0.03223	8605.592

| 11600	-3.25228	0.059845	0.059852	-0.03354	8605.592
11800	-3.25234	0.059908	0.059915	-0.03492	8605.592
12000	-3.25241	0.059978	0.059985	-0.03636	8605.592
12200	-3.25249	0.060056	0.060063	-0.03784	8605.592
12400	-3.25257	0.06014	0.060147	-0.03938	8605.592
12600	-3.25266	0.06023	0.060238	-0.04096	8605.592
12800	-3.25276	0.060326	0.060334	-0.04259	8605.592
13000	-3.25286	0.060427	0.060434	-0.04424	8605.592
13200	-3.25296	0.060532	0.060539	-0.04593	8605.592
13400	-3.25307	0.06064	0.060648	-0.04764	8605.592
13600	-3.25318	0.060752	0.060759	-0.04937	8605.592
13800	-3.25329	0.060865	0.060873	-0.05112	8605.592
14000	-3.2534	0.06098	0.060988	-0.05288	8605.592
14200	-3.25352	0.061096	0.061104	-0.05464	8605.592
14400	-3.25363	0.061212	0.06122	-0.0564	8605.592
14600	-3.25375	0.061328	0.061336	-0.05816	8605.592
14800	-3.25386	0.061443	0.061451	-0.0599	8605.592
15000	-3.25397	0.061557	0.061565	-0.06164	8605.592
15200	-3.25408	0.061668	0.061676	-0.06335	8605.592
15400	-3.25419	0.061777	0.061785	-0.06505	8605.592
15600	-3.25429	0.061883	0.061891	-0.06672	8605.592
15800	-3.25439	0.061985	0.061993	-0.06836	8605.592
16000	-3.25449	0.062083	0.062091	-0.06996	8605.592
16200	-3.25458	0.062177	0.062184	-0.07153	8605.592
16400	-3.25467	0.062266	0.062273	-0.07307	8605.592
16600	-3.25475	0.062349	0.062357	-0.07456	8605.592
16800	-3.25483	0.062428	0.062435	-0.076	8605.592
17000	-3.2549	0.0625	0.062508	-0.07741	8605.592
17200	-3.25496	0.062567	0.062575	-0.07876	8605.592
17400	-3.25502	0.062627	0.062635	-0.08007	8605.592
17600	-3.25507	0.062682	0.062689	-0.08132	8605.592
17800	-3.25512	0.06273	0.062737	-0.08253	8605.592
18000	-3.25516	0.062771	0.062779	-0.08368	8605.592
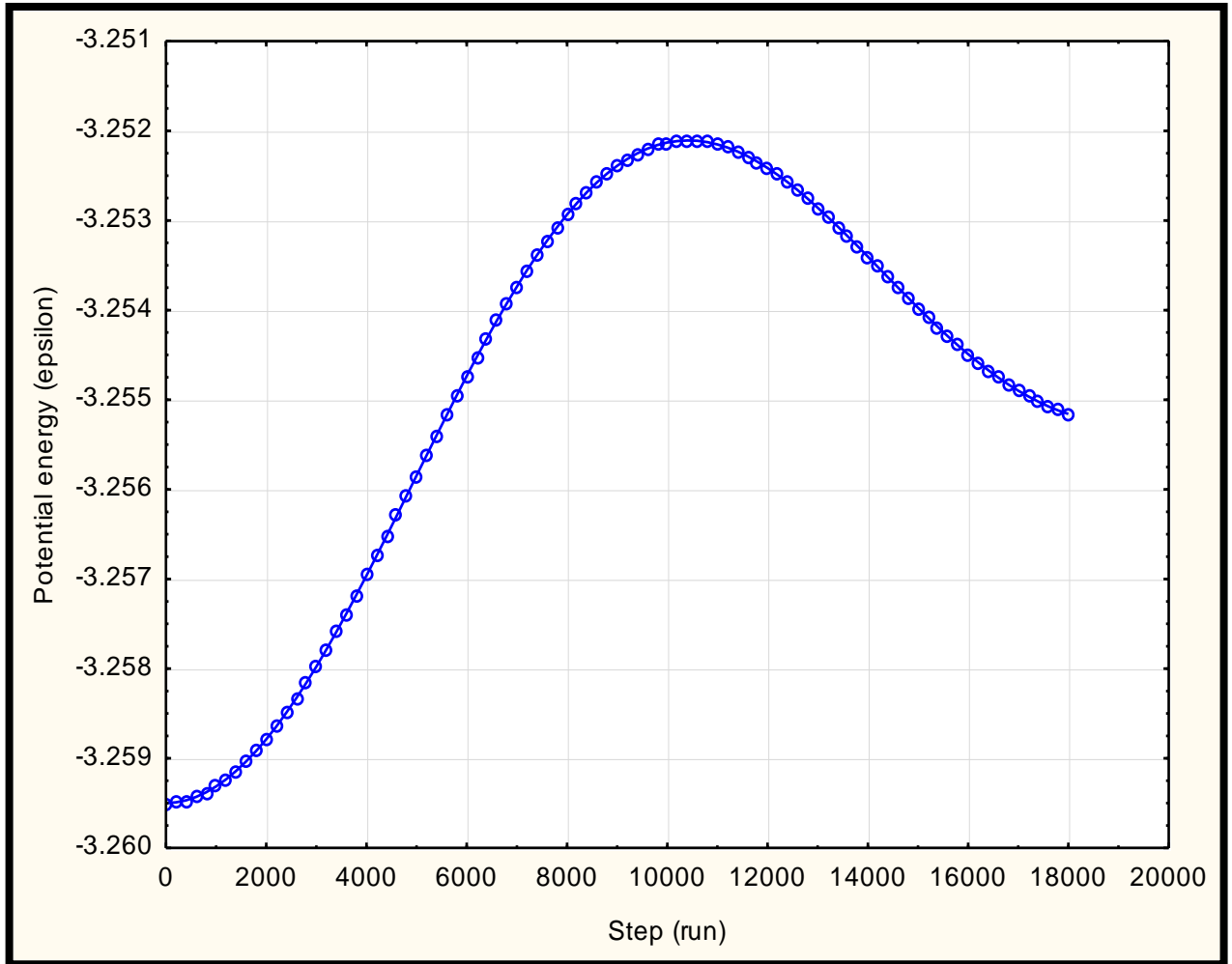
Figure (4-2) Potential energy vs. step (run) in crack

From Fig. (4-3) and Table (4-2), the decreases in kinetic energy lead to reduce the speed of the atoms because there is no crack initiation, the increases of kinetic energy (0.059667) at step (run) =10600, it is obvious that the rapid breaking of local atomic bonds in brittle fracture gives rise to a higher atomic kinetic energy at the crack tip [74].
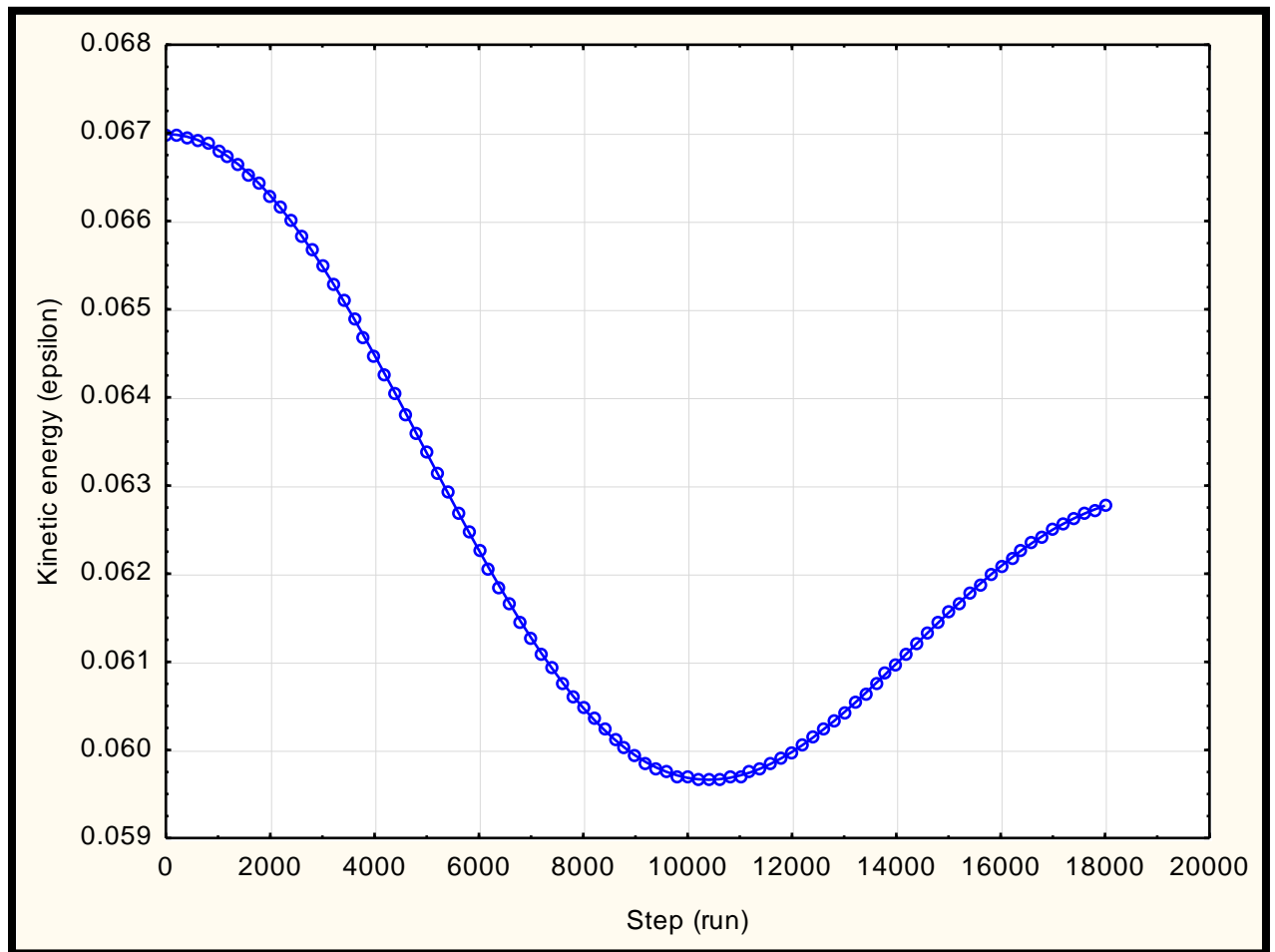

Figure (4-3) Kinetic energy vs. step (run) in crack

The conversion of energy from potential energy to kinetic energy in a closed system raises the system temperature [78]. Temperature units is reduced $(T^* = \frac{K_B T}{\epsilon})$. decrease in temperature because there is no crack initiation, the increase in temperature indicates that the crack propagated as shown in Fig. (4-4) and Table (4-2).
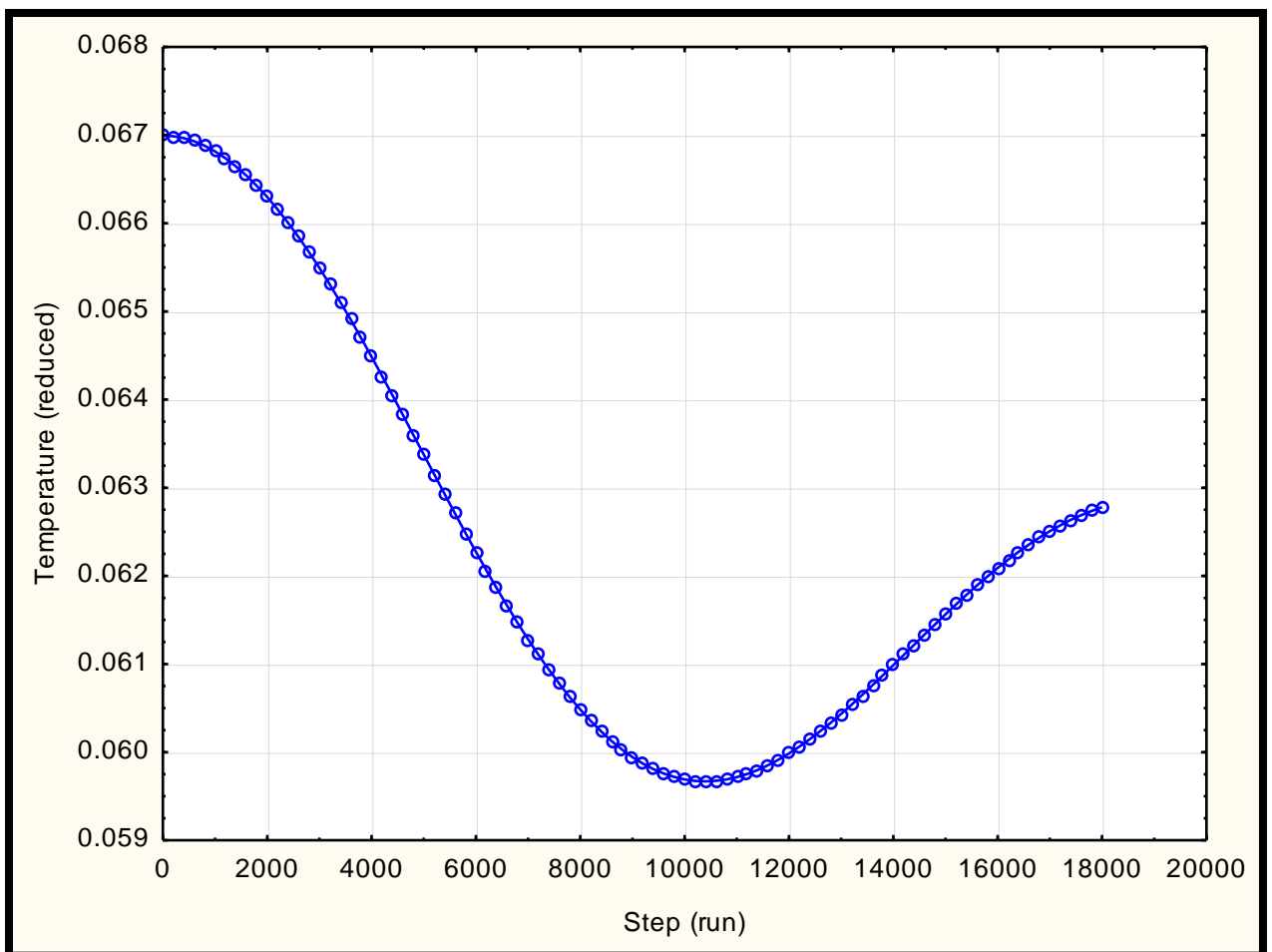
Figure (4-4) Temperature vs. step (run) in crack

pressure is external force per unit area. It is the force distribution normal to the surface . pressure unite is reduced ($p^* = \dfrac{p\sigma^3}{\epsilon}$).

From Fig. (4-5) and Table (4-2) , decreases in negative pressure because there is no crack initiation, the increase in negative pressure resulting from breaking the bonds between atoms.
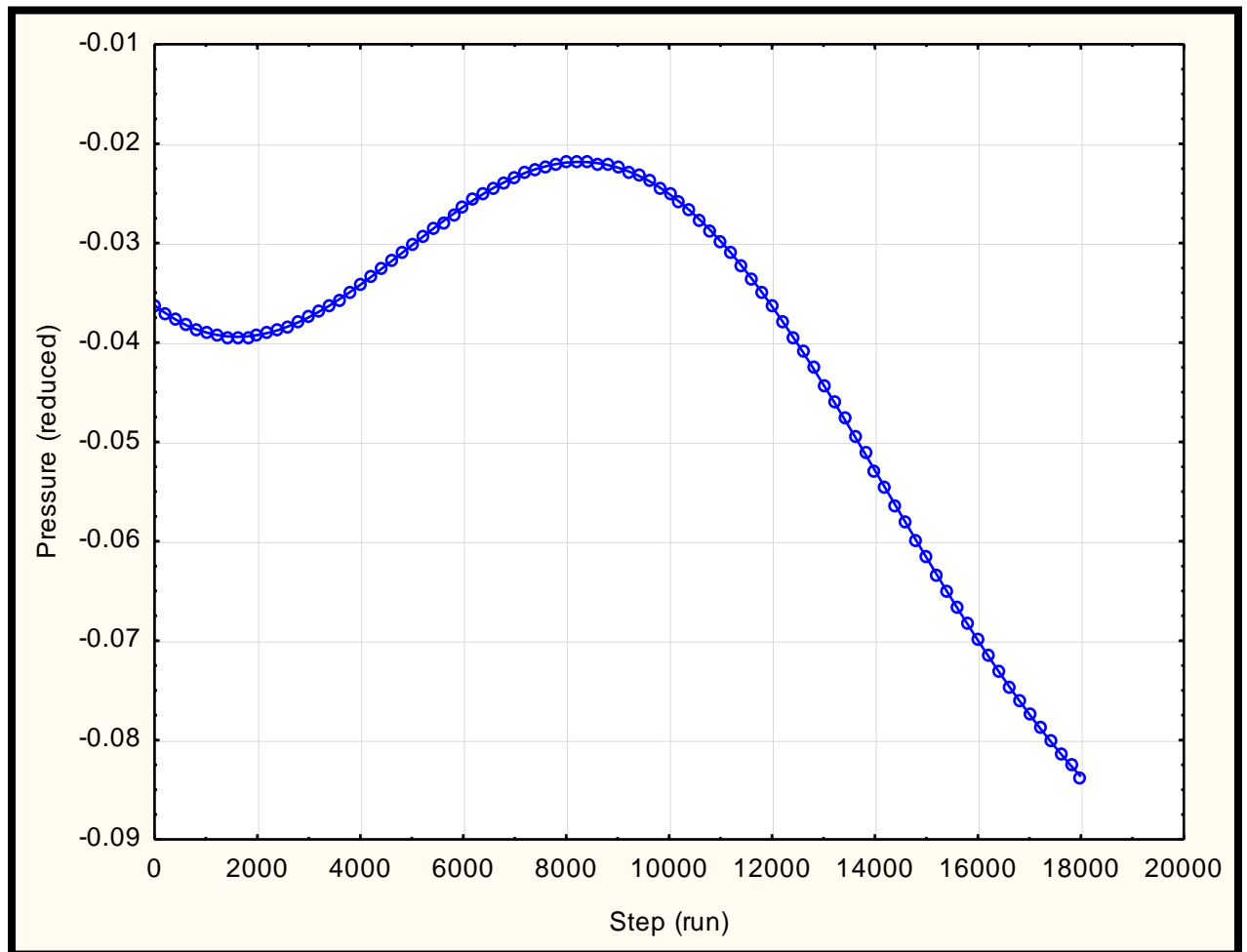

Figure (4-5) Pressure vs. step (run) in crack

62

In this thesis used NVE microcanonical ensemble simulations, so the volume or area of crack is constant as shown in Fig. (4-6) and Table (4-2).
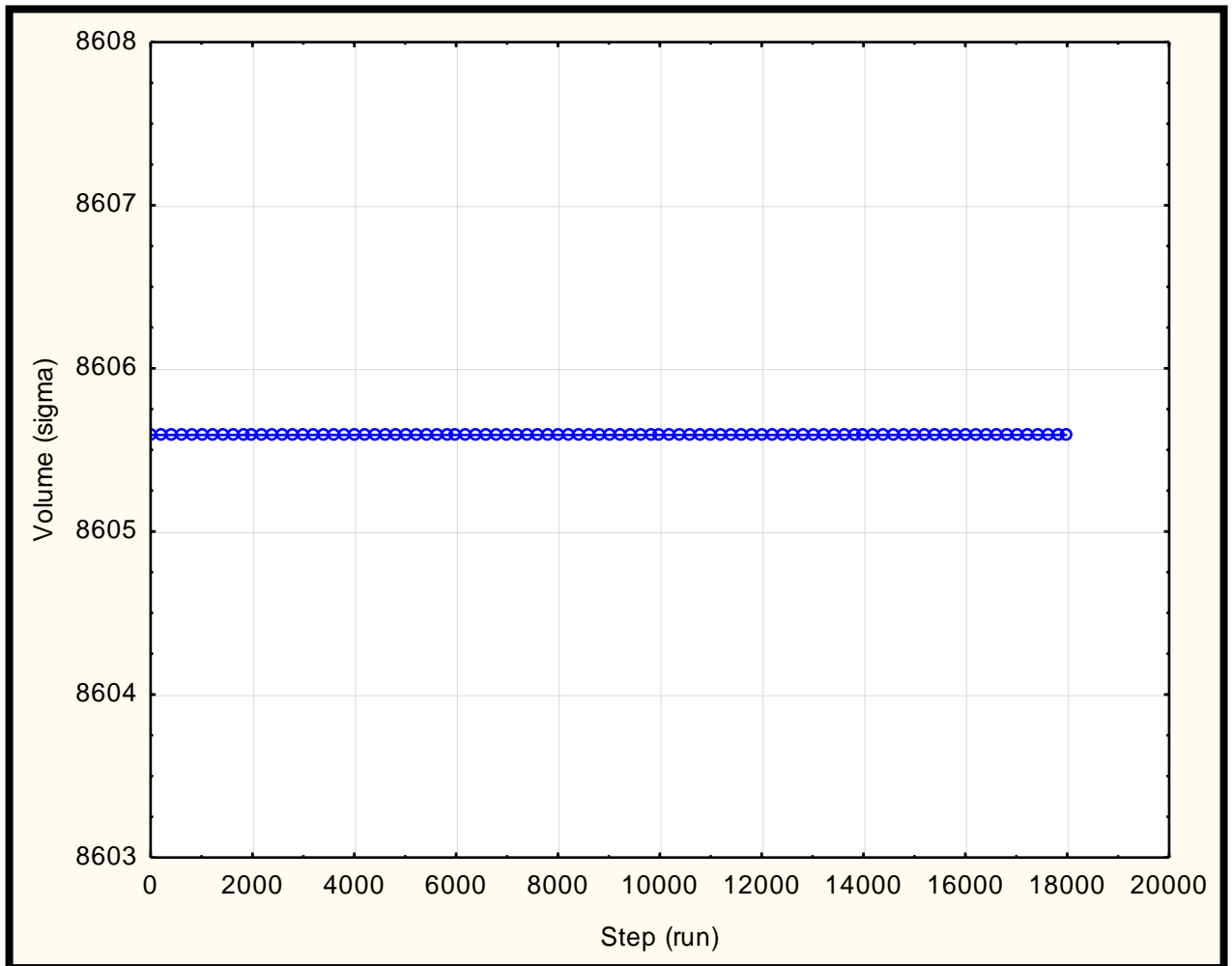

Figure (4-6) Volume vs. step (run) in crack

4-2 Modified Embedded Atom Method (MEAM) code

After the implementation of the simulation program the results of Modified Embedded Atom Method (MEAM) code as shown in the tables (4-3) and (4-4) . The total energy in each time step (E = K(t)+U(t)) is conserved by Newtonian dynamics.

the time step must be chosen small enough to ensure energy conservation and avoid large discretization errors [77]. From Fig (4-7) and Table (4-3) shows the response of total energy vs. run time for time step (0.0001 Ps) is stable at value (-636.4) while for (0.0005, 0.0006, 0.0007, 0.0008, 0.0009 and 0.001 Ps) the total energy decrease and then be stable for (0.002, 0.003 Ps) the total energy be unstable this means that the stable time step for numerical solution for Modified Embedded Atom Method (MEAM) equation so used time step (0.0001 Ps) for calculation.

Table 4-3 : Total energy vs. step (run) in MEAM

| Time step (Ps) / Step (run)	0.003	0.002	0.001	0.0009	0.0008	0.0007	0.0006	0.0005	0.0001
	Total energies (eV)								
0	-636.381	-636.381	-636.381	-636.381	-636.381	-636.381	-636.381	-636.381	-636.381
10	-637.886	-637.009	-636.541	-636.516	-636.494	-636.475	-636.456	-636.433	-636.381
20	-637.452	-637.106	-636.535	-636.502	-636.478	-636.462	-636.441	-636.421	-636.382
30	-637.497	-637.047	-636.548	-636.535	-636.485	-636.458	-636.435	-636.421	-636.383
40	-637.079	-636.949	-636.562	-636.519	-636.483	-636.466	-636.439	-636.42	-636.383
50	-637.142	-636.981	-636.565	-636.507	-636.499	-636.461	-636.442	-636.423	-636.383
60	-637.098	-636.999	-636.55	-636.509	-636.488	-636.47	-636.442	-636.422	-636.383
70	-637.293	-636.945	-636.542	-636.518	-636.482	-636.465	-636.448	-636.421	-636.383
80	-637.325	-637.121	-636.536	-636.477	-636.485	-636.455	-636.441	-636.425	-636.383
90	-637.34	-637.033	-636.523	-636.493	-636.457	-636.462	-636.437	-636.418	-636.383
100	-637.479	-637.025	-636.531	-636.497	-636.482	-636.459	-636.441	-636.426	-636.383
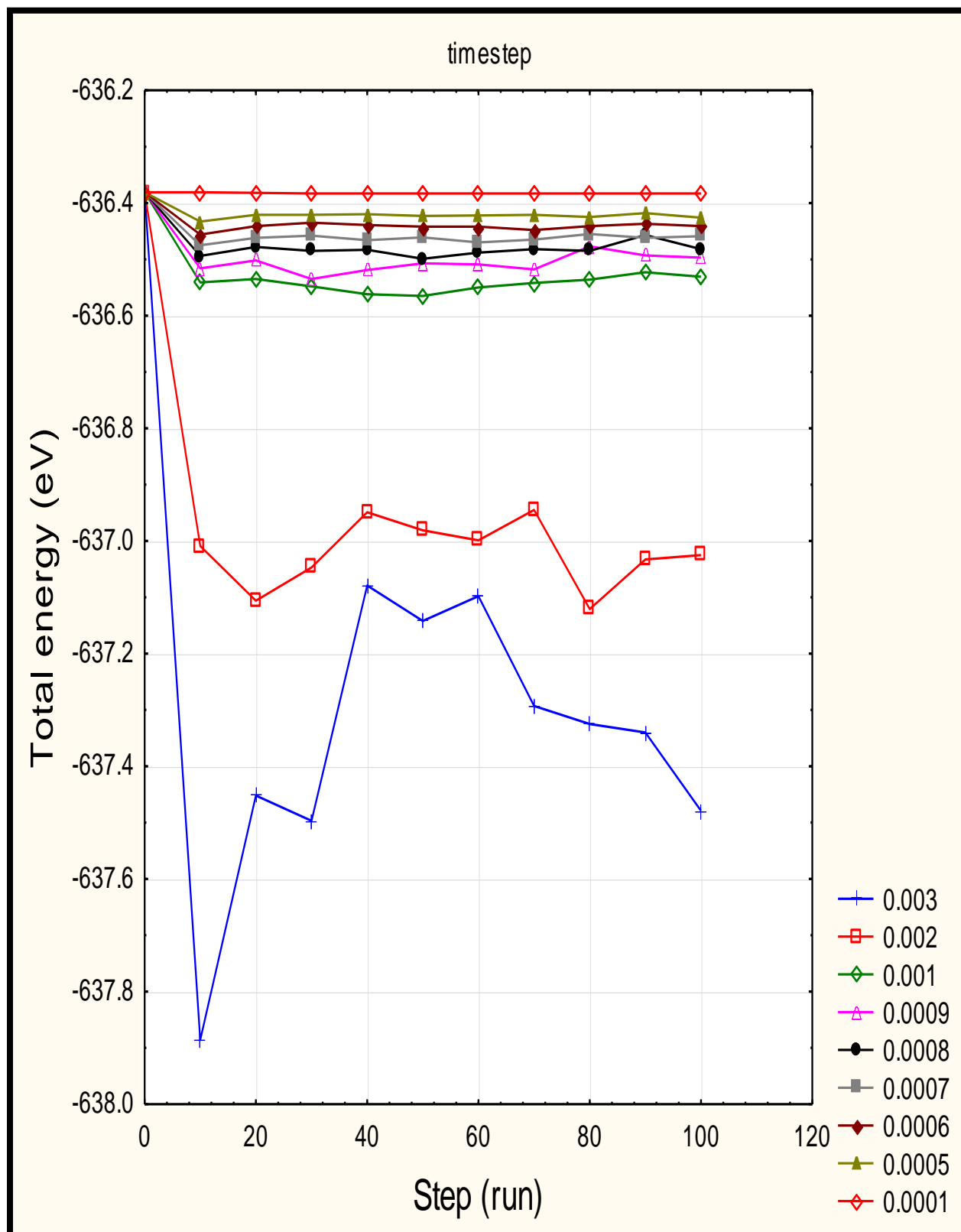
Figure (4-7) Total energy vs. step (run) in MEAM

Complex chemical bonds in SiC involve both ionic and covalent characters. There is charge transfer between Si and C atoms resulting in Coulomb interaction between ions, so the two-body interaction potential must contain at a minimum a steric repulsion as well as Coulomb interaction [18]. Potential energy in Modified Embedded Atom Method code (MEAM) is Coulomb potential, the potential energy is negative because of negative cohesive energy, in energy versus distance between two atoms plot in coulomb type of potential , see a drop in energy at the equilibrium position of two atoms. The potential energy of Modified Embedded Atom Method (MEAM) for SiC material as shown in Fig. (4-8) and Table (4-4), increases in negative potential energy because when embedded atom within the group of atoms (stable system) need sufficient energy in order to break the bonds between the atoms.

Table 4-4: Values of the MEAM at time step 0.0001 Ps

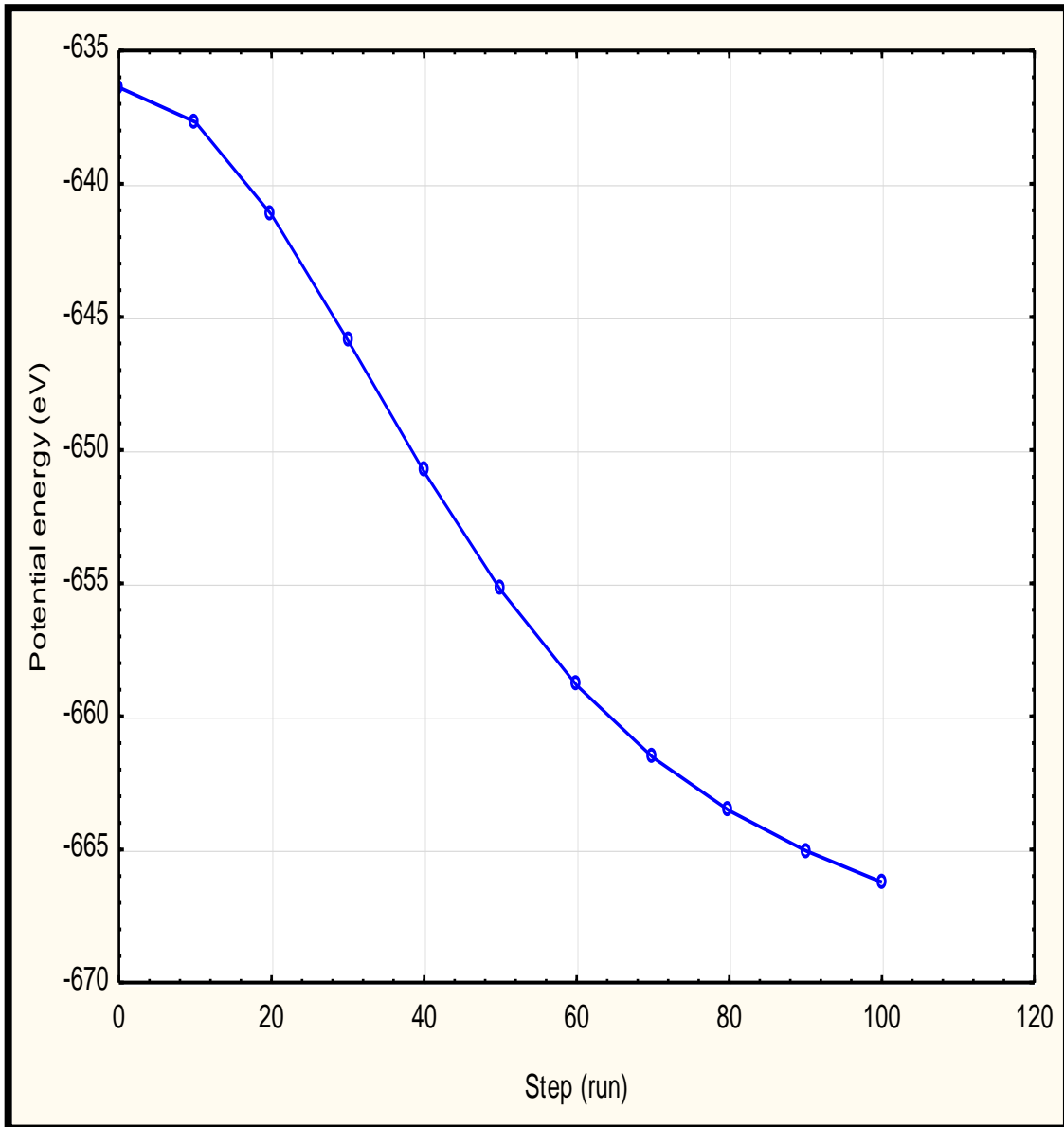| Step(run)	Potential energy (eV)	Kinetic energy (eV)	Temperature (Kelvin)	Pressure (bar)
0	-636.381	0	0	-76571.8
10	-637.678	1.296735	78.99198	-79820.8
20	-641.164	4.781635	291.2782	-88701.6
30	-645.879	9.496157	578.4683	-101052
40	-650.814	14.43089	879.0729	-114353
50	-655.249	18.86593	1149.237	-126525
60	-658.836	22.45288	1367.74	-136298
70	-661.546	25.16253	1532.801	-143221
80	-663.541	27.15851	1654.389	-147559
90	-665.047	28.66375	1746.082	-149832
100	-666.226	29.84359	1817.953	-150489

Figure (4-8) Potential energy vs. step (run) in MEAM

From Fig. (4-9) and Table (4-4), it is obvious that the rapid breaking of local atomic bonds gives to a higher atomic kinetic [74].
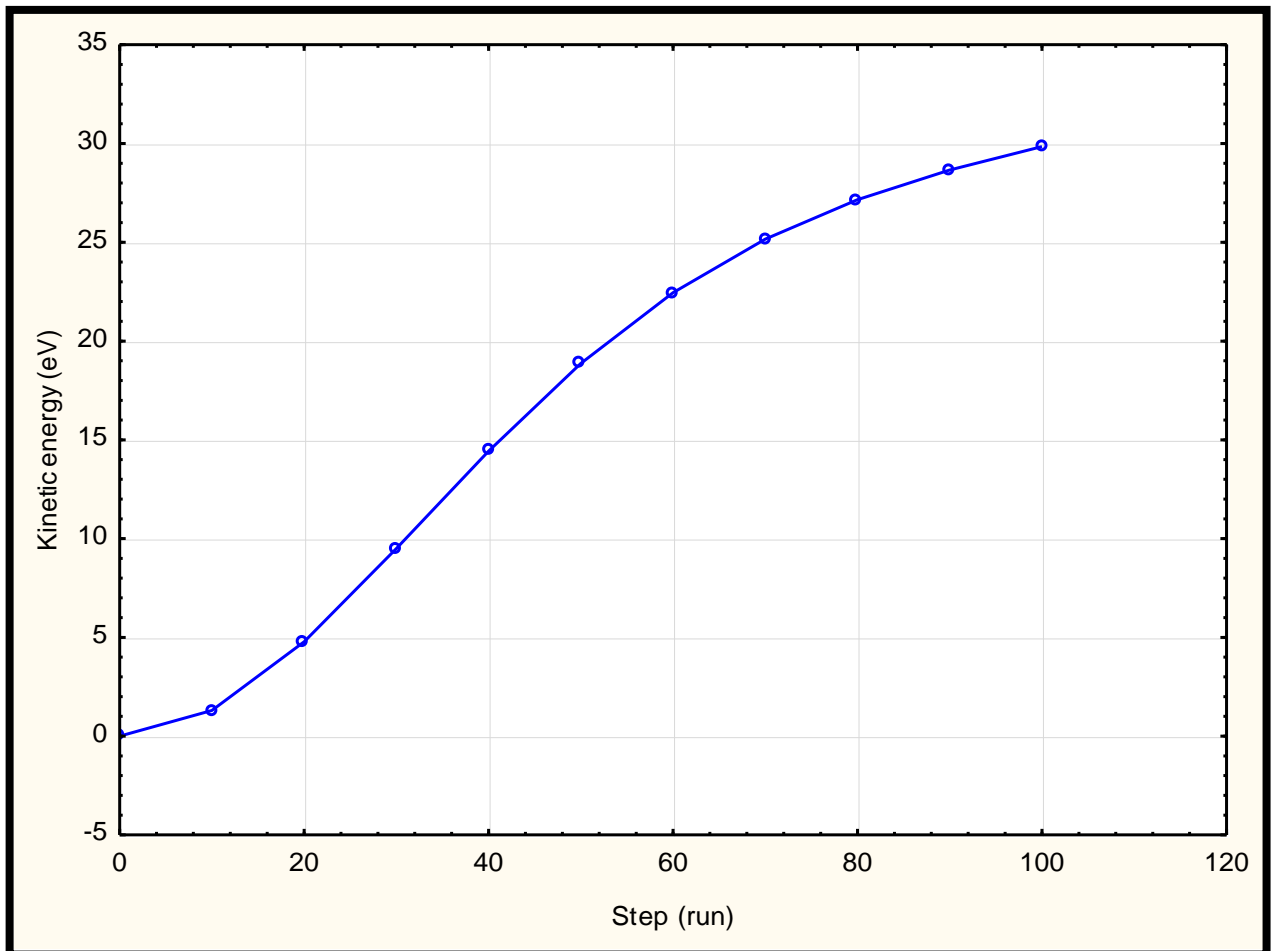

Figure (4-9) Kinetic energy vs. step (run) in MEAM

Although energy of the system is conserved, the temperature will increase when potential energy is transferred into thermal kinetic energy [46], resulting in breaking the bonds between atoms as shown in Fig. (4-10) and Table (4-4).
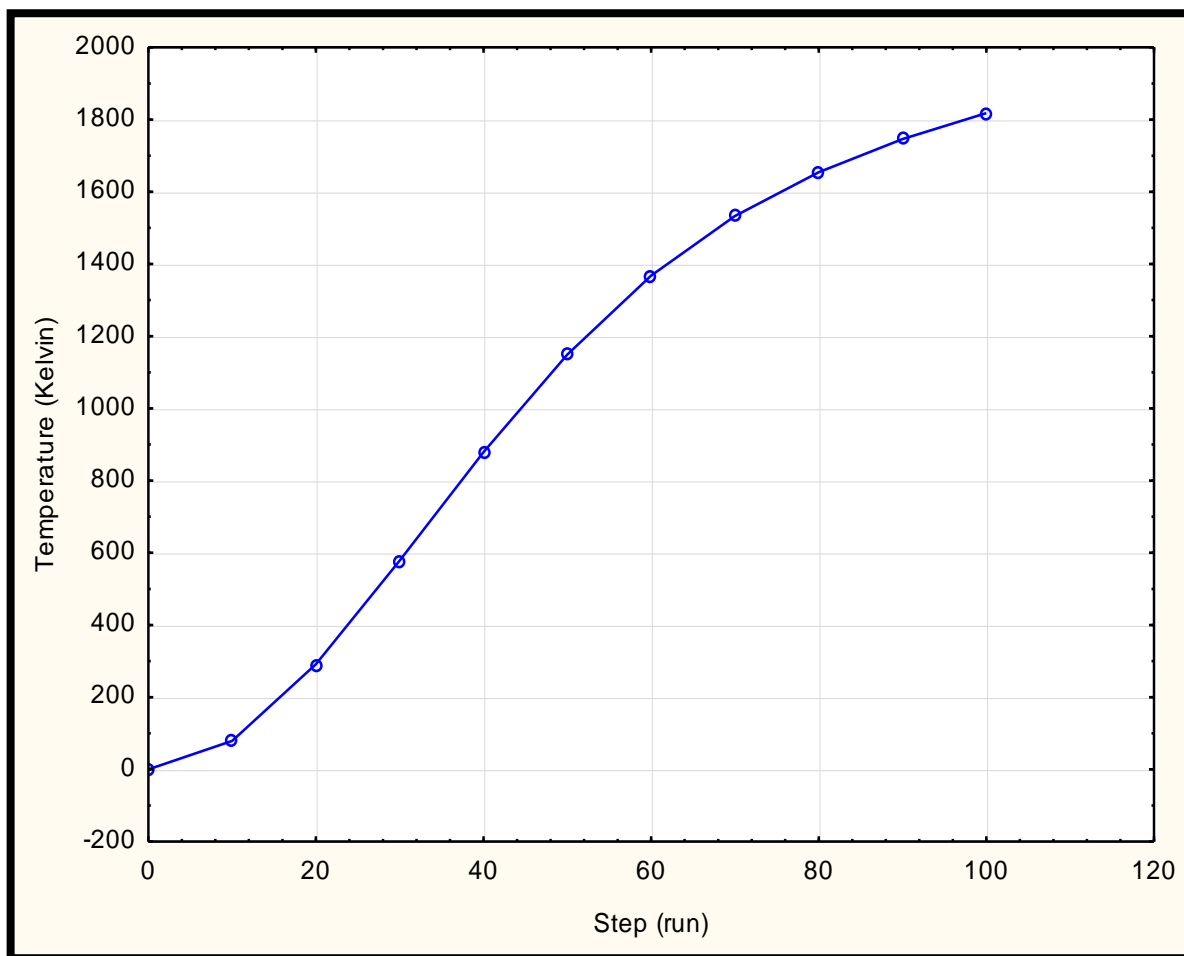

Figure (4-10) Temperature vs. step (run) in MEAM

From Fig. (4-11) and Table (4-4), an increases in negative pressure result of breaking the bonds between atoms.
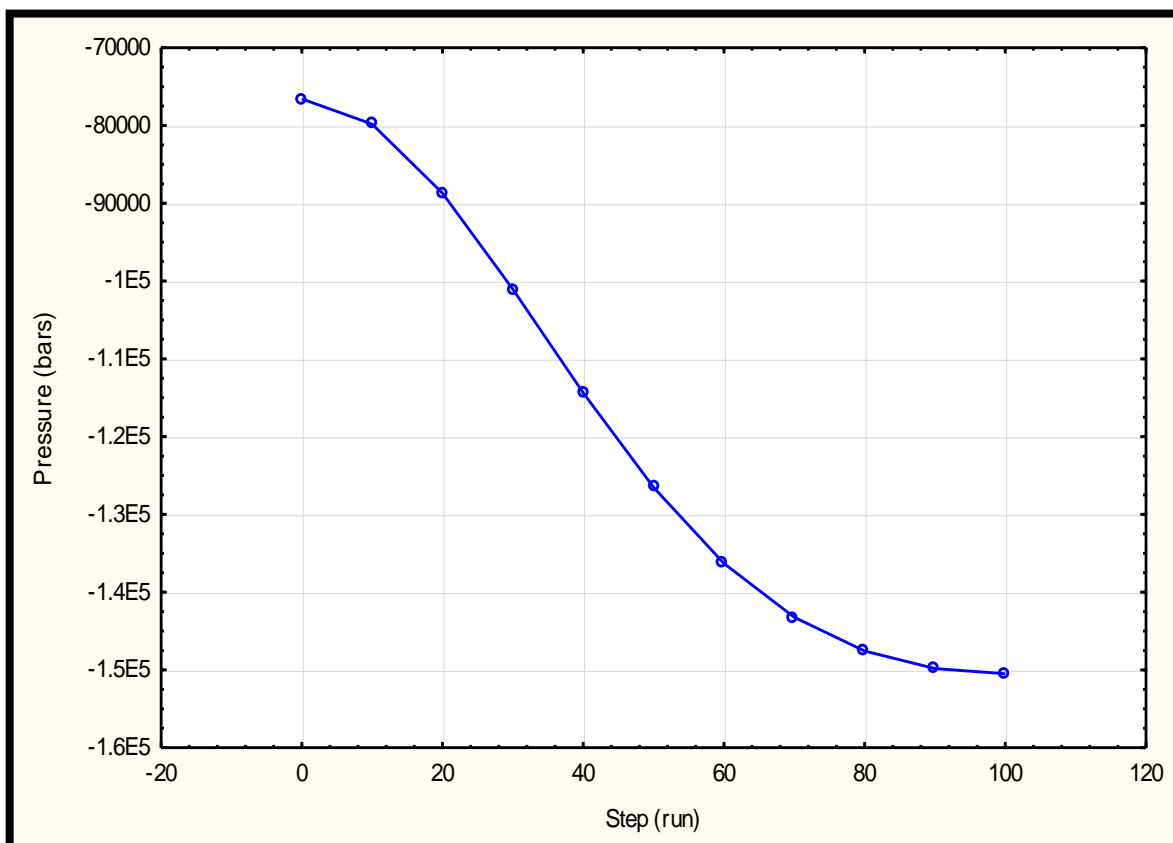

Figure (4-11) Pressure vs. step (run) in MEAM

70

4-3 Conclusions

1- Best time step in crack is (0.00001tau) , while in Modified Embedded Atom Method (MEAM) is (0.0001Ps).

2- In crack, (decreases then increases) in negative each of (pressure and potential energy) vs. step (run), while in modified embedded atom method, an increases in negative each of (pressure and potential energy) vs. step (run) .

3- In crack, decreases then increases each of (temperature and kinetic energy) vs. step (run), whereas in Modified Embedded Atom Method (MEAM) , an increases each of (temperature and kinetic energy) vs. step (run).

4- The volume in crack is constant .

4-4 Future works

1- Make the crack code work in three dimension by change the model.

2- Study the crack propagation by using perdynamic dynamic.

3- Added three dimension to Modified Embedded Atom Method (MEAM) code by change the model.

4- Change boundary conditions in Modified Embedded Atom Method (MEAM) code and crack code.

5- Add a program to draw such VMD and Ovito.
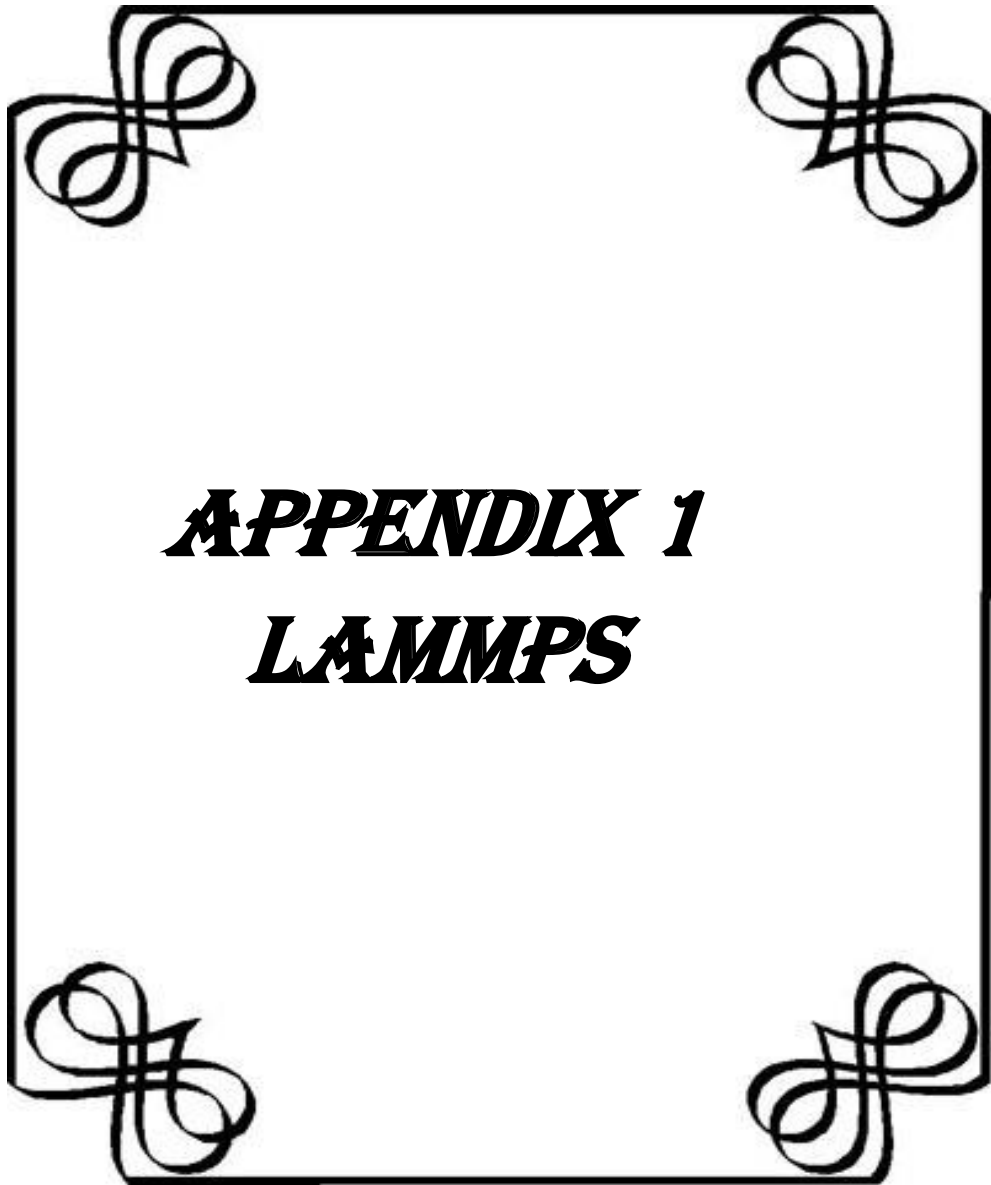
APPENDIX 1
LAMMPS

Appendix I

1-1 An introduction to LAMMPS

LAMMPS (Large-scale Atomic/Molecular Massively Parallel Simulator) is the molecular mechanics software that used in this thesis.

LAMMPS is written in C++, open source and developed by Sandia National Laboratories. It can be found on the web at

http://lammps.sandia.gov/index.html

It is primarily built for running in systems with multiple processors. This works as follows: A system containing atoms is split up into several subsystems that each processor needs to work with. This is called parallel processing, as opposed to serial processing. When a processor needs information about the system on another processor (to calculate the interaction energy between two atoms on different processors, for example), then it can send a request to the processor in question to do that calculation. LAMMPS uses MPI to do this. This might sound like a lot of extra work, but it is actually much faster than running the simulation on a single processor [73].

1-2 Installing LAMMPS

LAMMPS can be downloaded from

http://lammps.sandia.gov/download.html , via Github or Homebrew (for Mac), a personal package archive (for Ubuntu) or executables from **http://rpm.lammps.org/windows.html** (for Windows).

1-2-1 Installing LAMMPS on Windows

If one runs on Windows and has more than one processor core, one will need additional programs to implement MPI, these are given in the link above, and require a little extra work.

The windows installation will pack out to a folder called /LAMMPS + version number. The excecutables lmp_mpi.exe and lmp_serial.exe are both in the /bin subfolder. If want to run serial we must copy lmp_mpi.exe in sub folder that want to run [73].

1-2-2 Installing LAMMPS on Ubuntu

If you want to install LAMMPS follow these intructions:-

A- FFTW (to compute long-range interactions), Install fftw-2.1.5 tar.gz from **http:/www.fftw.org/download.html**

B- MPICH (to work in parallel), Install mpich2-0.93 tar.gz from **www.mpich.org/downloads/versionsl .**

In one line code have chosen.

sudo apt-get install build-essential mpich-bin libmpich1.0-dev fftw2 fftw-dev libxaw7-dev

From:http://ubuntuforums.org/showthread.php?t=1038282&highlight=LAMMPS&page=2   Download it from lammps.sandia.gov.

 In the terminal write the following:

tar xvf lammps15May15.tar.gz

cd lammps15May15

It will contain the following files: bench, doc, examples, lib, potentials, src, tools.

haid@ubuntu:~/Desktop/mkidr/lammps-15May15$ cd src

haid@ubuntu:~/Desktop/mkidr/lammps-15May15$ cd MAKE

To avoid future problems it will be better installing with the first line code now in the MAKE file will see a lot of makefiles.xxx. Most users think Makefile.linux is the one they should use because they use "linux." If open the Makefile.linux see that it requires MPICH and FFTW. Things that actually don't need (especially if starting the use of lammps). What to install is Makefile.serial. If open this file will see in the first line that it says: no MPICH, no FFTW.

If read carefully the Makefile.serial, in one line it says:
MPI library, can be src/STUBS dummy lib.

If go to STUBS will find a Makefile, this will create a dummy lib for MPI in accordance to the Makefile.serial. So in the STUBS file type:
haid@ubuntu:~/Desktop/mkidr/lammps-15May15/src/STUBS$ make   clean
haid@ubuntu:~/Desktop/mkidr/lammps-15May15/src/STUBS$ make

Then you go back to src and compile lammps
haid@ubuntu:~/Desktop/mkidr/lammps-15May15/src$ make   clean-all
haid@ubuntu:~/Desktop/mkidr/lammps-15May15/src$ make serial

It will work correctly, to verify your installation we will run some examples. First type
haid@ubuntu:~/Desktop/mkidr/lammps-15May15/src$./lmp_serial
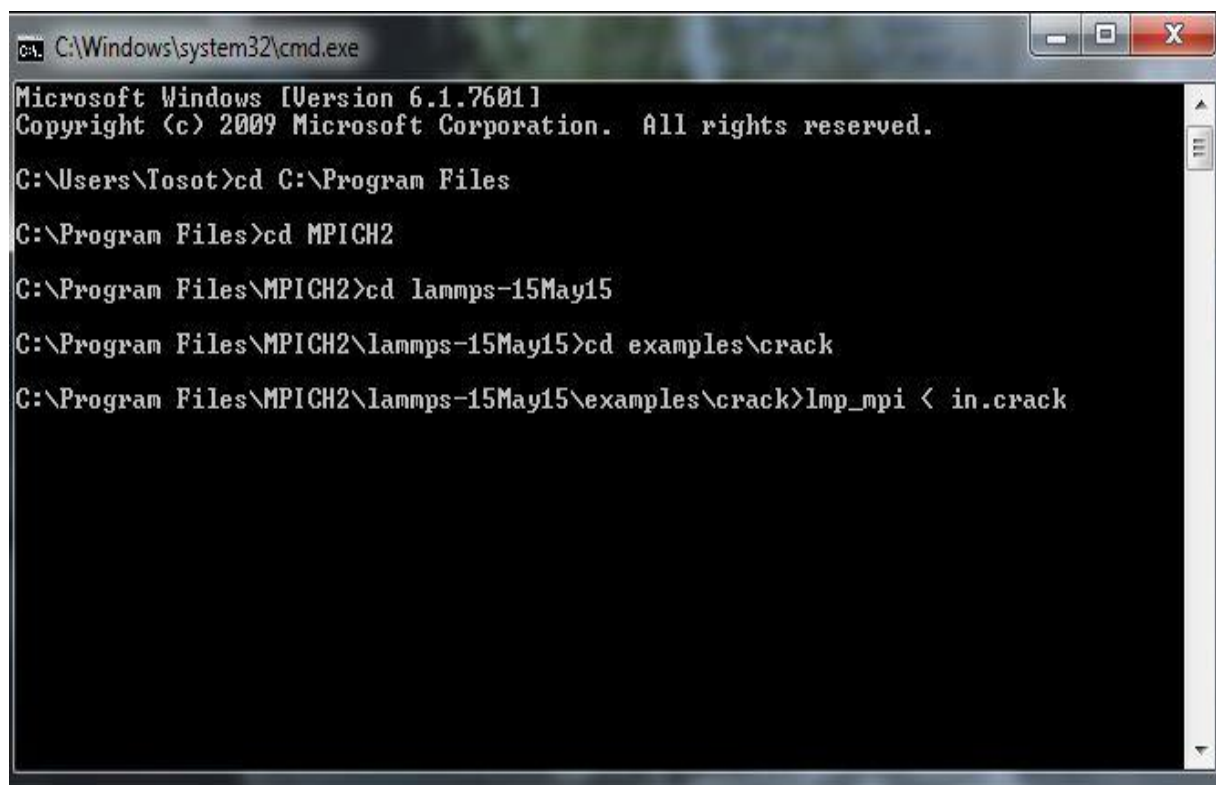

Should get:
LAMMPS (15 May 2015)
This is mean the installation process is ok [79].

74

1-3 Running LAMMPS

1-3-1 Running LAMMPS on Windows

LAMMPS is text-based, and accepts commands in the same way as for example MATLAB does. Just as for MATLAB, can write scripts that do the work for, called run-files. In order for LAMMPS to read the script, one should (in Windows) open the PowerShell/command prompt and navigate to the folder where the executables lie, one writes one of the following commands: lmp_mpi.exe < in.whatever, which means that open the executable lmp-mpi.exe and asks it to read the file in. whatever that lies in the home folder as in Figure (1).
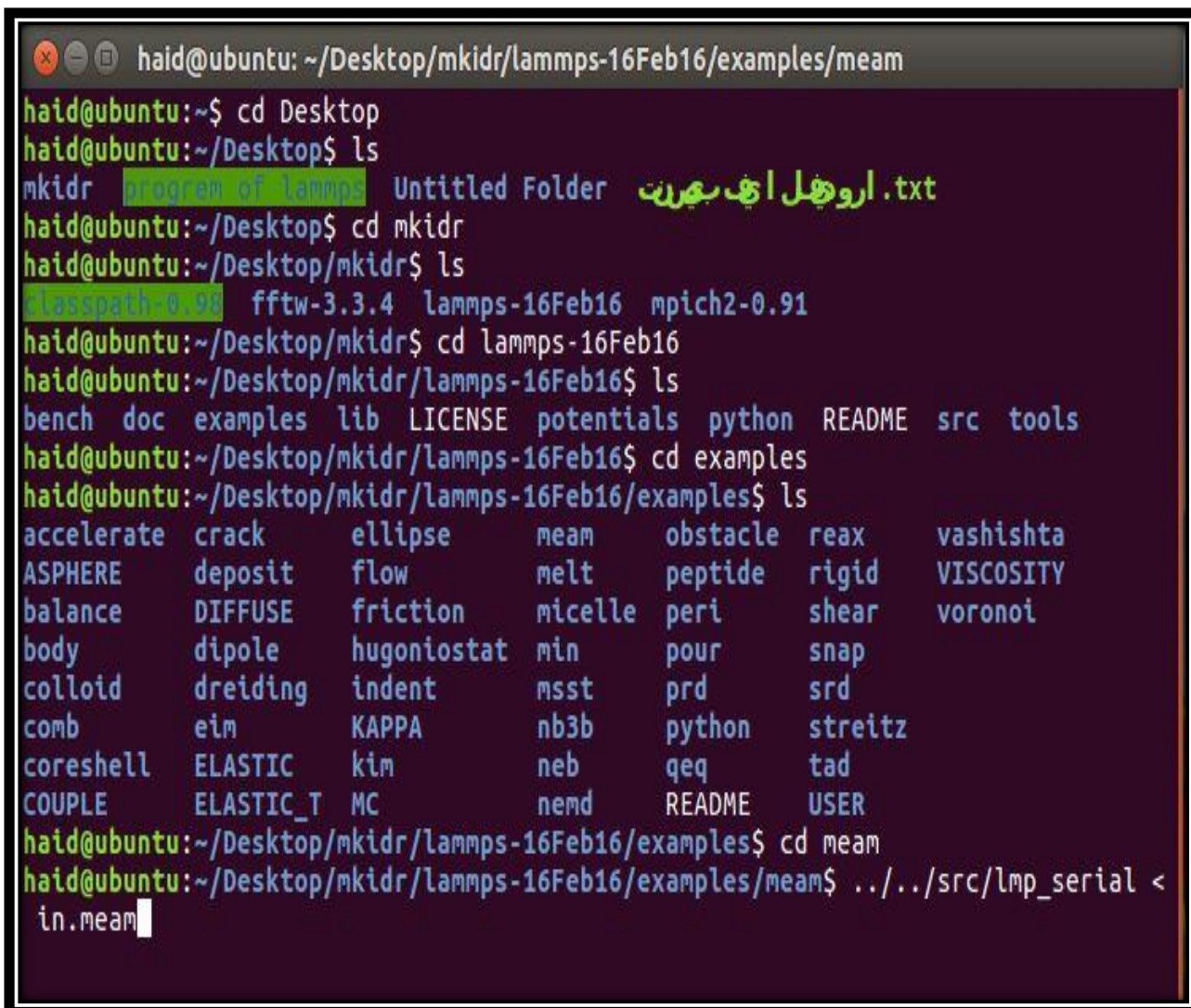
Figure (1): Running LAMMPS on Windows

If for some reason the process needs to stop immediately, one can press ctrl+c to kill the LAMMPS process [73].

1-3-2 Running LAMMPS on Ubuntu

Let's go to the examples file (cd ../examples), Choose any, and get deep in learning the meaning of the codes. Each example has one or more lammps input files. For instance will choose "meam" (cd meam). Will run as shown in Figure (2) [79].

Figure (2): Running LAMMPS on Ubuntu

1-4 Simulation Procedures

1-4-1 Procedures:

1- First task in order to draw a simulation is to download LAMMPS software to personal computer or laptop, which is itself a free source and is easily available on Sandia National Laboratories website.

2- Three basic files or components are always required for running any simulation. They are as follows:

a) In file (program file to create models and performing simulation)

b) Potential file (contains data about inter atomic bond energy and force field between atoms)

c) Executable file (lmp_win_no-mpi.exe, required to run the commands in the in file).

3-The next step is to open command prompt screen (dos environment) by typing "cmd" in address bar or in start icon.

4-Then the screen will display the path address in which all the aforementioned files are present.

5-After that next to the path address type lmp_win_no-mpi.exe< in file name then press enter.

6-Then automatically the in file will be executed by the .exe file and if there is any error in the in file then it will be displayed in the command prompt screen and subsequent rectification will be required.

1-4-2 Output of Simulation:

1- After successful running of the in. file, get three out-put files as follows:

a) DUMP file (containing the atomic co-ordinates of the final structure after simulation and also for deformation studies it contains the stress component values)

77

b) Log file (containing thermodynamic data e.g. temperature, pressure, volume, and total energy after a particular no of steps)

c) Log. lammps file

2- Now to see the final structure of experimented sample after simulation, have to open dump file containing atomic coordinates, through VMD software which need to be installed in the system separately [3].

1-5 Thermodynamic Properties in LAMMPS

The solution of the classical equations of motion results exclusively in a set of trajectories, which are comprised of atomic positions, r, and velocities, v, (or equivalently momenta, p) as a function of time, *t*. Every thermodynamic property is formulated as a function of these trajectories. Since, classical thermodynamics is a continuum theory formulated without knowledge of the atomic nature of matter, it does not provide relationships between thermodynamic quantities and atomic trajectories. For that we require statistical mechanics, called statistical thermodynamics, when limited to equilibrium systems. Make no attempt here to derive any of these relationships. Simply present some relationships and link them to variables available in LAMMPS [80].

1-5-1 Number of Particles of Component i, Ni

In the four ensembles described in chapter one, the number of particles (atoms or molecules) is held constant. Therefore, this extensive variable is always an input to the simulation. It is a constant and has no fluctuation during the course of the simulation.

1-5-2 Volume of the system, *V*

In the NVE and NVT ensembles, the volume of the simulation cell is a fixed input. It does not fluctuate with time. In the NpT and NpH ensembles, the volume fluctuates in response to the barostat.

1-5-3 Temperature, *T*

The temperature is related to the kinetic energy, K.E, via the equipartition theorem. The kinetic energy is related to the velocities via classical mechanics.

$$\frac{3}{2}NK_BT = K.E = \frac{1}{2}\sum_{i=1}^{N}\sum_{\alpha=1}^{3}m_i v_{i,\alpha}^2 \tag{1}$$

$$T = \frac{2E_{ink}}{3NK_B} \tag{2}$$

Unlike the volume, the temperature fluctuates in all four ensembles. The NVT and NpT ensembles, in which the temperature is specified, are controlled by thermostats that do not keep the temperature exactly at the set point temperature at all times. Instead, a proper thermostat allows the temperature to fluctuate about the set point temperature in a manner that is still capable of rigorously generating trajectories that correspond to the ensemble [80].

1-5-4 Pressure, *p*

In three-dimensions, the pressure tensor is a symmetric 3x3 tensor, with each component defined by a kinetic and potential contribution,

$$P_{\alpha\beta} = P_{K.E,\alpha\beta} + P_{P.E,\alpha\beta} \tag{3}$$

The kinetic contribution to the $\alpha\beta$ element of the pressure is

$$P_{K.E,\alpha\beta} = \frac{1}{V}\sum_{i=1}^{N}m_i v_{i,\alpha}v_{i,\beta} \tag{4}$$

Since the velocities in different dimensions are not correlated, when $\alpha \neq \beta$, the average value of the $P_{K.E,\alpha\beta}$ is zero. However, $\alpha = \beta$, have twice the kinetic energy in that dimension.

$$P_{K.E,\alpha\beta} = \frac{\delta_{\alpha\beta}}{V} \sum_{i=1}^{N} m_i \, v_{i,\alpha}^2 \qquad (5)$$

If use the equipartition theorem relate the kinetic energy in terms of the temperature and average over all three dimensions, have the pressure from the ideal gas law, where the potential energy is zero,

$$p = \frac{N}{V} K_B T = \frac{2}{3} \frac{K_B T}{V} = \frac{1}{3V} \sum_{i=1}^{N} \sum_{\alpha=1}^{3} m_i \, v_{i,\alpha}^2 \qquad (6) \text{ for ideal gas only}$$

Thus the potential energy contribution to the pressure can be seen as a deviation from the ideal

$$P_{P.E,\alpha\beta} = \frac{1}{V} \sum_{i=1}^{N} r_{i,\alpha} f_{i,\beta} \qquad (7)$$

When $\alpha \neq \beta$, the average value of the $P_{P.E,\alpha\beta}$ is not necessarily zero, depending on the state of stress within the system.

If the pressure tensor is not of interest, the scalar pressure reported by LAMMPS is the thermodynamic pressure [80],

$$p = \frac{1}{3} \sum_{\alpha=1}^{3} p_{\alpha\alpha} = \frac{1}{3V} \sum_{i=1}^{N} \sum_{\alpha=1}^{3} m_i \, v_{i,\alpha}^2 + \frac{1}{3V} \sum_{i=1}^{N} \sum_{\alpha=1}^{3} r_{i,\alpha} f_{i,\alpha} \qquad (8)$$

$$p = \frac{N K_B T}{V} + \frac{\sum_{i}^{N} r_i \cdot f_i}{dV} \qquad (9)$$

Where (N) is the number of atoms in the system, (K_B) is the Boltzmann constant, (T) is the temperature , (d) is the dimensionality of the system (2 or 3 for 2d/3d) , and (V) is the system volume (or area in 2d). the second term is the virial, equal to(–dU/dV), computed for all pairwise as

well as 2-body, 3-body, 4-body , many body, and long –rang interactions, where (r_i) and (f_i)are the position and force vector of atom (i) [81].

Like the temperature, the pressure fluctuates in all four ensembles. The NpT (Constant pressure –Temperature) and NpH (Constant pressure –enthalpy) ensembles, in which the pressure is specified, are controlled by barostats that do not keep the pressure exactly at the set point temperature at all times. Instead, a proper barostat allows the pressure to fluctuate about the set point pressure in a manner that is still capable of rigorously generating trajectories that correspond to the ensemble**.**

1-5-5 Kinetic Energy, *K.E*

The kinetic energy is not a traditional thermodynamic variable. However, it is an important property in the atomic-level description of matter. The K.E is defined by the sum of the kinetic energy of all particles in the system, as given in equation (1). In this work, the kinetic energy is defined exclusively as a function of velocities. Explicitly, the kinetic energy is not a function of particle positions.

If the system does not have net zero momentum, then there is a center of mass velocity that exists in the simulation. The kinetic energy can then be broken into two parts: kinetic energy of the center of mass of the system and the peculiar kinetic energy, which is the sum of kinetic energy of each particle based on velocities relative to the system center of mass velocity. Importantly, when the equipartition theorem is used to calculate temperature, it relies on peculiar velocities [80].

1-5-6 Potential Energy, *P.E*

The potential energy is not a traditional thermodynamic variable. However, it is an important property in the atomic-level description of matter[73]. The P.E is defined by the sum of all interactions between all particles in the system as given by the interaction potential can be written as

$$U(r) = \sum_{i=1}^{N} \sum_{j>i} \emptyset |r_i - r_j| \qquad (10)\ [82]$$

where Ø (r) is the Lennard-Jones potential, Embedded-Atom Method potential and are all examples of interaction potentials that define the potential energy.

1-5-7 Internal Energy, *U* (or total energy, *E*)

The internal energy is the sum of the kinetic and potential energies. It is also called the total energy. Often in thermodynamics, we here of the excess internal energy, which subtracts the K.E form the total energy. However, in general, the internal energy includes both contributions.

$$U = E = K.E + P.E \qquad (11)$$

In the NVE (Constant Volume- Energy) ensemble, the internal energy should be constant, as it is a measure of the conservation of energy of the classical equations of motion. It truth it fluctuates based on the numerical approximations to the solution of these ordinary differential equations. In the other three ensembles, the internal energy fluctuates [80].

1-6 Working with LAMMPS

LAMMPS is text-based, which means that it accepts input either as typed in, or by scripts. In this section, will present how scripts work, and the meaning of commands used in programs.

LAMMPS input scripts are usually named as in.file name (input.file name). They are divided into commands, variables, fixes and computes. Variables are formulae for generating variable that can be used by fixes and computes. Fixes are in short a collection of rules for how the simulation will behave. Computes calculates properties of either the entirety of the system or a subset of it. Commands are everything else [73].

The structure of an input script in Lammps is the one that follows:

1. Initialization

2. Atom definition

3. Settings

4. Run a simulator

The first step is to set the units that are going to be used, define if it is going to be 2D or a 3D simulation, and decide which kind of boundary conditions are going to be considered, the next step is to choose the lattice type (fcc, bcc, diamond, etc.) and its dimensions. Once it is done, a simulation box is defined and the atoms are created inside it. Then, the force fields that will describe the interaction between particles are chosen.

This interaction can be described using potential files or, on the other hand, changing some parameters in a formula, as it in Lennard-Jones potential [36].

1-6-1 Input Script in Crack [82]

In this part the input script used to perform the simulation is described with all the details needed.

1-6-1-1 Initialization

Definition of the units that are going to be used during the simulation. The "LJ" (Lennard-Jones) units are:

mass=mass or m

distance = sigma, where $x^* = x/\text{sigma}$

time =tau, where $t^* = t(\ epsilon/m/sigma\hat{}\ 2)\hat{}1/2$

energy = epsilon, where $E^* = E/epsilon$

velocity = $sigma/tau$ where $v^* = v\ tau/sigma$

temperature = reduced LJ temperature, where $T^* = T\ Kb/epsilon$

pressure = reduced LJ pressure, where $p^* = p\ sigma\hat{}3/epsilon$

units LJ

Definition of the simulation dimensions, in this case 2D.

dimension 2

Boundary conditions in each direction. For (x) and (y) directions the boundary is type (s), thus the position of the face is set so as to encompass the atoms in that dimension, it is shrink-wrapped or non-periodic. In z direction the boundary is periodic, which means that particles interact across the boundary.

boundary s s p

1-6-1-2 Atom, and Lattice Definition

Definition atoms attributes. The atomic type is the one that matches better with LJ simulation, makes the atomic properties atomic. just atoms are defined.

atom_style   atomic

The "neighbor" command sets the extra distance beyond force cutoff with a bin style to create an operation that scales linearly with the number of atoms per processor. Not very important command. just makes the run time shorter.
specify parameters for neighbor list, where $r_{nbr} = r_{cut} + 0.3$.

neighbor   0.3 bin

Define parameters for neighbor list, delay value = N ,where N = delay building until this many steps since last build .The delay setting means never build new lists until at least N steps after the previous build.

neigh_modify   delay 5
Make the atomic structure as hexagon with reduced density rho*(for LJ units) equal to 0.93

create geometry
lattice   hex 0.93

Definition the region that is going to be studied. make a region of atom in a box. The X range is 0 to 100, the Y range is 0 to 40 and the Z range is -0.25 to 0.25.

region   box block 0 100 0 40 -0.25 0.25

Create the simulation box, allowing a max of five species

create_box   5 box

Create type-1 atoms in the box

create_atoms   1 box

Define the mass of atoms. type (1 to 5) have mass equal to (1).

mass   1 1.0
mass   2 1.0
mass   3 1.0
mass   4 1.0
mass   5 1.0

1-6-1-3 Force Fields

In this section choice of the interatomic potential that is going to be used and the directory to find the parameters.

Define the interatomic potential between atoms, pairwise interaction via the Lennard-Jones potential. The pair_style of "lj/cut 2.5" indicates a standard Lennard -Jones potential with a length cutoff of 2.5 sigma. The

keyword "pair_coeff" sets the pairwise force field coefficients for one or more pairs of atom types. An asterisk is used in conjunction with the(I,J) types and means all types from 1 to N. Here, we set the coefficients to the default value in epsilon and sigma.

LJ potentials

pair_style   lj/cut 2.5

The keyword "pair_coeff" sets the pairwise force field coefficients for one or more pairs of atom types. An asterisk "*" is used in conjunction with the I,J types and means all types from 1 to N. Here, set the coefficients to the default value in epsilon and sigma. Where epsilon = 1.0, sigma = 1.0, cutoff = 2.5.

pair_coeff   * * 1.0 1.0 2.5

1-6-1-4 Settings

Define groups of atoms, first should define region, then based on the region define groups.

define groups

In Group 1 in the X range is infinity to infinity, the Y range is infinity to 1.25 and the Z range is infinity to infinity.

region   1 block INF INF INF 1.25 INF INF
group   lower region 1

In group 2 in the X range is infintiy to infinity, the Y range is 38.75 to infinity and the Z range is infinity to infinity.

region   2 block INF INF 38.75 INF INF INF
group   upper region 2

Group boundary is addition of group lower and upper.

group   boundary union lower upper

Group moblie is substraction of all atoms from boundary atoms.

group   mobile subtract all boundary

In Group of left opper in the X range is infintiy to 20, the Y range is 20 to infintiy and the Z range is infinity to infinity.

region   leftupper block INF 20 20 INF INF INF
group   leftupper region leftupper

In Group of left ower in the X range is infintiy to 20, the Y range is infinity to 20 and the Z range is infinity to infinity.

region   leftlower block INF 20 INF 20 INF INF
group   leftlower region leftlower

Assign to the different group different atom types

set   group leftupper type 2

set   group leftlower type 3

set   group lower type 4

set   group upper type 5

Compute the average temperature of the atoms in the mobile group.

initial velocities

compute   new mobile temp

Create random velocity on the atoms in the   mobile group, at a temperature of 0.01K.

velocity   mobile create 0.01 887723 temp new

Set the Velocity of the atoms in the upper group along Y direction equal to 0.3.

velocity   upper set 0.0 0.3 0.0

Define a linear velocity on the groups of atoms in the mobile group.

velocity   mobile ramp vy 0.0 0.3 y 1.25 38.75 sum yes

1-6-1-5 Run the Simulator

The process was performed under micro-canonical ensemble, apply an NVE (Constant Volume- Energy) ensemble on all atoms, specify ensemble where fixid = 1, atoms = all and ensemble = nve.

fixes

fix   1 all nve

Apply a value of zero force to the atoms in the boundary groups.

fix   2 boundary setforce NULL 0.0 0.0

Set the timestep equal to 0.003

run

timestep   0.003

Output the result every 200 steps on the screen

thermo   200

thermo_modify   temp new

Not very important

neigh_modify   exclude type 2 3

Export an output file for visualization

#dump   1 all atom 500 dump.crack

#dump   2 all image 250 image.*.jpg type type &

zoom 1.6 adiam 1.5

#dump_modify   2 pad 4

#dump   3 all movie 250 movie.mpg type type &

\#   zoom 1.6 adiam 1.5

\#dump_modify   3 pad 4

Run for 5000 steps

run   5000

1-6-2 Input Script in MEAM [81]

1-6-2-1 Initialization

Definition of the units that are going to be used during the simulation. The "metal" units are:

mass = grams/mole

distance = Angstroms

time = picoseconds

energy = eV

velocity = Angstroms/picosecond

force = eV/Angstrom

torque = eV

temperature = Kelvin

pressure = bars

dynamic viscosity = Poise

charge = multiple of electron charge (1.0 is a proton)

dipole = charge*Angstroms

electric field = volts/Angstrom

density = gram/cm^dim

units metal

Boundary conditions in each direction. For x, y and z directions the boundary is periodic, which means that particles interact across the boundary.

boundary p p p

1-6-2-2 Atom Definition

Definition atoms attributes. The atomic type is the one that matches better with metal simulation, makes the atomic properties atomic.
just atoms are defined.

atom_style   atomic

The "neighbor" command sets the extra distance beyond force cutoff with a bin style to create an operation that scales linearly with the number of atoms per processor. Not very important command. Just makes the run time shorter.
specify parameters for neighbor list, where $r_{nbr} = r_{cut} + 0.3$.

neighbor   0.3 bin

define parameters for neighbor list, delay value = N ,where N = delay building until this many steps since last build .The delay setting means never build new lists until at least N steps after the previous build.

neigh_modify   delay 10

Read them in from a data or restart file, via the read data or read restart command, Contain molecular topology information , read_data-Read in a data file containing information LAMMPS needs to run a simulation (data.***)

read_data   data.meam

1-6-2-3 Force Fields

In this section we choose of the interatomical potential that is going to be used and the directory to find the parameters. The "*" indicates that the potential is going to be applied between all the types of atoms defined.

pair_style   meam
pair_coeff * * library.meam Si C sic.meam Si C

1-6-2-4 Run the Simulator

The process was performed under micro-canonical ensemble, apply an NVE (Constant Volume- Energy) ensemble on all atoms, specify ensemble where fixid = 1, atoms = all and ensemble = nve.

fix   1 all nve

Set the timestep equal to 0.001

timestep   0.001

Output the result every 10 steps on the screen

93

thermo   10

Export an output file for visualization

#dump   1 all atom 50 dump.meam

#dump   2 all image 10 image.*.jpg element element &

axes yes 0.8 0.02 view 60 -30

#dump_modify   2 pad 3 element Si C
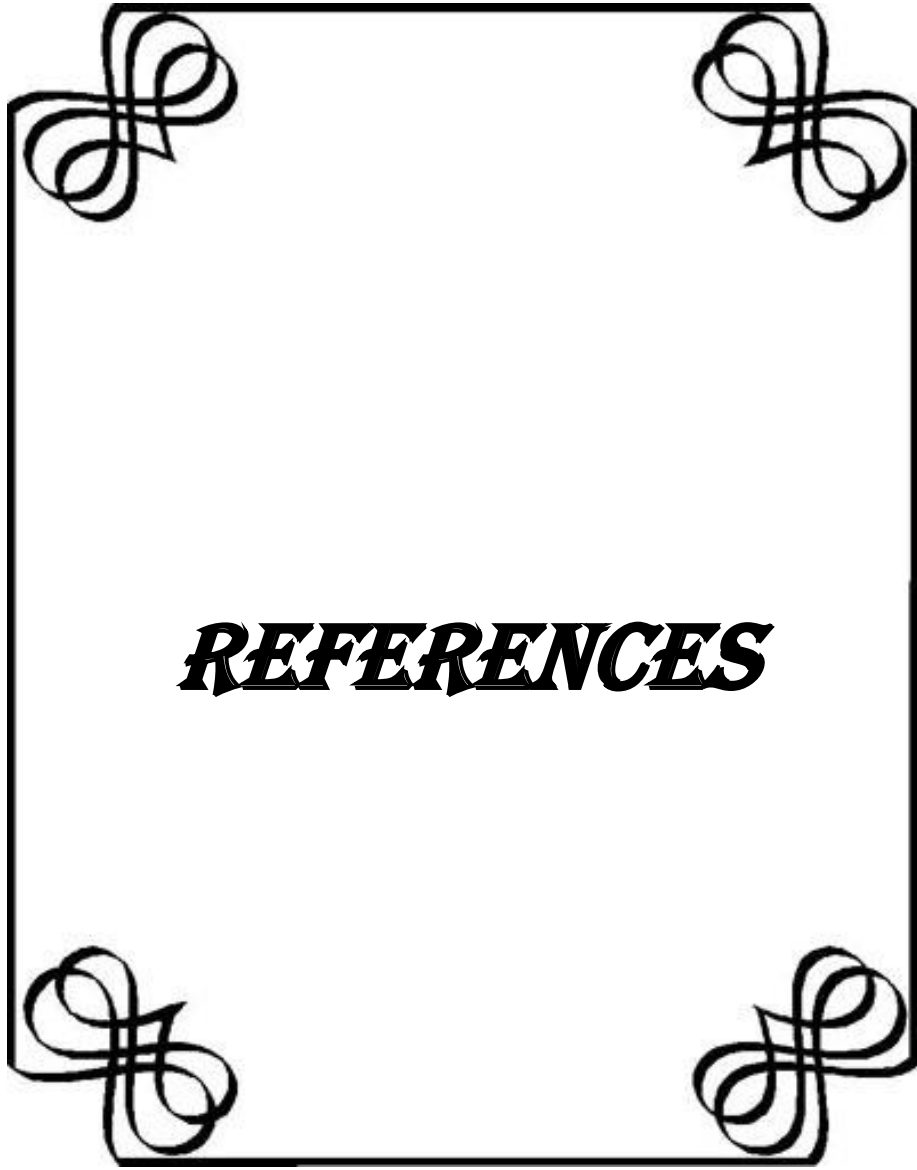
#dump   3 all movie 10 movie.mpg element element &

axes yes 0.8 0.02 view 60 -30

#dump_modify   3 pad 3 element Si C

Run for 5000 steps

run   5000

REFERENCES

1- Xinran Zhang ,'' Computational Modeling of Li Diffusion Using Molecular Dynamics", A paper for graduation with Honors in Physics faculty of the Department of Physics, Wake Forest University, (2015) pp.1-31.

2- Satyanarayan Dhal and Yadlapalli Raja, "Effect of Size and Strain Rate on Deformation Behaviour of Cu50Zr50 Metallic Glass: A molecular Dynamics Simulation Study", A Thesis of Department of Metallurgical & Materials Engineering National Institute of Technology Rourkela-769008, (2012) pp.1-63.

3- Ashis Das and Gaurav Singh, " Plastic Deformation and failure studies near a void for Copper-Aluminium alloy via Molecular Dynamics Simulation",
 A thesis of Department of Metallurgical and Materials Engineering National Institute of Technology, Rourkela, (2014) pp.1-50.

4- B.J. Alder and T. E. Wainwright, " Studies in Molecular Dynamics. l" ,General Method, J. Chem. Phys. 31(2), (1959).

5- A. Rahman, "Correlations in the Motion of Atoms in Liquid Argon", Physics Review. 136 (2A), (1964) pp. 405-411.

6- Jarosaw Meller, "Molecular Dynamics", Encyclopedia of Life Sciences, Cornell University, Ithaca, New York, USA Nicholas Copernicus University, Torun´, Poland, (2001) pp. 1-8.

7- Michael P. Allen, "Introduction to Molecular Dynamics Simulation", John von Neumann Institute for Computing, http://www.fz-juelich.de/nic-series/volume23, (2004) pp. 1-28.

8- Xue Yang, "Atomistic Simulation Of Plasma Interaction With Plasma Facing Components In Fusion Reactors", PhD. Thesis, Purdue University, West Lafayette, Indiana,(2013) pp. 1-141.

9- William D. Callister, Jr.,"Fundamentals of Materials Science and Enginerring" , John Wiley & Sons, Inc, University of Utah, (2001) pp.147-196.

10- William G. Hoover, "Simulation of Brittle Fracture via Molecular Dynamics", G, Iacucci (ed), Computer Simulation in Physical Metallurgy- © ECSC, EEC, EAEC, Brussels and Luxemhourg, (1986) pp. 145-158.

11- Mnrray S., Daw and Michael I. Baskes, "Application of the embedded atom method to hydrogen embrittlement", Springer Science, (1987) pp. 196-213.

12- Mnrray S. Daw and M. I. Baskes "Embedded-atom method: Derivation and application to impurities, surfaces, and other defects in metals", Physical Review B, V.29, N.12, (1984) pp. 6443-6453.

13- Mnrray S. Daw and M. I. Baskes, "Semiempirical, quantum mechanical calculation of hydrogen embrittlement in metals", Physical Review Letters , V.50, N.17, (1983) pp. 1285–1288.

14- Mnrray S. Daw , Stephen M. Foiles and Michael I. Baskes "The embedded-atom method: A review of theory and applications", Materials Science Reports- Elsevier Science Publishers B.V. All rights reserved, (1993) pp. 251–310.

15- S. Nouranian, M.A. Tschopp, S.R. Gwaltney, M.I. Baskes, and M.F. Horstemeyer, "An interatomic potential for saturated hydrocarbons based on the modified embedded-atom method", physics.chem-ph., (2014) pp. 1–29.

16- CH. Henager, Jr., F. Gao, SY. Hu, G. Lin, EJ. Bylaska and N. Zabaras, "Simulating Interface Growth and Defect Generation in CZT –Simulation State of the Art and Known Gaps. Pacific Northwest National

Laboratory", Report- Prepared for the U.S. Department of Energy under Contract DE-AC05-76RL01830,USA, (2012) pp. 1-81.

17- M.I. Baskes, "The Modified Embedded Atom Method. Association for information and image management" ,Assoclation for information and image Management 1100 wayne Avenue, Suite 1100 Silver Spring, Maryland 20910 (1994) pp. 3-28.

18- Daan Frenkel and Berend Smit, "Understanding Molecular Simulation for Algrithms to Application" .University of Amsterdam the Netherlands, Academic Press A Division of Harcourt, Inc. (2002) pp. 1-658.

19- Michele Meo and Marco Rossi, "Prediction of Young's modulus of single wall carbon nanotubes by molecular-mechanics based finite element modeling", Composites Science and Technology, Department of Mechanical Engineering, University of Bath, Claverton Down, Bath BA2 7AY, (2006) pp. 1597–1605 .

20- Erik Fransson and Johannes Laurell Hakansson "Local and Global Ordering in Barium Zirconate, a Model Potential Study", Thesis for the degree of Master of Science in Engineering Physics, Department of Applied Physics Division of Materials and Surface Theory Chalmers University of Technology Gothenburg, Sweden, (2014) PP.1-58.

21- Lammps molecular dynamics simulator, http://lammps.sandia.gov/ ,(2014).

22- Wang, Mingchao, Yan, Ceng, Ma, Lin, Hu, Ning and Chen, Mingwei, "Effect of defects on fracture strength of graphene sheets" ,Computational Materials Science,(2012) pp. 236-239.

23- Bohumir Jelinek, Sabastien Groh, Mark F. Horstemeyer, Jeffery Houze, Seong-Gon Kim, Gregory J. Wagner,Amitava Moitra and Michael I. Baskes, "Modified embedded atom method potential for Al, Si, Mg, Cu,

and Fe alloys", Physical review.B, Condensed matter 85(24):245102,(2012).

24- Minh-Quy Le and Romesh C. Batra , "Single-edge crack growth in graphene sheets under tension" , Computational Materials Science, (2013) pp. 381-388.

25- G. D. Samolyuk, Stas I. Golubov, Y. N. Osetsky, and R. E. Stoller, "Molecular dynamics study of influence of vacancy types defects on thermal conductivity of β-SiC", Journal of Nuclear Materials 418, (2011) pp. 174-181.

26- Mazdak Ghajari, Lorenzo Iannucci and P. T. Curtis, "A peridynamic material model for the analysis of dynamic crack propagation in orthotropic media", Computer Methods in Applied Mechanics and Engineering 276, (2014) pp. 431-452.

27- Laalitha S. I. Liyanage, Jeff Houze, Sungho Kim, Mark A. Tschopp, Seong-Gon Kin, Michael I. Baskes and Marks F. Horstemeyer, "Structural, elastic and thermal properties of cementite(Fe_3C) calculated using Modified Embedded Atom Method", Physical Review B 89, (2014).

28- Alireza Tabarraei and Xiaonan Wang, "A molecular dynamics study of nanofracture in monolayer boron nitride", Materials Science & Engineering A 641, (2015) pp. 225-230.

29- Ebrahim Asadi , Mohsen Asle Zaeem, Sasan Nouranian, and Michael I. Baskes, "Two-phase solid–liquid coexistence of Ni, Cu, and Al by molecular dynamics simulations using the modified embedded-atom method", Science Direct, Acta Materialia 86, (2015) pp. 169-181.

30- Qi-lin Xiong, Zhen-huan Li and Xiao-geng Tian, "Fracture behaviors of pre-cracked monolayer molybdenum disulfide: A molecular dynamics study" , Beilstein Journal of Nanotechology, (2016) pp. 1411-1420.

31- Naigen Zhou, Chi Zhang, Xiang Zeng, Jiren Yuan and Lang Zhou, "A molecular dynamics study of the growth rate of SiC crystal and its dependence on the temperature" , Interational Journal of Modern Physics B, Volume 30 (2016) pp. 1-12.

32- Lu Xie, "Simulations du dépôt par pulverization plasma et de la croissance de couches minces", PhD. thesis, UniversIté D'orléans, (2013) PP.1-155.

33- Dhatri Gaddamanugu,"Finite Element Modelling and Molecular Dynamic Simulations of Carbon Nanotubes/Polymer Composites". Texas A&M University, (2009) pp.1-83.

34- Hoang,K.C.; Fu,Y. and Song,J.H. "An hp-proper orthogonal decomposition–moving least squares approach for molecular dynamics simulation". Computer Methods Applied Mechanics Engineering, University of Colorado at Boulder, Boulder, CO 80309, (2016) pp.548–575.

35- Fredrik Hedman, "Algorithms for Molecular Dynamics Simulations". Stockholms University, (2006) pp.1-93.

36- J. M. Seminario and Perla B. Balbuena, "Molecular dynamics: From classical to Quantum methods" . Theroretical and computational chemistry, University Columbia U.S.A., (1999) pp.1-946.

37- Maria Cano Colino, "Molecular Dynamics Simulation of EPSP Synthase". Universitat Autònoma de Barcelona, (2007) pp.1-41.

38- A.J. Stone, "The theary of intermolecular forces", Clarendon Press.Oxford, Department of Chemistry ,University Cambridge, (1996) pp. 1-41.

39- Gemma Safont Camprubí ,"Mechanical properties at nano-level", University Lund, (2011) pp.1-28.

40- Nneoma Ogbonna ,"Molecular Dynamics Simulation" . African Institute for Mathematical Sciences Muizenberg, South Africa., (2004) pp. 2-37.

41- Mihai Ciocoiu,"Materials behavior : Research methodology and mathematical models", CRC Press, Taylor& Francis Group, Apple Academic Press, (2015) pp.1-361.

42- Sale,K.L. "Molecular Modelig of Nitroxidesspin Labels: Methods Development and Applications". The University Florida ,College of Arts and Sciences, (2002) pp.1-325.

43- Rangel-Vazquez,N.A. and felix, F.R. "Computational Chemistry Applied in the Analyses of Chitosan /Polyvinylpyrrolidone/ Mimosa Tenuiflora" . Science Publishing Group, (2014) pp.1-97.

44- Robert K. Poole, "Globin and other Nitric oxide -Reactive proteins, part B", Department of Molecular Biology and Biotechnology , The University of Sheffield, UK, (2008) pp.1-654..

45- H. Fehske, R. Schneider, and A. Weibe, "Computational many-particle physics",Springer, (2008) pp.1-780.

46- Jiaxi Zhang, "Molecular dynamics study of crack propagation behavior and mechanisms in Nickel", MSC. Thesis, The Ohio State University, (2011) pp.1-58.

47- Beena Rai,"Molecular modeling for the design of novel performance chemical and materials", CRC Press, Taylor& Francis Group, pp.1-382. (2012).

48- Daniel Schopf, "Effective Potentials for Numerical Investigations of Complex Intermetallic Phases", Institut für Theoretische and Angewandte Physik ,Universität Stuttgart, (2013) pp.17-238.

49- Kivilcim Basak Vural," Adsorption of Gold Atoms on Anatase TiO2(100) -1×1 Surface", MSc. Thesis, University Middle East Technical , (2009) pp.1-50.

50- John A. Keith, Josef Anton, Payam Kaghazchi, and Timo Jacob, "Modeling Catalytic Reactions on Surfaces with Density Functional Theory. 1st ed", (2012) pp.1-38.

51- Stefan Wippermann, "Understanding substrate-supported atomic-scale nanowires from ab initio theory", University Paderborn, (2010) pp.1-184.

52- Kim, lurii, "First-principles study on electronic and structural properties of Cu(In/Ga)Se alloys for solar cells", University Lappeenranta of Technology, LUT school of Technology, Department of Mathematics and Physics, (2015) pp.1-40.

53- Vorgelegt Von, "Interface Dipole Formation in Organic Surface Functionalizations", PhD. Thesis, Von der Fakultät für Mathematik, Informatik und Naturwissenschaften der RWTH Aachen University, (2012) pp. 8-274.

54- Fabiano Corsetti, "On the properties of point defects in silicon nanostructures from ab initio calculations", PhD. Thesis ,Thomas Young Centre ,Imperial College London, (2012) pp.1-259.

55- S. Dalgic, and S. Guler, "The Atomic Structure of Lattice Mismatched Si/Ge Bulk Heterostructures by Using the Density Functional Theory", Physics Department, Faculty of Science, Trakya University, 22100, Edirne (TURKEY) (2011) pp.1-4.

56- Geoffrey Tse, "Study of Piezoelectricity on III/V semiconductors from atomistic simulations to computer modeling", PhD. Thesis , University of Manchester, (2012) pp.1-213.

57- Samir Lounis,"Theory of Magnetic Transition Metal Nanoclusters on Surfaces", Reihe Materie und Material / Matter and Materials,41(2007) pp.1-189.

58- EVA D. Zurek,"Density Functional Theory (DFT) Studies of Solids and Molecules", PhD. Thesis ,University Stuttgart, (2006) pp.7-161.

59- Sara Galasso, "Generalization of the Eliashberg equations and Density Functional Theory applied to the analysis of the fundamental properties of iron-basedsuperconductors", PhD. Thesis, Politecnico di Torino, Porto Institutional Repository, (2015) pp.1-84.

60- Jiawei Xian, "Electronic Properties of Gold Nanoclusters from GW Calculations", PhD. Thesis, pp.1-109 (2012).

61- Sami Auvinen, "Computational Modeling of The Properties of TiO2 Nanoparticles". University Lappeenranta of Technology,(2013) pp.13-59.

62- Vorgelegt Von, "Surface Functionalization with Amino-based Self-Assembled Monolayers", PhD. Thesis, Von der Fakultät für Mathematik, Informatik und Naturwissenschaften der RWTH Aachen University, (2015), pp.1-211.

63- Mohammed Suleiman Hussein Suleiman,"Theoretical Investigation of Structural, Electronic and Optical Properties of some Group10,11 and 12Transition-Metal Nitrides", PhD. Thesis ,University Witwatersrand, Johannesburg, (2013) pp.1-278.

64- Paolo Giannozzi, Scuola Normale Superiore and Piazza dei Cavalieri, "Density Functional Theory For Electronis Structure Calculations", Università di Pisa, (2005) pp.1-35.

65- Jianlin Chang, "Ab initio calculations of semiconductor surfaces and molecular clusters", PhD. Thesis, Queen's University Kingston, Ontario, Canada , (1997) pp.1-139.

66- MARAL Mianpour, "Theoretical Studies of Nanostructure Formation and Transport on Surfaces", PhD. Thesis ,University of Central Florida, (2013) pp.1-208.

67- R.M. Martin, "Pseudopotentials", Cambridge University, (2004) pp.205-231.

References ....……………………

68- Jian-Hua Zhang, Shun-Qing Wu, Yu-Hua Wen, and Zi-Zhong Zhu, "An EAM potential for the dynamical simulation of Ni-Al alloys Journal Atomic Molecular Sciences", Department of Physics and Institute of Theoretical Physics and Astrophysics, Xiamen University, Fujian 361005, China, Vol. 1, No. 3,(2010) pp. 253-261.

69- S.Y. Hu, M.I. Baskes, M. Stan, and L.Q. Chen, "Atomistic calculations of interfacial energies, nucleus shape and size of h0 precipitates in Al–Cu alloys". Acta Materialia, 54, (2006) pp. 4699–4707.

70- M.I. Baskes, "Modified embedded-atom potentials for cubic materials and impurities", physical Review B, Vol. 46, NO. 5, (1992) pp. 2727-2742.

71- Hanchen Huang, Nasr M. Ghoniem, J immy K. Wong, and Michael I. Baskest, "Molecular dynamics determination of defect energetics in B-Sic using three representative empirical potentials", Modelling and Simulation in Materials Science and Engineering, University of California, (1995) pp.615-627.

72- Markus J. Buehler and Huajian Gao, "Chapter 1 modeling dynamic fracture using large-scale atomistic simulations", Massachusetts Institute of Technology, Department of Civil and Environmental Engineering 77 Massachusetts Avenue Room 1-272, Cambridge, MA., 02139, USA, (2007) pp. 1-67.

73- Kristian Berg Keilen, "Polymer failure modeled by Molecular Dynamics", Materials Science and Engineering, Norwegian University of Science and Technology, Department of Engineering Design and Materials, (2014) pp. 1-127.

74- Farid, F. Abraham, Dominique Brodbeck, William E. Rudge and Xiaopeng Xu, "A molecular dynamics investigation of rapid fracture mechanics". IBM Research Division, Almaden Research Center, 650

Harry Road, San Jose, CA 95120-6099, U.S.A. ,Vol. 45, No. 9, (1997) pp. 1595-1619.

75- Petucci,J.; LeBlond,C and Karimi M. Molecular dynamics simulations of brittle fracture in fcc crystalline materials in the presence of defects. pp. 130-139. (2014).

76- Ravi Kiran Siripurapu, "Molecular Dynamics Study of Zirconium and Zirconium Hydride", MSc. Thesis, Department of Mechanical Engineering, University of Saskatchewan, (2013) pp. 1-94.

77- Tommy Andersson, "One-shot free energy calculations for crystalline materials", MSc. Thesis, University chalmers of technology, (2012) pp. 1-57.

78- Justin M. Petucci, "A Study of crack propagation in metals in the presence of defects", MSc. Thesis, Indiana University of Pennsylvania, (2013) pp. 1-104.

79- http://katter-world.blogspot.com/2010/05/install LAMMPS on ubuntu.

80- David Keffer, "Evaluating Thermodynamic properties in LAMMPS", Department of Materials Science & Engineering University of Tennessee, Knoxville, (2016) pp. 1-10.

81- LAMMPS User's Manual .http://lammps.sandia.gov. (2016).

82- Nneoma Ogbonna, "Molecular dynamics simulation", African Institute for Mathematical Sciences, (2004).

الخلاصة

في هذه الرسالة، تم دراسة التصدع وتعديل طريقة غمر الذرة (MEAM) باستخدام المحاكاة الديناميكية الجزيئية، محاكاة (lammps) لنشر التصدع في الشبيكة السداسية وفي تعديل طريقة غمر الذرة لمادة السليكون كاربيد (SiC). ميكانيكية التصدع تتضمن نشوء الانخلاعات وتوليد التراص غير المتكامل.

في كود التصدع كانت الخطوات الزمنية المستخدمة (0.03،0.04.0.044، 0.02، 0.01، 0.009، 0.008، 0.007، 0.006، 0.005، 0.004، 0.003، 0.002، 0.001 و reduced 0.00001) وفي تعديل طريقة غمر الذرة الخطوات الزمنية المستخدمة (0.003، 0.002، 0.001، 0.0009، 0.0008، 0.0007، 0.0006، 0.0005 و Ps 0.0001)، الخطوة زمنية يجب اختيارها صغيرة بما يكفي لضمان الحفاظ على الطاقة وتجنب الاخطاء الكبيرة المنفصلة ، وبالتالي فان افضل خطوة زمنية مختارة في كود التصدع هي (reduced 0.00001) وفي تعديل طريقة غمر الذرة هي (Ps 0.0001) . في كود التصدع

الزيادة في الطاقة الكامنة (النقصان في السالبيه) بسبب عدم ابتداء التصدع، وحين يبدا التصدع بالتوسع فان قيمة الطاقة الكامنة تكون مساوية الى 302511ϵ- في خطوة التشغيل 10600، وهذ ناتج من تكسر الاواصر بين الذرات، بينما الزيادة في درجة الحرارة تشير الى انتشار التصدع. الزيادة (النقصان في السالبيه) في الضغط للنظام بسبب عدم نشوء التصدع ومن ثم النقصان (الزيادة في السالبيه) في الضغط بسبب تكسر الاواصر بين الذرات عند انتشار التصدع. في هذا الكود فان حجم او مساحة التصدع هو ثابت.

في تعديل طريقة غمر الذرة (MEAM) ، الزيادة في الطاقة الكامنة بالسالبة لان غمر ذرة بمجموعة من الذرات (نظام مستقر) تحتاج الى طاقة كافية من اجل كسر الاواصر بين الذرات. وزيادة الطاقة الحركية للنظام يمكن ان تعزى الى الزيادة السريعة والمضطردة في تكسر الاواصر بين الذرات الموضعية . على الرغم من طاقة النظام محفوظة فان درجة حرارة النظام تزداد عندما يتم تحويل الطاقة الكامنة الى طاقة حركية نتيجة تكسر الاواصر بين الذرات. و يزداد الضغط بالسالب نتيجة كسر الاواصر بين الذرات

دراسة الخصائص الميكانيكية لمادة SiC باستخدام المحاكاة الديناميكية الجزيئية (LAMMPS)

رسالة مقدمة إلى مجلس كلية التربية / جامعة القادسية

وهي جزء من متطلبات نيل درجة الماجستير في علوم الفيزياء

تقدمت بها

شروق حيدر عبد النبي المحنة

بكالوريوس فيزياء / كلية التربية

جامعة القادسية 2014

بأشراف

أ.م.د هشام محمد علي حسن البيرماني

1438هـ   2017 م